OFFICE OF CIVILIAN RADIOACTIVE WASTE MANAGEMENT

1. QA: QA

SPECIAL INSTRUCTION SHEET

Page: 1 of: 1

Complete Only Applicable Items

This is a placeholder page for records that cannot be scanned or microfilmed

2. Record Date	3. Accession Number
08/18/2000	MOL.20000829.0005
4. Author Name(s)	**5. Author Organization**
RICHARD A. SILVA	N/A

6. Title
SUBSURFACE TRANSPORTER SAFETY SYSTEMS ANALYSIS

7. Document Number(s)	8. Version
ANL-WER-ME-000001	REV. 01
9. Document Type	**10. Medium**
REPORT / DESIGN DOCUMENT	OPTIC/PAPER

11. Access Control Code
PUB

12. Traceability Designator
DC #25003

13. Comments
THIS IS A ONE-OF-A-KIND DOCUMENT DUE TO THE COLORED GRAPHS ENCLOSED, AND CAN BE LOCATED THROUGH THE RPC.

OFFICE OF CIVILIAN RADIOACTIVE WASTE MANAGEMENT
ANALYSIS/MODEL COVER SHEET

1. QA: QA

- Complete Only Applicable Items

2. ☒ Analysis — Check all that apply	3. ☐ Model — Check all that apply
Type of Analysis: ☒ Engineering; ☐ Performance Assessment; ☐ Scientific	Type of Model: ☐ Conceptual Model; ☐ Abstraction Model; ☐ Mathematical Model; ☐ System Model; ☐ Process Model
Intended Use of Analysis: ☐ Input to Calculation; ☐ Input to another Analysis or Model; ☐ Input to Technical Document; ☒ Input to other Technical Products	Intended Use of Model: ☐ Input to Calculation; ☐ Input to another Model or Analysis; ☐ Input to Technical Document; ☐ Input to other Technical Products
Describe use: Input to Waste Emplacement/Retrieval System Description Document and other System Description Documents that are Direct Inputs to the Site Recommendation Consideration Report	Describe use:

4. Title:

Subsurface Transporter Safety Systems Analysis

5. Document Identifier (including Rev. No. and Change No., if applicable):

ANL-WER-ME-000001 REV 01

6. Total Attachments:	7. Attachment Numbers - No. of Pages in Each:
3	I-4, II-13, III-3 (CD-ROM Media)

	Printed Name	Signature	Date
8. Originator	Richard A. Silva \ Douglas D. Orvis	Richard A. Silva / Douglas D. Orvis	07/13/2000
9. Checker	Kenneth J. Herold	Kenneth J. Herold	7/19/00
10. Lead/Supervisor	Frank J. Bierich	Frank J. Bierich	07-19-00
11. Responsible Manager	Daniel G. McKenzie III	Daniel G. McKenzie III	7/19/00

12. Remarks:

1. Doug Orvis contributed to the analysis by providing the Fault Tree Analysis and the related conclusions.
2. Lewie Booth checked the Fault Tree Analysis and the related conclusions
3. John Cron provided significant technical and editorial changes and/or revisions from REV 00 to REV 01

The following TBV/TBD are contained in this document:

TBV: 245, 246, 253, 274, 308, 690,3130, 3133, 3138, 3142, 4208
TBD: 330, 3936

OFFICE OF CIVILIAN RADIOACTIVE WASTE MANAGEMENT

ANALYSIS/MODEL REVISION RECORD

Complete Only Applicable Items

2. Analysis or Model Title:

Subsurface Transporter Safety Systems Analysis

3. Document Identifier (including Rev. No. and Change No., if applicable):

ANL-WER-ME-000001 REV 01

4. Revision/Change No.	5. Description of Revision/Change
00	Initial Issue.
01	The revision of this analysis incorporated design changes from the Viability Assessment Design to the Site Recommendation Consideration Report Design and the Enhanced Design Alternative II, including the Waste Package Transporter, the Site Layout, and applicable System Description Documents. This revision was an extensive change and, therefore, the entire analysis has been revised.

CONTENTS

INTENTIONALLY LEFT BLANK

FIGURES

INTENTIONALLY LEFT BLANK

TABLES

INTENTIONALLY LEFT BLANK

ACRONYMS AND ABBREVIATIONS

Acronyms

CCF	Common-Cause Failure
DBE	Design Basis Event
ESF	Exploratory Studies Facility
FRA	Federal Railroad Administration
FTA	Fault Tree Analysis
MGR	Monitored Geologic Repository (replaces the term MGDS)
SR	Site Recommendation
TBD	To Be Determined
TBM	Tunnel Boring Machine
TBV	To Be Verified
T.E.P	Test and Evaluation Program
WHB	Waste Handling Building
WP	Waste Package

Abbreviations

C.G.	Center of Gravity
DC	Direct Current
ft	Feet
g	Acceleration due to gravity
hr	Hour
in	Inches
KE	Kinetic Energy
km	Kilometers
lb/lbs	Pound/Pounds
lb_f	Pounds force

ACRONYMS AND ABBREVIATIONS (CONTINUED)

m	Meters
mm	Millimeters
mph	Miles per Hour
MT	Metric Ton (1,000 kg)
N	Newton
PE	Potential Energy
psi	Pound per Square inch (lb/in^2)
s	Second
Sta.	Station
yr	Year

1. PURPOSE

The purpose of this document, as stated in the development plan *Subsurface Transporter Safety Systems Analysis* (CRWMS M&O 2000a), is to revisit and revise the initial issue of this analysis, which investigated a Waste Package (WP) Transporter runaway condition and the results of such a condition. The main reason to revise the initial document is due to the major changes of the WP Transporter design, dimensions, and gross weight. These changes are in response to recently issued Enhanced Design Alternatives requirements affecting the WP Transporter and the emplacement of WPs.

The objective of this activity includes a review of the previously established runaway scenario, a discussion and description of new runaway scenarios, and a re-evaluation of the maximum attainable transporter speed under three primary conditions: frictionless, standard rolling resistance, and with standard and/or dynamic braking systems. The intended use of this analysis is to provide safety-related and design information as inputs to associated System Description Documents and the Site Recommendation (SR) Consideration Report - Volume 1, Section 2.

Under the presented runaway conditions, transporter derailment and/or tip-over is identified and analyzed. The use and effectiveness of impact limiters and other energy absorbing systems are also discussed. A fault-tree analysis is developed, based on previous fault-tree analyses, to determine the probability of a runaway-to-WP breach scenario. The determination of such an event as credible or incredible is presented. Different methods and concepts of uncontrolled descent mitigation are introduced as a means of mitigating and/or preventing a runaway scenario.

The conclusion of this analysis provides a description of potential runaway scenarios and their related effects, i.e., derailment, tip-over, impact, etc., and an estimate of the frequency (annual probability of occurrence) of such scenarios. The use of this analysis will support justification for or against the elimination of Runaway Train design basis events (DBE).

INTENTIONALLY LEFT BLANK

2. QUALITY ASSURANCE

The quality assurance classification of repository structures, systems, and components has been performed in accordance with QAP-2-3, *Classification of Permanent Items.* The WP emplacement equipment has been classified as quality affecting *Classification of the MGR Waste Emplacement System* (CRWMS M&O 1999a). The *Classification of the MGR Waste Emplacement System* (CRWMS M&O 1999a) lists the Waste Retrieval System, the Waste Package Transporter, and the locomotives with a designation of QL-1, high safety or waste isolation significance.

This design activity has been developed in accordance with AP-3.10Q, *Analysis and Models,* and has been evaluated in accordance with QAP-2-0, *Conduct of Activities.* The activity evaluation (CRWMS M&O 1999c) addressing the Quality Assurance classification has determined that this design activity is quality-affecting and subject to the requirements of the *Quality Assurance Requirements and Description* document (DOE 2000).

Attachment III of this analysis includes electronic media (CD-ROM) containing the actual Microsoft Excel 97 SR-2 spreadsheet data file entitled *SSTSSA Calculation Rev 01.xls.* This data file has been managed in accordance with AP-SV.1Q, *Control of the Electronic Management of Data.*

In order to ensure accuracy and completeness of the information generated in this document, access to the information on the personal computer was controlled with password protection. As an attachment to the document, the properties inherent to the CD-ROM media, i.e., read-only, provide adequate controls to protect the data file, and provide controls to ensure that the data are readily retrievable. In addition, the data file was archived on the network "H" drive, which was backed up daily by the Enterprise Server Team Department per project policy. When the work was complete, the data file, as a CD-ROM attachment to this document, was hand carried to Engineering Document Control for transfer to the Records Processing Center.

The formal to-be-verified (TBV) and to-be-determined (TBD) tracking system described in AP-3.15Q, *Managing Technical Product Inputs,* is applicable to this analysis.

INTENTIONALLY LEFT BLANK

3. COMPUTER SOFTWARE AND MODEL USAGE

Microsoft Excel 97 SR-2 was used to develop seven figures (Figure 11 through Figure 16, and Figure 19). This software was appropriate to the application. The calculations used to create these figures are described in Sections 6.3 and 6.4. Hand calculations for each figure were made and the results compared with the data in the figures. The data were found to be without significant error. These checks are presented in Attachment II. Therefore, the routines used within Microsoft Excel 97 SR-2 are "simple and easily understood" and comply with Section 5.1 of AP-SI.1Q, *Software Management.*

MicroStation Version 05.07.01.14 for Windows x86, a computer aided design (CAD) software package, was used to create Figure 21, and the dimensions shown have been hand verified within Section 6.5. It has been shown that the preliminary CAD dimensions in Figure 21 were within a level of accuracy deemed adequate for the conceptual design.

The Project-standard suite of office automation software for word processing has been used in the preparation of this analysis. The remaining figures have been drawn using various CAD software programs and are used solely for visual display of equipment designs. These are commercially available software programs that are approved for the Project and, therefore, no qualifications are needed.

INTENTIONALLY LEFT BLANK

4. INPUTS

4.1 DATA AND PARAMETERS

The data and parameters used in this analysis are given in the following sections and have been determined to be appropriate for use in this analysis. The qualification status of the input is indicated, as well as the documentation of TBV or TBD parameters, in accordance with AP-3.15Q, *Managing Technical Product Inputs.*

4.1.1 The physical dimensions and general arrangement of the WP Transporter used in this analysis are shown in Figure 1 through Figure 3 (used throughout) (CRWMS M&O 2000b, Section 6.2.1.3 and 6.4.5.1).

4.1.2 The physical layout of the Exploratory Studies Facility (ESF), including the North Ramp and North Ramp Curve, is shown in Figure 4 and is based on the *ESF Layout Calculation* (CRWMS M&O 1996, Section 7.4.2) as used in the *Site Recommendation Subsurface Layout* analysis (CRWMS M&O 2000d, Section 4.1.5.1). As stated in Assumption 5.14, this analysis does not investigate the use of the South Ramp. The ESF layout is used in Assumption 5.1 and Table 3. (TBV-4208)

4.1.3 The system shall transport and emplace WPs with the characteristics defined in Table 1. These values are used throughout this analysis (CRWMS M&O 1999b). (TBV-246)

Table 1. Waste Package Characteristics

Characteristic	Value
Length	3.48 m to 5.96 m (11.4 ft to 19.5 ft) (TBV-246)
Diameter	1.32 m to 2.11 m (4.33 ft to 6.92 ft) (TBV-246)
Weight	72,100 kg maximum (79.5 tons) (TBV-246)

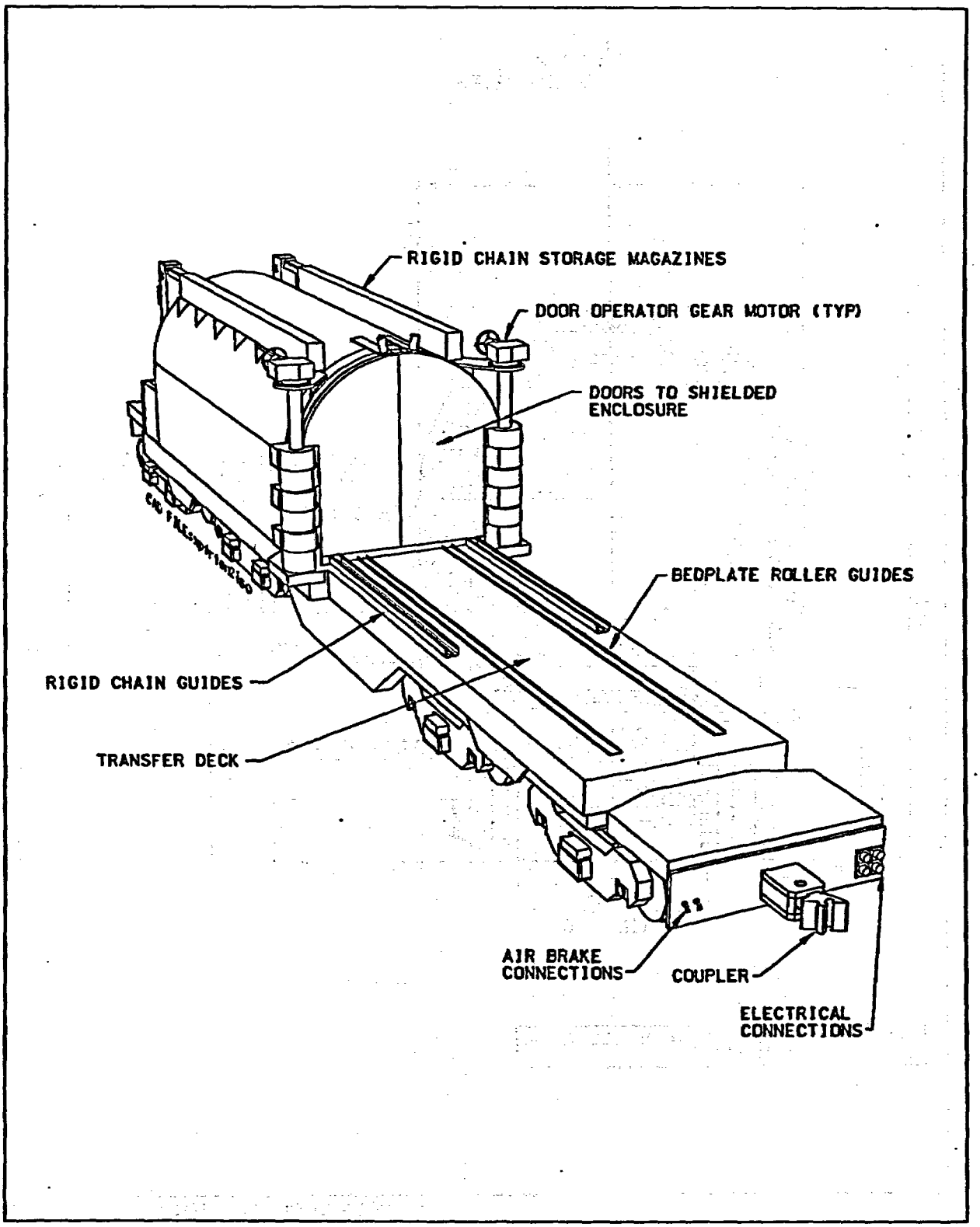

Figure 1. Waste Package Transporter Isometric View

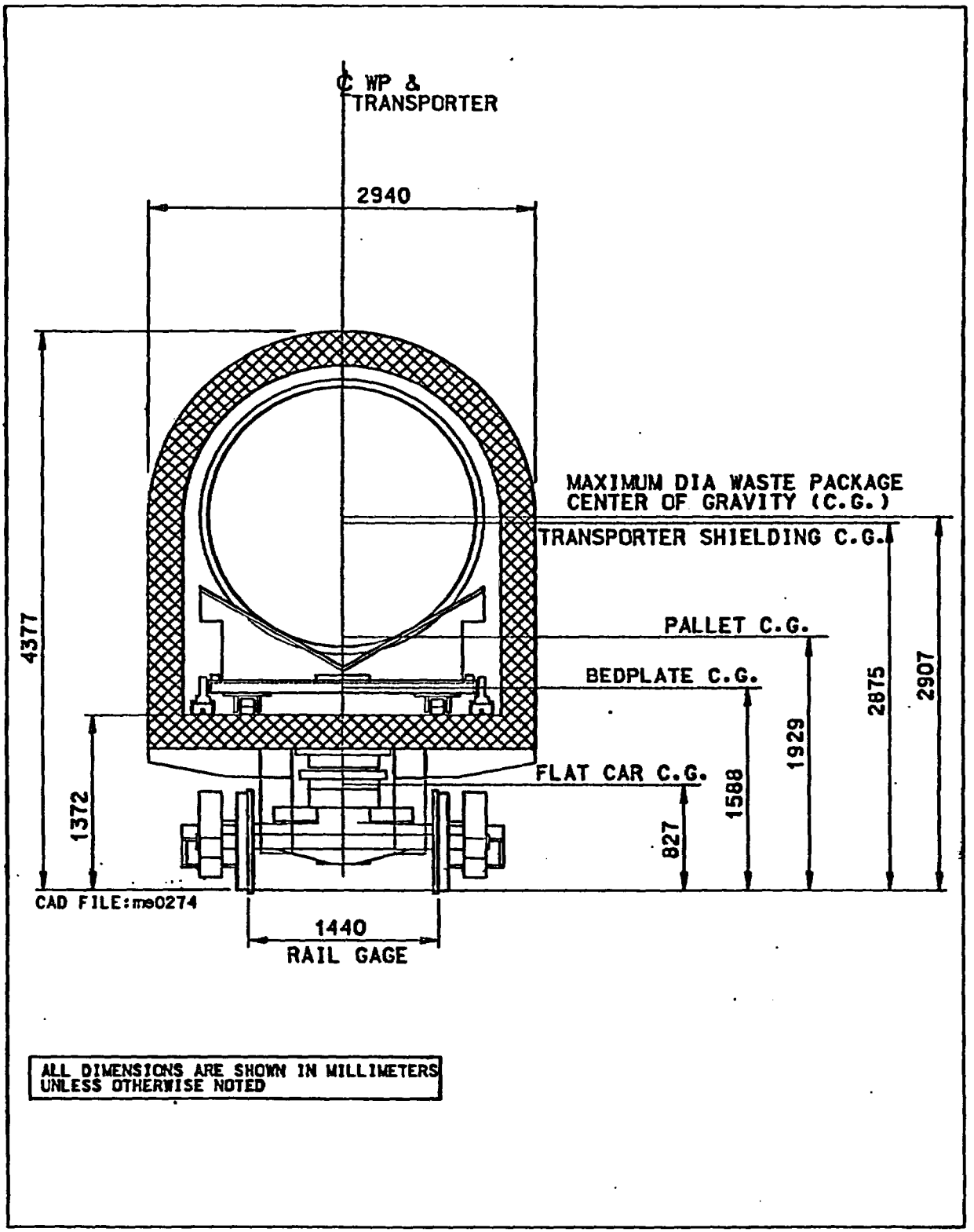

SOURCE: CRWMS M&O 2000b, Section 6.4.5.1

Figure 2. Waste Package Transporter Center of Gravity

INTENTIONALLY LEFT BLANK

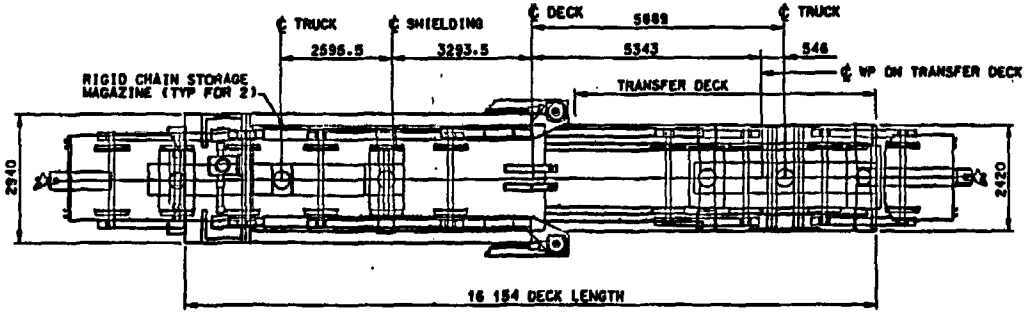

PLAN VIEW

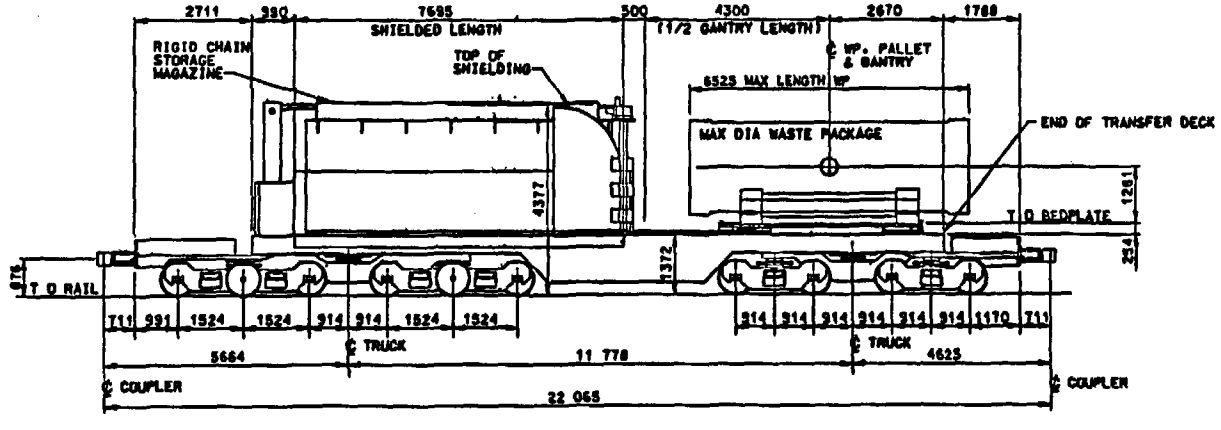

ELEVATION VIEW

CAD FILE:

ALL DIMENSIONS ARE SHOWN IN MILLIMETERS UNLESS OTHERWISE NOTED

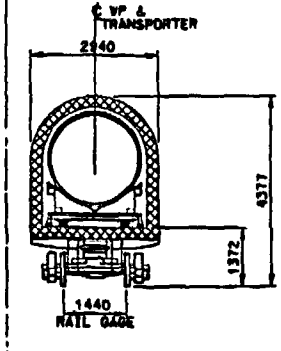

SECTION VIEW

SOURCE: CRWMS M&O 2000b, Section 6.2.1.3

Figure 3. WP Transporter

INTENTIONALLY LEFT BLANK

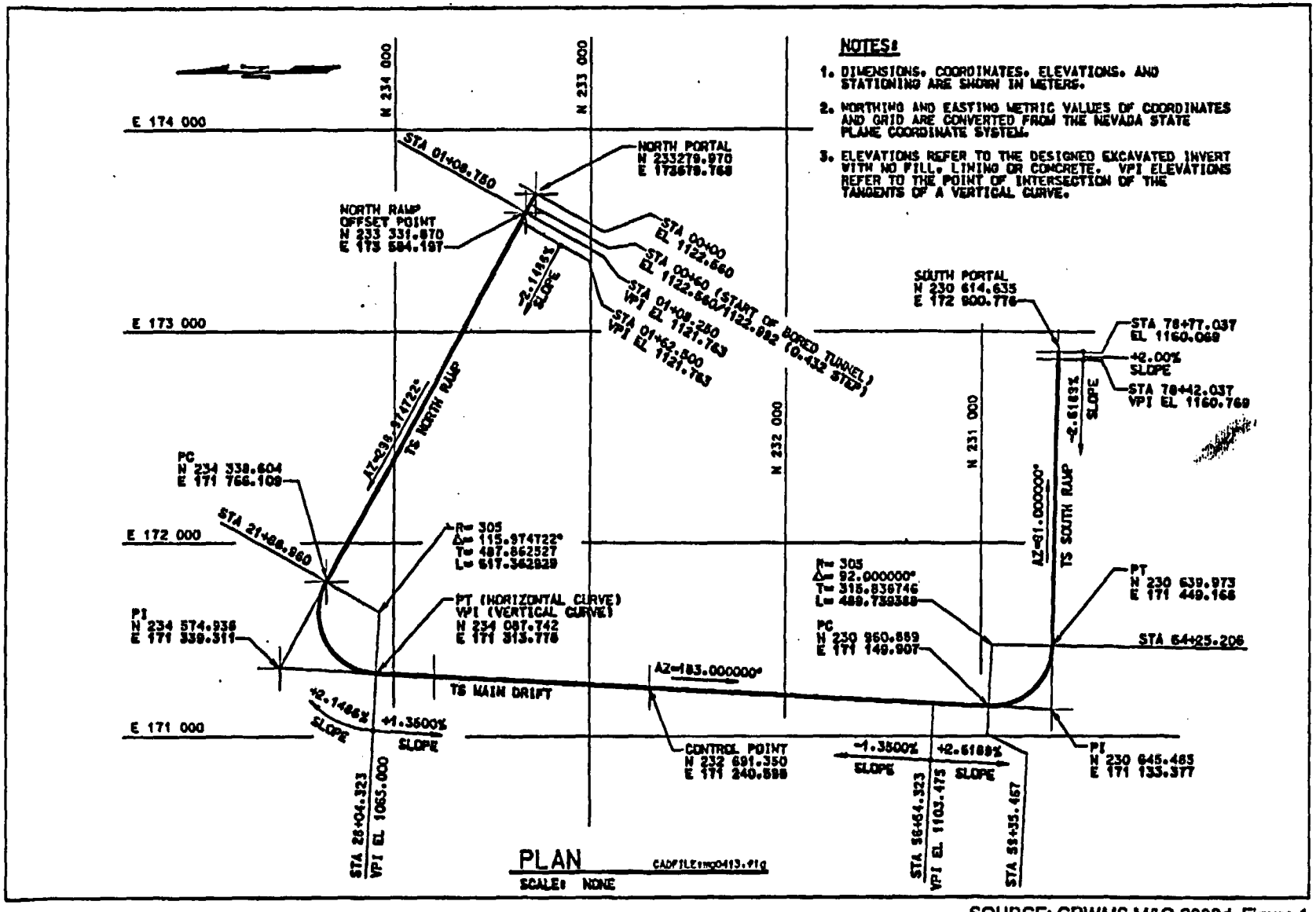

SOURCE: CRWMS M&O 2000d, Figure 1

Figure 4. Exploratory Studies Facility

4.1.4 The center of gravity from top-of-rail for the WP, bed plate, pallet, shielding, and WP Transporter are given in Table 2 (used throughout).

Table 2. Waste Package Transporter Physical Characteristics

	Transporter Rail Car	Transporter Shielding	Bed Plate	Waste Package (TBV-246)	Pallet	Total
Weight	136 MT (149.91 tons)	153.4 MT (169.09 tons)	10.0 MT (11.023 tons)	[a]85.0 MT (93.696 tons)	3 MT (3.31 tons)	[b]387.4 MT (427.04 tons)
Center of Gravity (From Top of Rail)	827 mm (32.6 in)	2,875 mm (113.2 in)	1,588 mm (62.5 in)	2,907 mm (114.5 in)	1,929 mm (75.9 in)	N/A

(Source: CRWMS M&O 2000b, Section 6.4.5.1 and Section 6.4.3)

NOTES: [a]Assumption 5.4 states that the maximum WP weight, for this analysis only, is assumed as 85,000 kg (93.696 tons) and is used as a bounding weight for the WP in subsequent calculations.

[b]Assumption 5.16 states that a 400 MT (441 tons) bounding weight for the loaded transporter is used in subsequent calculations, except as noted in Section 6.4.3 for use in tip-over calculations.

4.1.5 The subsurface repository layout for SR is presented in Table 3 and Figure 5. The details of the subsurface layout, including lengths and grades, are presented in Table 3. The information in Table 3 was extracted from *Site Recommendation Subsurface Layout* (CRWMS M&O 2000d, Attachment II) and *ESF Layout Calculation* (CRWMS M&O 1996, Section 7.4.2). This information is used to determine runaway speeds and braking distances, as discussed in Section 6.3, and to determine tip-over and/or derailment speeds, as discussed in Section 6.4. (TBV-4208)

4.1.6 For waste emplacement and retrieval, two Transport Locomotives are currently envisioned to haul the WP Transporter. Each locomotive is a 50-ton, 4-axle, 8-wheel unit with two direct-current electric motors rated at 170 hp each. The locomotive is powered by a single 650-volt overhead conductor (catenary wire) through a pantograph mounted on the locomotive (CRWMS M&O 1998b, Section 7.3.1). These input parameters are used in the locomotive description (Section 6.1.2) and in the calculation of rolling resistance (Attachment III, Table III-1).

Table 3. SR Site Layout Location Data

From Point	Description	To Point	Description	Grade (%)	[a] Total Slope Length from North Portal (m)	Slope Length of Segment (m)	[b] Plan Length of Segment (m)	[a] Vertical Distance (m)	Curve Radius (m)
	North Portal Entrance	[c] A	Top of North Ramp	N/A	0.0	162.50	N/A	N/A	N/A
[c] A	Top of North Ramp (Sta. 01+62.50)	[c] B	Top of Northern Curve of ESF Loop (Sta. 21+86.96)	-2.14862	162.50	2,024.93	2,024.46	43.50	N/A
[c] B	Top of Northern Curve of ESF Loop (Sta. 21+86.96)	C	Top of North Ramp Extension Curve	-2.06	2,187.43	270.0	269.9	5.56	N/A
C	Top of North Ramp Extension Curve	D	End of North Ramp Extension Curve	-2.06	2,457.4	340.9	340.8	7.02	305
D	End of North Ramp Extension Curve	E	Point on the North Ramp Extension	-2.06	2,798.3	999.1	998.9	20.58	N/A
E	Point on the North Ramp Extension	F	Intersection of the North Ramp Extension and the Test and Evaluation Program (T.E.P.) Observation Drift #2	-2.06	3,797.4	71.8	71.8	1.48	N/A
F	Intersection of the North Ramp Extension and the T.E.P. Observation Drift #2	G	Grade break in the North Ramp Extension	-2.06	3,869.2	273.00	273.0	5.62	N/A
G	Grade break in the North Ramp Extension	H	Intersection of the East Main North Extension and the North Ramp Extension	-1.38	4,142.2	173.4	173.3	2.39	305
H	Intersection of the East Main North Extension and the North Ramp Extension	I	Intersection of the centerline of the east turnout of Postclosure Test Drift #1 and the East Main North Extension	-1.35	4,315.6	359.6	359.5	4.85	N/A

Ref. 1996

TITLE: ESF Layout Calculation
DI: BABEAD000-01717-0200-00003 REV 04

7.4.2 ELEVATIONS

The elevations of the vertical control points shown below refer to the excavated invert. It should be noted that the starting point for the bored tunnel is approximate; the actual station will be field determined.

LOCATION	ELEVATION	SOURCE
North Portal @ Sta 00+00	1122.560 m	Design Input (Table 1)
Launch Chamber Face @ Sta 00+60	1122.560 m	Design Input (Table 1)
Start of Bored Tunnel @ Sta 00+60	1122.992 m	Design Input (Table 1)
VPI @ Sta 01+08.250	1121.763 m	Design Input (Table 1)
VPI @ Sta 01+62.500	1121.763 m	Design Input (Table 1)
VPI @ Sta 28+04.323	1065.000 m	Design Input (Table 1)
VPI @ Sta 56+54.323	1103.475 m	Calculated (Section 7.2)
VPI @ Sta 78+42.037	1160.769 m	Calculated (Table 4)
South Portal @ Sta 78+77.037	1160.069 m	Established (Section 7.3)

TABLE 2
VERTICAL CURVE DATA SHEET

[1]VERTICAL CURVE @ STATION 01+08.250

CURVE TYPE: EQUAL-TANGENT PARABOLIC
CURVE LENGTH: 35.000 m

CONTROL PT	STATION	ELEV. @ EXC. INV	ELEV. @ SPRINGLINE
VPC	00+90.750 m	1122.025 m	1125.835 m
VPI	01+08.250 m	1121.763 m	1125.573 m
VPT	01+25.750 m	1121.763 m	1125.573 m

[1]VERTICAL CURVE @ STATION 01+62.500

CURVE TYPE: EQUAL-TANGENT PARABOLIC
CURVE LENGTH: 50.000 m

CONTROL PT	STATION	ELEV. @ EXC. INV	ELEV. @ SPRINGLINE
VPC	01+37.500 m	1121.763 m	1125.573 m
VPI	01+62.500 m	1121.763 m	1125.573 m
VPT	01+87.500 m	1121.220 m	1125.030 m

Note: Parabolic type curves are designed to provide smooth transitions into and out of vertical curves.

[1] Curve data, except for elevation @ excavated invert, from Table 1, Section 4.1. Calculated elevation @ excavated invert based on a 7.62 m diameter tunnel (See Ref. 5.13 and Design Criterion 4.2.4)

TABLE 3
VERTICAL CURVE DATA SHEET

VERTICAL CURVE @ STATION 28+04.323

CURVE TYPE: EQUAL-TANGENT PARABOLIC
CURVE LENGTH: 30.000 m

CONTROL PT	STATION	ELEV. @ EXC. INV	ELEV. @ SPRINGLINE
VPC	27+89.323 m	1065.322 m	1069.132 m
VPI	28+04.323 m	1065.000 m (see note 1)	1068.810 m (see note 3)
VPT	28+19.323 m	1065.202 m	1069.012 m

VERTICAL CURVE @ STATION 56+54.323

CURVE TYPE: EQUAL-TANGENT PARABOLIC
CURVE LENGTH: 30.000 m

CONTROL PT	STATION	ELEV. @ EXC. INV	ELEV. @ SPRINGLINE
VPC	56+39.323 m	1103.272 m	1107.082 m
VPI	56+54.323 m	1103.475 m (see note 2)	1107.285 m (see note 3)
VPT	56+69.323 m	1103.868 m	1107.678 m

Note: Parabolic type curves are designed to provide smooth transitions into and out of vertical curves.

[1] From Table 1, Section 4.1
[2] From Section 7.2
[3] Calculated elevation @ springline based on a 7.62 m diameter tunnel (See Ref. 5.13 and Design Criterion 4.2.4)

TABLE 4
VERTICAL CURVE DATA SHEET

VERTICAL CURVE @ STATION 78+42.037

CURVE TYPE: EQUAL-TANGENT PARABOLIC
CURVE LENGTH: 30.000 m

CONTROL PT	STATION	ELEV. @ EXC. INV	ELEV. @ SPRINGLINE
VPC	78+27.037 m	1160.376	1164.186 m
VPI	78+42.037 m	1160.769 m (see note 1)	1164.579 m (see note 2)
VPT	78+57.037 m	1160.469 m	1164.279 m

Note: Parabolic type curves are designed to provide smooth transitions into and out of vertical curves.

[1] VPI invert elevation = Portal elevation + (0.02)(20 m + 30/2 m) = 1160.069 m + 0.7 m = 1160.769 m

[2] Calculated elevation @ springline based on a 7.62 m diameter tunnel (See Ref. 5.13 and Design Criterion 4.2.4)

7.4.3 STATION CALCULATIONS

North Portal
Station (See Section 4.1) = 00+00.000

VPI - North Ramp
Station (See Section 4.1) = 01+08.250

North Ramp Offset Point
Station (See Section 4.1) = 01+08.750

VPI - North Ramp
Station (See Section 4.1) = 01+62.500

North Ramp PC
Station = 2566.073 - 487.863+108.750 = 21+86.960

North Ramp PT/VPI
Station = 2186.960+617.363 = 28+04.323

VPI - Main Drift
Station =2804.323+2850.000 (See Section 4.1) = 56+54.323

South Ramp PC
Station = 2804.323+(c_1-487.863)+(c_2-315.837) = 59+35.467

South Ramp PT
Station = 5935.467+489.739 = 64+25.206

VPI - South Ramp
Station = 6425.206+(b_2-315.837)-20-15 = 78+42.037

South Portal
Station = 6425.206+(b_2-315.837) = 78+77.037

7.4.4 SLOPE CALCULATIONS (EXCAVATED INVERT)

TUNNEL SEGMENT	STA (m)	ELEV (m)	SLOPE
North Portal	00+00.000	1122.560	
to			0.0000 %
Launch Chamber Face	00+60.000	1122.560	
to			0.432 m step
Start of Bored Tunnel	00+60.000	1122.992	
to			Varies[1]
VPI	01+08.250	1121.763	
to			0.0000 %
VPI	01+62.500	1121.763	
to			- 2.1486 %
VPI	28+04.323	1065.000	
to			+ 1.3500 %
VPI	56+54.323	1103.475	
to			+ 2.6189 %
VPI	78+42.037	1160.769	
to			- 2.0000 %
South Portal	78+77.037	1160.069	

[1] Actual (existing) slope varies in this tunnel segment (See Reference 5.15)

8.0 CONCLUSIONS

The geometric parameters which define the "TS Loop" portion of the ESF have been defined in Section 7 of this calculation. Pertinent coordinate geometry data from the preceding calculations is shown on Figure 3. Also included on Figure 3, for reference only, are borehole locations (See Reference 5.16 and Design Criterion 4.2.3), fault trace locations (See Reference 5.8), and the North and South Ramp Extension drifts.

As discussed in Section 7.3, it is recommended that an independent survey be performed to tie in control used at the North Portal to that to be used for construction of the South Portal box cut and to confirm the as-built position of the TBM and last tangent baseline in the South Ramp approximately 1000 m prior to hole-out.

9.0 ATTACHMENTS

Attachment I: Stormwater Calculations at South Portal Pages I-1 to I-3

From Point	Description	To Point	Description	Grade (%)	[e]Total Slope Length from North Portal (m)	Slope Length of Segment (m)	[b]Plan Length of Segment (m)	[a]Vertical Distance (m)	Curve Radius (m)
I	Intersection of the centerline of the east turnout of Postclosure Test Drift #1 and the East Main North Extension	J	Grade brake in North Main	−1.35	4,675.1	40.9	40.9	0.55	305
J	Grade brake in North Main	K	Intersection of the North Main and the Exhaust Main	−2.07	4,716.0	381.4	381.4	7.89	305
K	Intersection of the North Main and the Exhaust Main	L	Grade Brake in the North Main	+0.99	5,097.4	798.4	798.4	7.90	N/A
[c]B	Top of Northern Curve of ESF Loop (Sta. 21+86.960)	[c]M	End of North Ramp Curve (Sta. 28+04.323)	−2.14862	2,187.43	617.50	617.36	46.95	305
[c]M	End of North Ramp Curve (Sta. 28+04.323)	[d]N	Control Point on ESF Loop	+1.350	2,604.93	1,398.44	1,398.31	18.88	N/A

13.27

NOTES:

[a]Vertical distance is found by the following relationship:

Vertical distance = slope length × $\sin(\theta)$

where: $\theta = \tan^{-1}\frac{\%\text{Grade}}{100}$

[b]Horizontal distance is found by the following relationship:

Horizontal distance = slope length × $\cos(\theta)$

[c]Site Layout information involving the ESF is extracted from CRWMS M&O 1996, Section 7.4.2

[d]ESF Control Point information extracted from Figure 4 (CRWMS M&O 2000d, Figure 1)

[e]The total slope length is considered the total distance from the North Portal entrance (Sta. 00+00.00) to the beginning of the particular layout section (i.e. "From Point").

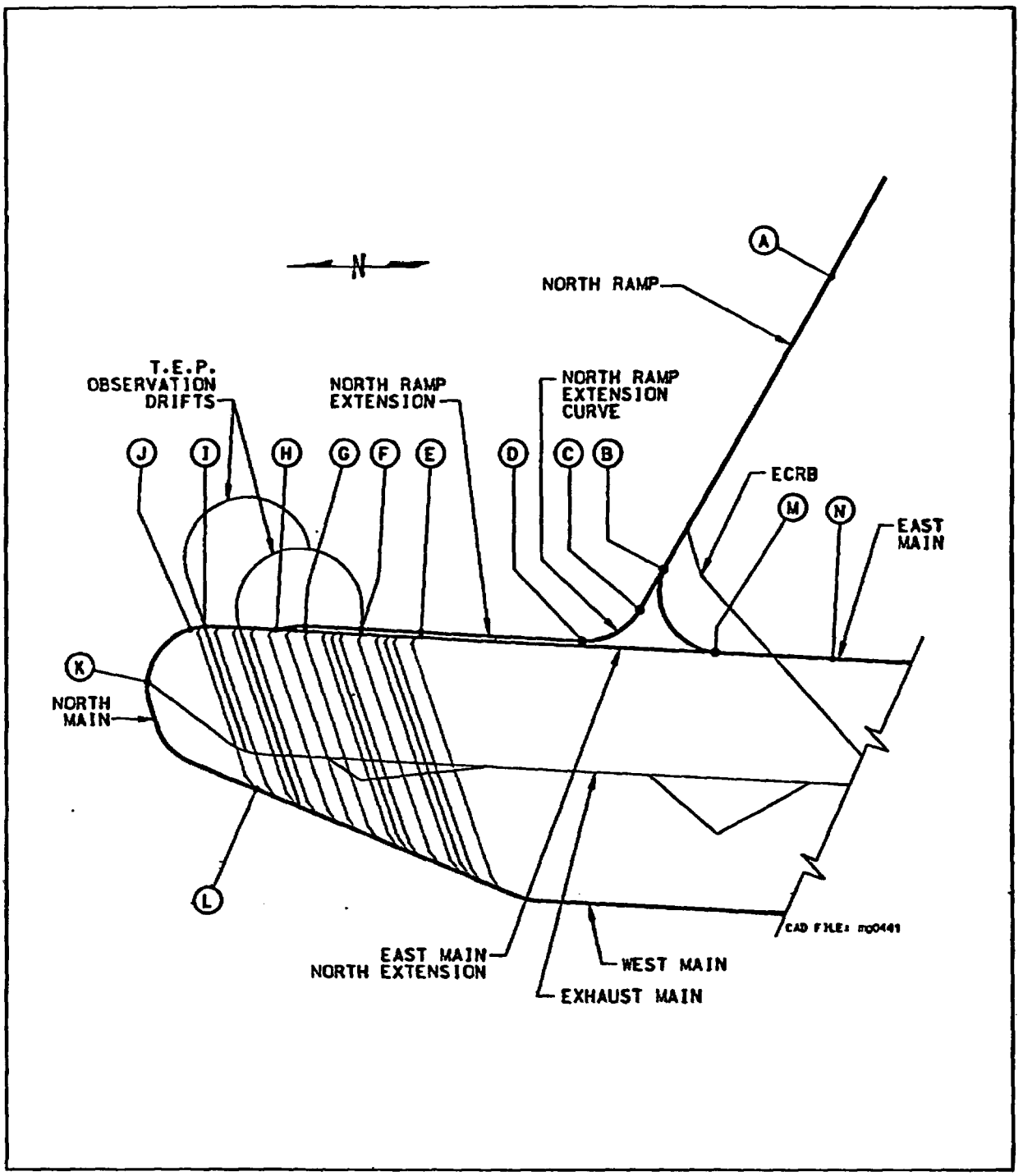

NOTES: 1. Balloon callout locations are approximate.
2. Exact balloon information is presented in Table 3.

Figure 5. SR Partial Site Layout

4.2 CRITERIA

The criteria used in this analysis are given below.

4.2.1 The system shall operate, where practical, on the track provided by the Subsurface Emplacement Transportation System, which has a track gauge of 1.44 m (56.5 in) (used in Section 6.4) (CRWMS M&O 2000c, Para. 1.2.4.5). (TBV-274)

4.2.2 The system shall operate within the Subsurface Emplacement Transportation System curvatures, which have a 305 m (1,000 ft) minimum radius curve (used throughout) (CRWMS M&O 2000c, Para. 1.2.4.6). (TBV-253)

4.2.3 The system speed shall be limited to 8 km/hr when transporting a WP (used throughout) (CRWMS M&O 2000c, Para. 1.2.2.1.2).

4.2.4 The portions of the system supporting emplacement shall operate over a maximum grade of ±2.5 percent outside the emplacement drifts and a maximum grade of ±1 percent within the emplacement drifts (see Assumption 5.14) (used throughout Section 6.3) (CRWMS M&O 2000c, Para. 1.2.4.3).

4.2.5 The portions of the system supporting retrieval, recovery, and restoration shall operate over a maximum grade of ±2.7 percent outside the emplacement drifts and a maximum grade of ±1 percent within the emplacement drifts (see Assumption 5.14) (used throughout Section 6.3) (CRWMS M&O 2000c, Para. 1.2.4.4).

4.2.6 The system shall lift the WP no higher than the maximum lift heights specified Table 4 (used in Section 6.6) (CRWMS M&O 2000c, Para. 1.2.2.1.3). (TBV-245)

Table 4. Maximum WP Lift Heights

WP Lift	Maximum Lift Height
WP in a Vertical Orientation	2 m (6.6 ft)
WP in a Horizontal Orientation	2.4 m (7.9 ft)

4.2.7 The portions of the system supporting retrieval, recovery, and restoration shall have an operational life of 160 years after initiation of waste emplacement (used in Assumption 5.13) (CRWMS M&O 2000c, Para. 1.2.1.2).

4.2.8 The portions of the system supporting emplacement shall have an operational life of 40 years following the start of emplacement (used in Assumption 5.13) (CRWMS M&O 2000c, Para. 1.2.1.1).

4.2.9 The system shall be designed to retrieve all emplaced WPs within 34 years after the initiation of retrieval operations (used in Section 5.7) (CRWMS M&O 2000c, Para. 1.2.1.5).

4.2.10 The portions of the system supporting retrieval, recovery, and restoration shall include provisions that support a deferral of closure for up to 300 years after initiation of waste emplacement (used in Section 5.13) (CRWMS M&O 2000c, Para. 1.2.1.3).

4.2.11 The system shall be designed to recover a minimum of (TBD-330) WPs (used in Assumption 5.7) (CRWMS M&O 2000c, Para. 1.2.1.7).

4.2.12 The system shall be designed to emplace and retrieve a minimum of 11,000 WPs (used in Section 5.6) (CRWMS M&O 2000c, Para. 1.2.1.6).

4.2.13 The system shall ensure that an uncontrolled descent down the North or South Ramp by system equipment carrying a WP is limited to less than 1.0×10^{-6} events per year (used in Section 6.8.1) (CRWMS M&O 2000c, Para. 1.2.2.1.1).

4.2.14 The system shall be capable of transporting and emplacing WPs at an annual throughput of (TBD-3936) (CRWMS M&O 2000c, Para. 1.2.1.4).

4.3 CODES AND STANDARDS

4.3.1 Association of American Railroads

S-401-99 Freight Car Brake Design Requirements. *Manual of Standards and Recommended Practices: Section E-Brakes and Brake Equipment* (AAR 1999).

M-926-99 Brake Shoes – High Friction Composition Type. *Manual of Standards and Recommended Practices: Section E-Brakes and Brake Equipment* (AAR 1999).

4.3.2 Department of Labor – Mine Safety and Health Administration

30 CFR 75 Mandatory Safety Standards – Underground Coal Mines (1998).

INTENTIONALLY LEFT BLANK

5. ASSUMPTIONS

The assumptions used in this analysis are listed below. The basis for the assumption is included as part of the assumption statement.

5.1 *Assumption*: Slope calculations for the North Ramp will use -2.14862 percent grade from Station 01+62.50 to the start of the North Ramp Curve, Station 21+86.960.

Basis: A minor deviation of line and grade occurred in the ESF as a result of a problem with the Tunnel Boring Machine (TBM) guidance. This occurred in the North Ramp between Station 00+60 and Station 01+08. The TBM trajectory was corrected to -2.14862 percent grade at approximately Station 01+62.500 (CRWMS M&O 1997a, p. 43 and CRWMS M&O 1996, Section 7.4.4).

Slope from Station 00 to Station 21+86.960:

$$\text{Slope} = \frac{\text{Elevation Change}}{\text{Distance}} \times 100 = \frac{1{,}122.560 - 1{,}078.265}{2{,}186.960} \times 100 = 2.02541 \text{ percent}$$

(Eq. 1)

Slope from Station 01+62.50 to Station 21+86.960:

$$\text{Slope} = \frac{\text{Elevation Change}}{\text{Distance}} \times 100 = \frac{1{,}121.763 - 1{,}078.265}{2{,}186.960 - 162.50} \times 100 = 2.14862 \text{ percent}$$

(Eq. 2)

Relative Error of two slopes:

$$\text{Error} = \frac{\text{Actual Slope} - \text{Estimated Slope}}{\text{Actual Slope}} \times 100$$

$$= \frac{2.14862 - 2.02541}{2.14862} \times 100 = 5.73438 \text{ percent}$$

(Eq. 3)

This deviation over the length of the North Ramp (2,186.960 m) will not be assumed to be negligible. Therefore, slope calculations for the North Ramp will use –2.14862 percent grade from Station 01+62.50 to the start of the North Ramp Curve, Station 21+86.960 (see Section 4.1.2). This assumption will not be considered TBV since the slope of the ESF is constant and, therefore, further confirmation is not required.

Used In: This assumption is used in the velocity calculations in Section 6.3.

5.2 *Assumption*: The gravitational constant of 9.80665 m/s^2 (32.1740 ft/s^2) will be used throughout and rounded to the appropriate number of significant digits.

Basis: The acceleration of gravity is not constant. Gravity (g) varies with latitude and altitude. The standard acceleration of gravity is 9.80665 m/s^2 (32.1740 ft/s^2) for mean sea level at 45°N latitude. Even though the approximate latitude and elevation of the North Ramp entrance differs from 45°N latitude and sea level, the resulting deviation in the gravitational constant will be assumed negligible (Avallone and Baumeister 1987, p. 1-26). This assumption will not be considered TBV since slight variations in gravitational constant do not significantly impact the results of this analysis and, therefore, further confirmation is not required.

Used In: This assumption is used in the velocity and stopping distance calculations in Section 6.3.

5.3 *Assumption*: For this analysis, the weight of each WP is assumed uniformly distributed throughout the volume of the WP. (TBV-308)

Basis: Radioactive waste material will be placed in symmetrically oriented basket assemblies, which will result in a uniform distribution of weight and a center of gravity located near the center of the WP (CRWMS M&O 1998a, Section 4.3).

Used In: This assumption is used in the determination of tip-over and derailment in Section 6.4.

5.4 *Assumption*: The maximum WP weight, for this analysis only, is assumed as 85,000 kg.

Basis: This bounding condition allows for increases in the 72,100-kg WP weight (Section 4.1.3) without affecting the analysis results. This assumption will not be considered TBV since slight variations in WP weight will be within the bounded weight and does not significantly impact the results of this analysis. Therefore, further confirmation is not required.

Used In: This assumption is used throughout the analysis.

5.5 *Assumption*: The calculations for a WP Transporter tip-over assume that the entire transporter is a rigid body and the center of gravity is located at a fixed point above the centerline of the rails.

Basis: The WP Transporter design may utilize springs within the suspension of the railcar trucks (see Figure 6) that, under normal operating conditions, would allow the WP Transporter to sway back and forth shifting the center of gravity from the center of the rails. It is also assumed that there will be no tip-over of the WP within the WP Transporter. This assumption will not be considered TBV since this provides a simplified representation of the WP Transporter and, therefore, further confirmation is not required.

Used In: This assumption is used for the tip-over calculations in Section 6.4.3.

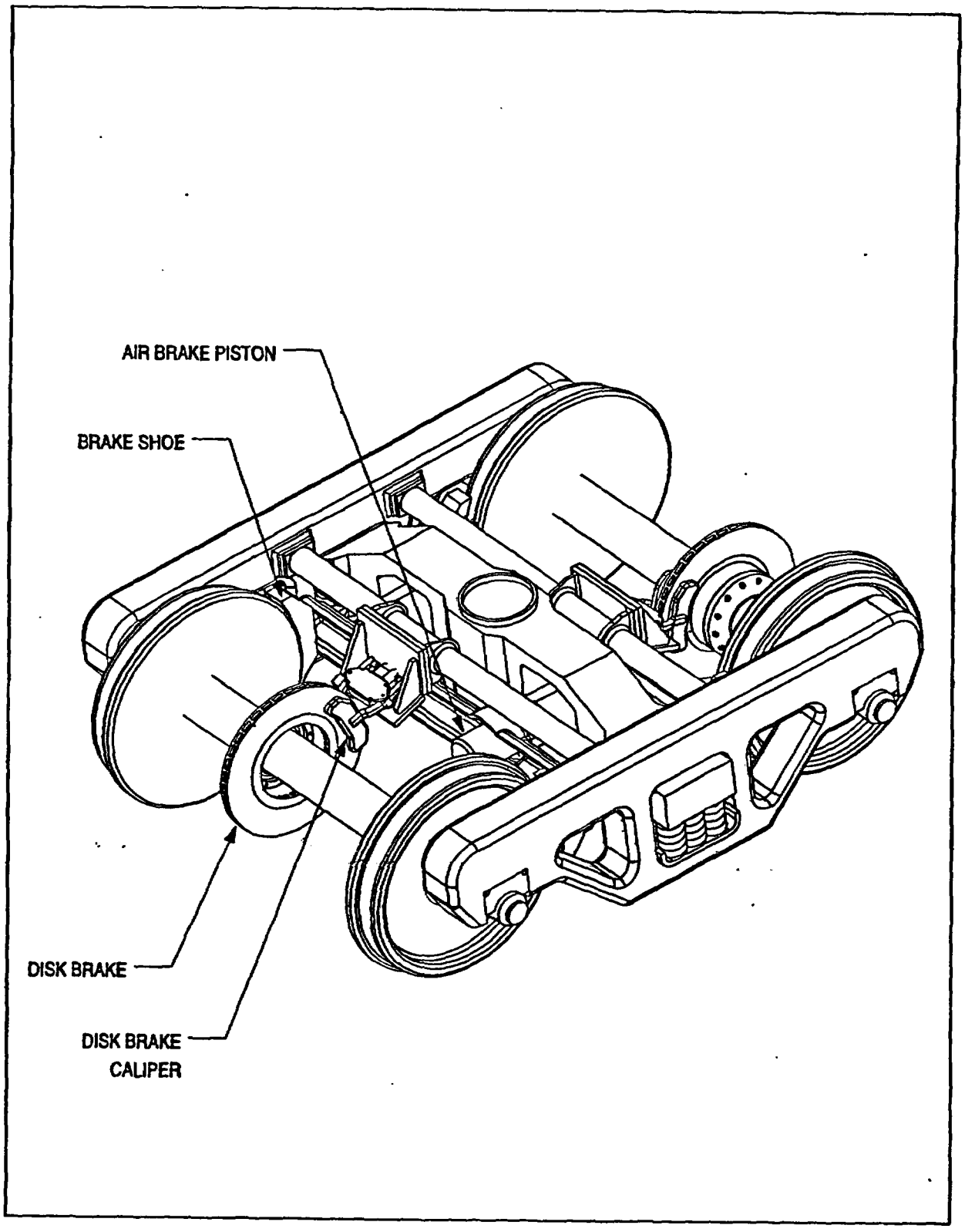

Figure 6. Waste Package Transporter Conceptual Two-Axle Truck Design

5.6 *Assumption*: The mass moment of inertia of the WP Transporter is assumed negligible.

Basis: The initial determination of the WP Transporter tip-over speed neglects the mass moment of inertia so that a bounding limit for tip-over velocity can be established. In dynamic motion calculations, the mass moment of inertia increases the energy required to tip the WP transporter, thereby increasing the speed in the curve necessary to tip. The calculation presented herein establishes the minimum required speed, or bounding limit, for WP Transporter tip-over. This assumption will not be considered TBV since this provides a simplified representation of the WP Transporter and, therefore, further confirmation is not required.

Used In: This assumption is used for the tip-over calculations in Section 6.4.3.

5.7 *Assumption*: The fault-tree model developed in *Application of Logic Diagrams and Common-Cause Failures to Design Basis Events* (CRWMS M&O 1997b) is assumed to be representative of the braking, control, and communication systems of the transporter train and is an appropriate baseline for the present analysis of potential design alternatives. The present analysis incorporates by reference the assumptions that were developed and justified in the cited document, as summarized in bullets below (TBV-3133).

Basis: The fault-tree model was developed in accordance with Civilian Radioactive Waste Management System Management and Operations (CRWMS M&O) procedures for qualified analyses. Further, the basic design and operational concepts represented in that model have not changed.

Assumptions from *Application of Logic Diagrams and Common-Cause Failures to Design Basis Events* (CRWMS M&O 1997b, Sections 4.3.2 through 4.3.16) are carried forward to this analysis as described in Section 6.8.3. The following summarizes those assumptions:

- Transporter train consists of a primary locomotive, a shielded WP transporter, and a secondary locomotive.
- Braking systems include dynamic brakes on both locomotives, a fail-safe air-release service brake with wheel shoes on all three vehicles, and a manually actuated parking brake.
- The air-release service brake design is represented by those provided by a typical mine-locomotive vendor; operators in the central control room can intervene at any time to take control of operating and braking the train.
- Published human error rates for errors of commission, omission, checking errors, and failure to recover from initial human errors are applicable.
- Initial error by train driver that could lead to a runaway is represented by an error of commission using controls that are in a "well-arranged functional group."

- Time spent on the North Ramp per descent is based on 4 km/hr (1.11 m/s or 2.5 mph) and 2,187 m (7,175 ft), giving a residence time of 0.55 hr per descent.

- Inspection intervals of component unavailability used in the calculations are based on 720 hours.

- Generic failure rate data for components are assumed to be applicable to the Monitored Geologic Repository (MGR).

- The failure probability of a system can be estimated from the failure probability of a principal component.

- Redundant components are subject to common-cause failures (CCF) and can be quantified using the "beta-factor" method.

- Controls of the two locomotives are interconnected via a radio-link rather than hardwired.

- Two locomotives have identical airbrake systems consisting of a single air reservoir and a single operating control valve.

- Transporter brake air supply and controls are hardwired to the primary locomotive, but have no direct connection to the secondary locomotive.

- Successful application of brakes to any one of the three vehicles is sufficient to stop a loaded transporter train.

- A rate of 456 trips per year for a loaded transporter is used within this analysis. A rate of 524 trips per year is compared to 456 trips per year in Assumption 5.8, and Sections 6.8.3.2.1 and 6.8.3.2.3

Criterion 4.2.14 defines the waste emplacement rate so that the overall MGR rates can be met (CRWMS M&O 2000c, Para. 1.2.1.4) (TBD-3936). Since the goal of the fault tree analysis (FTA) is to explore whether or not the runaway frequency can be reduced by several orders of magnitude, i.e., by a factor of about 1.7×10^{-3} (see Section 6.8.2.1), variations in emplacement rate are viewed as insignificant. Moreover, the fault-tree modeling is based on incomplete physical designs and the data used for fault-tree quantification are estimates, so any variations in assumed emplacement rate is unimportant at this stage of the design evolution.

It is also noted that Criterion 4.2.11 requires the ability to recover WPs; i.e., to transport the WPs back to the surface. The number of recoveries is expected to be very small (TBD-330). The frequency of transporting WPs up the North Ramp and during potential recovery operations leads to a small increase in the potential number of exposures. This undefined, but expected to be small, fractional increase is assumed to be negligible and is not addressed in this analysis.

It is further noted that Criteria 4.2.12 and 4.2.9 require that the system be able to retrieve 11,000 WPs within a 34-year period, respectively. This represents an average rate of about 324 trips per year. Even if the retrieval period were, for example, 24 years, the average annual rate would be 458 trips per year. Thus, the retrieval rate is expected to be less than the emplacement rate assumed in the baseline fault-tree analysis in Section 6.8.

Used in: The fault-tree model that is used as the baseline for the new analyses is presented in Section 6.8.3.

5.8 *Assumption*: The fault-tree model developed in *Application of Logic Diagrams and Common-Cause Failures to Design Basis Events* (CRWMS M&O 1997b) is assumed to be representative of the braking, control, and communication systems of the Transporter train that are subject to CCFs and human error (TBV-3133 and TBV-3138). The system design is exclusive of those potential design features that are postulated per Assumption 5.9.

Basis: A key characteristic of the service brake system is the fail-safe or "dead-man" actuation. The brakes are applied to the wheels by spring force. The train operator releases the brakes by putting force on a valve control lever or pedal that increases the pressure in the brake airline. Should the driver release the lever or pedal, or should an air leak occur, the reduced system pressure would allow the spring-actuated brake shoes to be applied to the wheels of the primary locomotive and the transporter. This concept of operation led to assumptions made in constructing the baseline fault tree as listed in the bullets below.

These assumptions involve the assumed design of the brake system and were derived in *Application of Logic Diagrams and Common-Cause Failures to Design Basis Events* (CRWMS M&O 1997b). These assumptions are as follows:

- The "runaway initiated" fault-tree event was modeled in a fault tree (CRWMS M&O 1997b, Section 7.2.1) to include three causes: human error, failure in the electrical drive system, and failure in the control or communications link to the main control room. A detailed design of the locomotive control panels is not available, so reference was made to control design concepts having primary control by on-board drivers, with the capability of intervention and override by the main control room operators. The rate of initiation of this event by human error was estimated to be 5×10^{-4} per trip. Assuming 456 trips per year gives a frequency of 2.28×10^{-1} per year. It should be noted that if the emplacement rate is changed to 524 trips per year, the initiation frequency is increased to 2.62×10^{-1} per year) (TBV-3133).

$1.0E\text{-}3 \times .5 = 5E\text{-}4$

- The "failure to slow or stop..." event was developed in a fault tree (CRWMS M&O 1997b, Section 7.2.2) through an OR gate to the two events "human operators fail to slow or stop train" or "hardware failure prevents ability to stop or slow." The "fail-safe" feature was assumed to be defeated by operator actions. The probability that humans fail to respond to the initiation of a runaway took credit for both on-board drivers and control-room operators via an

AND gate with a net probability of 2.5×10^{-3} per demand (or execution of the event) (TBV-3133).

- The sub-tree for the hardware failure contributions, event HARDWR in *Application of Logic Diagrams and Common-Cause Failures to Design Basis Events*, (CRWMS M&O 1997b, Section 7.2.2.3), includes failure of the control/actuation circuitry and the mechanical components of the brakes. The sub-tree included the dynamic brake system and the emergency brake system as diverse and redundant to the service brakes as means of stopping the train. In the quantification of the probabilities, however, no credit was taken for either of the alternative brake systems. It was noted that dynamic brakes are not intended for stopping in an emergency and the emergency brake design concept was not clearly defined. The probability of hardware contribution was estimated to be 8.09×10^{-5} per year; the value of NOSTOPHW.CAF in *Application of Logic Diagrams and Common-Cause Failures to Design Basis Events* (CRWMS M&O 1997b, Att. V) (TBV-3133).

- Potential CCFs of the brakes of all three vehicles were modeled in the fault tree; see event CCFALL in *Application of Logic Diagrams and Common-Cause Failures to Design Basis Events* (CRWMS M&O 1997b, Section 7.2.2.2). The analysis used the beta-factor method for quantifying the probabilities of CCFs (CRWMS M&O 1997b, Section 3.2.1, p. 12). The various CCFs may be attributed to errors in manufacturing, installation, maintenance, or testing. The beta-factor assumes that a certain fraction of documented failure rates for individual components or systems are attributed to CCFs (TBV-3133 and TBV-3138).

The hierarchy of CCFs was identified as:

- "intra-vehicle" - defined as CCFs of components or systems that are located in one locomotive, or in the transporter, such as the concurrent failure of two brake-release air cylinders, or concurrent failure of two channels of an electronic control system

- "like-vehicle" - defined as CCFs of components or systems that are located in different locomotives (e.g., concurrent failures of all brake cylinders in both locomotives)

- "all-vehicle" - defined as concurrent failures of all brake cylinders in the two locomotives and in the transporter as documented in *Application of Logic Diagrams and Common-Cause Failures to Design Basis Events* (CRWMS M&O 1997b, Section 3.2.2 p. 15). Three beta-factor values of 0.1, 0.01, and 0.001 were assumed to represent the respective intra-, like-, and all-vehicle CCFs, respectively (TBV-3133).

Used in: The assumption is used in the baseline fault-tree analysis presented in Section 6.8.2.2.2.

5.9 *Assumption:* Several representative design alternatives are assumed as potential means of reducing the frequency of potential transporter runaway events. The representative design alternatives are listed in the bullets below.

Basis: The baseline analyses presented in *Application of Logic Diagrams and Common-Cause Failures to Design Basis Events* (CRWMS M&O 1997b) indicate that design enhancements are required to drive the estimated frequency of runaway below 1.0×10^{-6} per year. This assumption will not be considered TBV since these are postulated design assumptions and, therefore, further confirmation is not required.

The design alternatives assumed in the evaluation are the following:

- Enhanced on-board systems:
  - Electronic interlock (or permissive) to ensure that dynamic brakes are engaged or that service brakes are set in a drag mode before an operator can start the train down the North Ramp. It is further assumed that the interlock system has a single electronic channel.
  - Alarm to alert operator when train speed exceeds normal operating range, or that the train is accelerating. It is further assumed that the alarm system has a single electronic channel and is independent of other electronic systems.
  - Automatic application of service brakes to control the speed of a normal descent, with human drivers and operators providing backup actuation. It is further assumed that the automatic brake application control system has a single electronic channel and is independent of other electronic systems.
  - Automatic actuation of emergency brakes by speed sensors, with human drivers and operators providing manual backup. It is further assumed that the automatic actuation system has two-channel redundancy.
  - Redundant and diverse hydraulically actuated disk brake caliper systems on locomotives (in addition to dynamic braking system) (see Section 6.1.2.1).
  - Redundant and diverse brake systems on transporter car. A hydraulic-operated disk brake system provides backup to the air-release brakes on the locomotives and transporter car. The basis for this alternative is presented in *Waste Package Transporter Design* (CRWMS M&O 1998a, Section 7.3.9) (TBV-3130).
  - A series of speed-retarder units mounted as an outboard system on the rails of the North Ramp to maintain the speed of an unbraked train at a predetermined maximum (well below the critical derailment and tip-over speed) before the train enters the North Ramp Curve or North Ramp Extension Curve. This alternative is described in Section 6.7.2.

Used in: The assumption is used in the fault-tree analysis of design alternatives presented in Section 6.8.3.

5.10 The bounding failure rate for rail-mounted hydraulic speed control units is assumed to be 0.2 per year. A more representative value of 0.29 failures per million hours is also used. It is further assumed that CCFs of such units may be calculated using a beta factor model with $\beta = 0.1$.

Basis: The bounding failure rate of 0.2 per year is based on the failure of all units at the end of a 5-year scheduled replacement period. The value of 0.29 per million hours is based on the failure rate for the hydraulic actuator, i.e., a mean value of 0.29 and a 60 percent confidence range of 0.057 to 0.88 per million hours (Arno 1981, p. 24). The beta factor of 0.1 is representative for CCFs as documented in *Application of Logic Diagrams and Common-Cause Failures to Design Basis Events* (CRWMS M&O 1997b, Section 3.2.2) (TBV-3138 and TBV-3142).

Used in: This assumption is used in Section 6.8.3.4.

5.11 *Assumption*: In the evaluation of a postulated design alternative that includes an automatic speed detection and brake actuation system on board the transporter locomotives, it is assumed that the automatic system has two-channel redundancy and is subject to both independent and CCF of the two channels. The probability of the event AUTODET ("Failure of Automatic Speed & Brake Actuation System to Apply Service Brakes") is assumed to be 1.82×10^{-7} per demand.

Basis: The probability of the event AUTODET is adopted from the probability of failure of a similar system, namely, the failure of a two-channel actuation system represented by event CONTLOC1 "Failure of Service Brake Control for Loco 1 & Transporter." The event CONTLOC1 is evaluated to be 1.82×10^{-7} per demand, which is the sum of the events under the OR gate: $1.65\times10^{-7} + 1.65\times10^{-8}$ (CRWMS M&O 1997b, Att. II, p. II-9) (TBV-3133).

Used in: This assumption is used in Section 6.8.3.1.

5.12 *Assumption*: The evaluation of a postulated design alternative includes a hydraulically actuated disk brake as a redundant and diverse backup to the air-actuated brakes. In the fault tree model, it is assumed that the probability of failure of the mechanical portions of the hydraulic system, which is denoted by event HARDHYD ("Failure of Hydraulic Disk Brake on Transporter"), is similar to the probability of failure of counterpart components in the air-brake system. It is further assumed that the probability of event HARDHYD is 5.19×10^{-3}.

Basis: The failures of those components are represented by the event SBTRANSP "Failure to Apply Service Brake Transporter" (CRWMS M&O 1997b, Att. II, p. II-3). The dominant contributor to the failure of the air-brake system was shown to be the failure of the air control valve on the primary locomotive with a probability of 5.19×10^{-3}; see event BKVALV1 (CRWMS M&O 1997b, Att. III, p. III-2) (TBV-3133).

Used in: This assumption is used in Section 6.8.3.2.2

5.13 *Assumption*: The preclosure period, from beginning of repository operations to permanent closure, is assumed to be 100 years (TBV-690).

Basis: This assumption is based on the performance requirement for retrieval, recovery, and restoration in Criteria 4.2.7, 4.2.8, 4.2.9, and 4.2.10. A preclosure operational period of 100 years is considered conservative since the MGR waste handling and emplacement activities are expected to span less than 40 years and the system shall have an operation life of 160 years. The criteria require that the repository maintain the option to retrieve waste for up to 300 years, which means that subsurface events (e.g., rock fall, earthquake, early failure of a WP, etc.) may need to be evaluated for a 300-year preclosure period, rather than 100 years. However, a factor of three increase in the preclosure period is not expected to change the event frequency category for these events (e.g., from a "Beyond Design Basis Event" to a Category 2 event) (Dyer 1999). The present analysis is concerned with the time duration when emplacement is occurring, which is expected to be less than 40 years, regardless of the time-period that the repository remains open for retrievability purposes.

Used In: This assumption is used throughout Section 6.8.

5.14 *Assumption:* The runaway scenarios and probability analysis will only investigate the North Ramp, North Ramp Curve, North Ramp Extension, and the northern portion of the East Main North Extension (see Figure 5).

Basis: During emplacement operations, the waste emplacement/retrieval system operates on the surface between the waste handling building (WHB) and the North Portal, and in the subsurface in the North Ramp, access mains, and emplacement drifts. During retrieval or abnormal conditions, the operations area may also extend to a surface retrieval storage site and South Portal on the surface, and the South Ramp in the subsurface (CRWMS M&O 2000c, p. 6).

As seen in Figure 4, the downward grade of the South Ramp is approximately 0.5 percent steeper than the North Ramp. However, the overall length of the South Ramp is appreciably shorter, 1416.8 m (Sta. 78+42.037 - Sta. 64+25.206 = 1416.831 m), as compared to the North Ramp, 2024.5 m (Sta. 21+86.960 - Sta. 01+62.500 =2024.46 m) (see Figure 4). Because of the longer distance of the North Ramp compared to the South Ramp, a runaway scenario for the North Ramp is considered a worst case scenario. Therefore, the runaway scenario for the North Ramp (Scenario 1 as discussed in Section 6.3.2.3) will be assumed indicative to both the North and South Ramp.

This assumption will not be considered TBV since direction of travel or the use of either the North or South Ramp does not significantly impact the results of this analysis and, therefore, further confirmation is not required.

5.15 *Assumption*: Rolling resistance due to ram-effect will be assumed negligible.

Basis: Ram-effect is the tendency for a train within a tunnel to push the air in front of the train and pull the air behind the train. However, the cross-sectional area of the train, 11.94 m^2 (see Section 6.3.2.1), is significantly smaller than the effective cross-sectional area, 36.17 m^2, of the 7.62-m diameter mains (CRWMS M&O 2000d, Section 4.1.7.1). Therefore, it is assumed that the air will pass around the WP transporter and not increase rolling resistance due to an increase in aerodynamic drag. This assumption will not be considered TBV since an increase in rolling resistance due to ram effect provides a lower bounding limit on rolling resistance and, therefore, further confirmation is not required.

Used In: This assumption is used in Section 6.3.2.

5.16 *Assumption*: WP Transporter weight is assumed to be 400 MT (441 tons).

Basis: Section 4.1.4 states that the WP Transporter weight is 387.4 MT. An upper bounding limit of 400 MT will be used throughout this analysis, except for Section 6.4.3, where the tip-over calculations use the weight and center of gravity parameters presented in Section 4.1.4. This assumption will not be considered TBV since slight variations in WP Transporter weight will be within the bounded weight and do not significantly impact the results of this analysis. Therefore, further confirmation is not required.

Used In: This assumption is used throughout.

INTENTIONALLY LEFT BLANK

6. ANALYSIS/MODEL

6.1 DESCRIPTION OF SUBSURFACE RAIL EQUIPMENT

Section 6.1 describes the functions of the subsurface rail equipment directly involved with the emplacement or retrieval of WPs. This equipment includes the WP Transporter (or transporter) as described in Section 6.1.1 and the transport locomotive as described in Section 6.1.2. The brake systems for the transporter and locomotive are described in detail within their respective sections. The subsurface rail system, also known as the Subsurface Emplacement Transportation System, includes all rail and rail-related equipment used for emplacement and retrieval operations, as described in Section 6.2.

6.1.1 Waste Package Transporter

The primary function of the WP Transporter is to safely transport WPs to and from the WHB and the emplacement drift transfer docks for both emplacement and retrieval operations. The transporter is a radiation-shielded railcar with the outline dimensions and pertinent features depicted in Figure 1 through Figure 3. The WPs are loaded on pallets within the WHB. A single WP pallet assembly is placed onto the extended bedplate—a thick steel plate that transfers the load of the WP pallet assembly to the deck of the transporter. Attached to the underside of the bedplate are rollers that allow smooth movement of the WP pallet assembly and the bedplate between the transfer deck and the shielded portion of the transporter. The bedplate is then retracted by a rigid chain mechanism into the shielded portion of the transporter. The transporter design contains the necessary flexibility to transport WPs of varying sizes and weights up to and including a WP that is 2.11-m in diameter, 5.96-m long (4.1.3), and weighs 85 MT (Assumptions 5.4).

Major components of the WP Transporter include radiological shielding, undercarriage (frame) including the transfer deck, couplers and connectors, brake systems, doors and door operators, bed plate and guides, rigid chain mechanisms, wiring, interlocks, and instrumentation and control systems.

6.1.1.1 Transporter Brake System

The transporter brake system is composed of primary (or service) and redundant brake systems that operate in conjunction with the transport locomotive (see Section 6.1.2.1). The primary brake system is envisioned to be similar to the brake systems used in the railroad and/or mining industry (CRWMS M&O 1998a, Section 7.3.9).

On commercial railcar air brake systems that are Federal Railroad Administration (FRA) certified for interchange service, compressed air is used to power one or more pneumatic cylinders that are mounted on the underside of the car body or within the railcar trucks. Railcars approved for interchange service are capable of traveling from one privately owned railroad to another, such as Norfolk and Southern to Union Pacific. These railcars conform to AAR Standard S-401-99 (Section 4.3.1), where each railcar has one or more brake cylinder pistons, a reservoir (air storage tank), associated air piping, and a control valve. Through a series of rods, levers, or other mechanical linkages, the brake cylinder force is transmitted to the brake shoes, which are then pressed against the tread of each wheel. The application of a brake shoe against

the wheel tread is called tread braking. Compressed air is supplied by an air compressor located on the locomotive and stored in the main reservoir of the railcar (Kratville 1997, Section 8; and NTSB 1998, p. 7 and Appendix C).

The control valve responds to signals sent by the locomotive operator. These signals are in the form of changes in air pressure within the main air line, or trainline. The trainline is the physical air connection from the locomotive to each railcar air brake system. Air is passed through the trainline by metal pipes within the railcar and through connecting flexible air hoses between rail cars (NTSB 1998, p. 7 and Appendix C).

When the air pressure within the trainline (also known as brake pipe pressure) is reduced, the control valve mechanically senses the pressure drop and delivers compressed air from the railcar reservoir to the brake cylinder(s). The amount of air sent to the brakes is proportional to the drop in brake pipe pressure (Kratville 1997, pp. 839-855 and NTSB 1998, p. 7 and Appendix C).

It is important to clarify the definition and use of emergency braking on commercial railcar air brake systems. Emergency braking is actuated by a rapid decrease in brake pipe pressure. The control valve senses the rapid drop in pressure and applies air at full pressure from the reservoir to the brake cylinders thereby creating maximum braking force (Air Brake Association 1998, p. 101).

To provide safe control, even when grades are steep, the WP Transporter will use two types of braking systems: Tread and Disk. The locomotive will use four types of braking systems: Tread, Disk, Parking, and Dynamic (see Section 6.1.2.1).

The WP Transporter primary brake system, as described in *Waste Package Transporter Design* (CRWMS M&O 1998a, Section 7.3.9), will be an automatic (fail-safe) tread-brake system that is activated by a decrease in air pressure. Unlike the standard-commercial AAR brake systems described above, a spring acting/air return cylinder provides the stopping force. Powerful and appropriately sized compression springs within the brake cylinder apply the required brake shoe force against the wheel, rather than using air pressure from a reservoir. With this system, compressed air is used to collapse the springs, thereby releasing the brake shoe from the transporter wheels. As air pressure is decreased, brake shoe force is proportionally applied by the springs. This eliminates the need for the WP Transporter to have a compressed air reservoir to apply brake pressure as compressed air is supplied by the locomotive compressor and reservoir. Typical air pressures stored in the locomotive air brake system reservoir are approximately 6.2 bar (90 psi) (CRWMS M&O 1998a, Section 7.3.9).

The secondary, or redundant, brake system for the transporter is envisioned to be a hydraulically applied disk brake system (see Assumption 5.9) (CRWMS M&O 1998a, Section 7.3.9). This braking system comprises a disk and a caliper mounted on each axle of the transporter trucks (see Figure 6). The calipers are hydraulically applied and spring released, which is not a fail-safe configuration. Pressure is applied to the brake calipers through a hydraulic connection to the locomotive hydraulic system (CRWMS M&O 1998a, Section 7.3.9).

Providing that slippage does not occur between the wheel and the rail, the WP Transporter primary braking (tread-braking) effectiveness is a function of wheel speed, brake shoe force, and the coefficient of friction between the brake shoe and the wheel tread. The friction between the

brake shoe and the wheel tread creates heat proportional to the shoe force and the wheel speed. The wheel, and partially the brake shoe, act as heat sinks and dissipate the heat generated. However, the temperature is at its greatest at the sliding surface of the brake shoe and the wheel. At some point during braking, sufficient heat may build in the shoe material and wheel to change both the wheel and the brake shoe surface characteristics. This molecular-level change in surface characteristics degrades the coefficient of friction and reduces the braking ability (NTSB 1998, p. 7).

The reduced braking ability from heat build-up is known as "heat fade" and is typically insignificant at low speeds. At low speeds, temperature will increase until the heat buildup is dissipated by the wheels and brake shoes at a rate equal to the amount generated, known as thermal equilibrium. Thermal equilibrium results in a constant coefficient of friction and braking ability. However, heat fade becomes significant as speeds and brake forces increase. There is a point where the heat generated surpasses the heat dissipated through wheels and brake shoes. At severely elevated temperatures, the brake shoe and/or wheel materials may deteriorate. In extreme conditions, enough heat may be generated to cause melting in both the brake shoe and the wheel.

With this in mind, tread braking is most effective soon after initial application of the brakes. Braking actually improves as the brake shoe and wheel tread surfaces warm up, but degrades as temperature drastically rises and heat fade becomes significant (NTSB 1998, p. 7).

6.1.2 Transport Locomotive

The primary function of the locomotive is to move the WP transporter containing the loaded WP pallet assembly from the WHB to the emplacement drift. The electric-powered locomotives will also be used to move the empty transporter and other rail equipment to and from the WHB or other surface facilities and the subsurface repository. Two transport locomotives will be used to move the WP Transporter through the North Ramp and the mains, one fore and one aft of the transporter (CRWMS M&O 2000c, p. 6).

The locomotives are supplied with electrical power through an overhead catenary (trolley wire)/pantograph system. The catenary system is a series of wires mounted to the crown of the drifts that carry a high-voltage direct current (DC). The rails act as the ground to complete the electrical circuit. The pantograph is positioned atop a tower, which is mounted above the rear truck of the each locomotive (see Figure 7). This pantograph configuration minimizes the horizontal travel of the pantograph on the overhead catenary wires when the locomotive travels through curves. As they are the primary source of power for the locomotives, the overhead catenary wires will be installed in all drift locations that are envisioned for locomotive travel (CRWMS M&O 1998b, Section 7.3.3.3).

6.1.2.1 Locomotive Brake System

The locomotive braking system consists of four brake systems: tread, disk, parking, and dynamic brakes. The tread (also known as service brakes) and disk brakes each would be capable of stopping the train independently, while the parking brakes hold the train in position once stopped. The dynamic braking systems would be used to assist in controlling the train speed as it descends the North Ramp and North Ramp Extension, but would not be used for a complete stop.

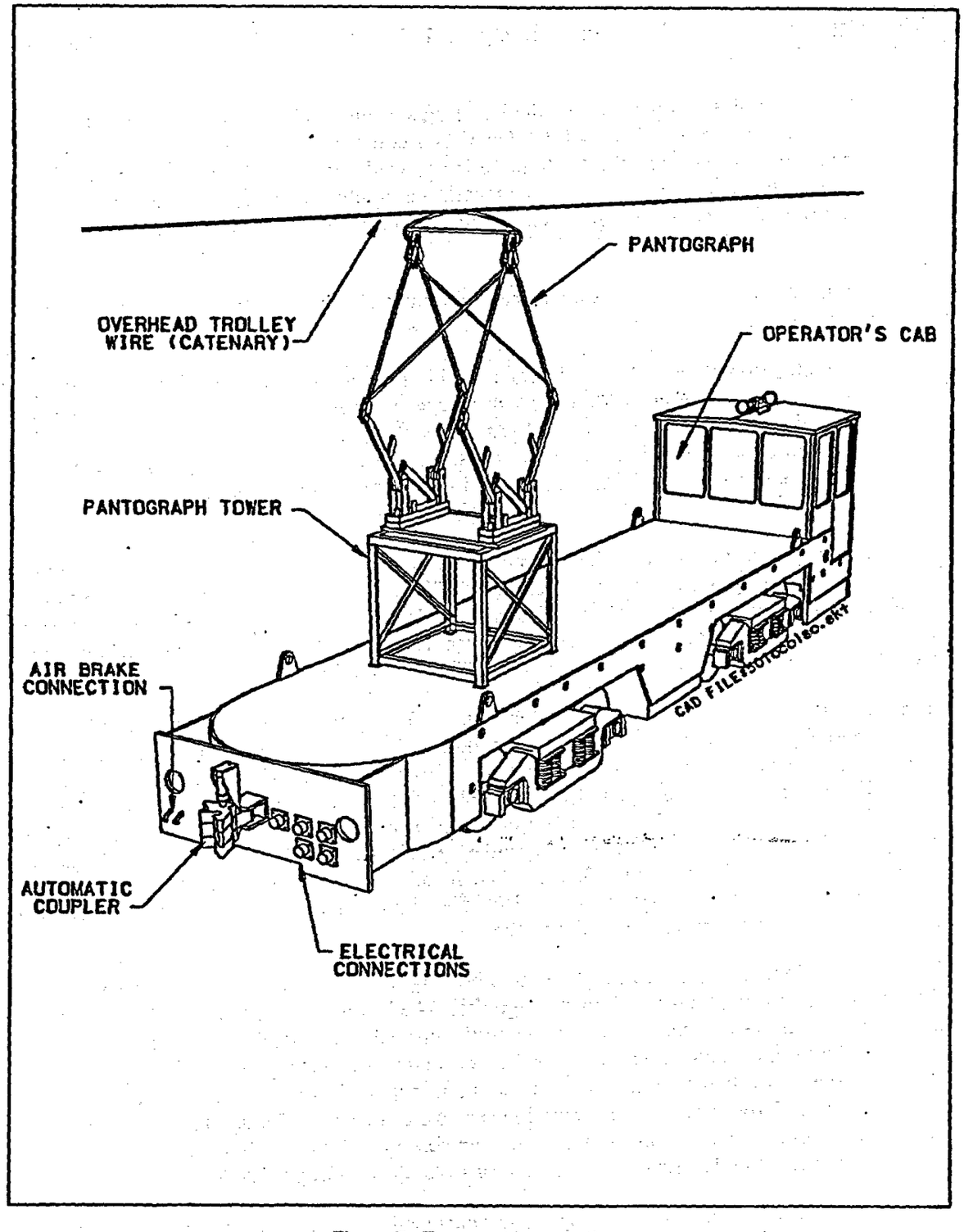

Figure 7. Transport Locomotive

The Department of Labor Mine Safety and Heath Administration regulation states (30 CFR 75.1404-1):

> "A locomotive equipped with a dual braking system will be deemed to satisfy the requirements of 30 CFR 75.1404 for a train comprised of such locomotive and haulage cars, provided the locomotive is operated within the limits of its design capabilities and at speeds consistent with the condition of the haulage road. A trailing locomotive or equivalent devices should be used on trains that are operated on ascending grades."

In addition, the Department of Labor Mine Safety and Heath Administration regulation states (30 CFR 75.1404):

> "Each locomotive and haulage car used in an underground coal mine shall be equipped with automatic brakes, where space permits. Where space does not permit automatic brakes, locomotives and haulage cars shall be subject to speed reduction gear, or other similar devices approved by the Secretary, which are designed to stop the locomotives and haulage cars with the proper margin of safety."

Like the transporter tread brakes, the locomotive tread brakes are automatic (fail-safe) air brakes that are activated by a decrease in air pressure. The stopping force is provided by powerful compression springs that, through a series of rods, levers, and linkages, push the brake shoes against the wheels. Air pressure is used to collapse the springs, thereby releasing the brake shoes from the locomotive wheels (CRWMS M&O 1998b, Section 7.3.3.7).

The disk brakes are the back-up, redundant, brake system that is installed within the transmission(s) of the locomotive. Each locomotive has two DC drive motors, one on each truck, which drives a transmission connected to the drive axle. The disk brake calipers are hydraulic-applied and spring released, which is not a fail-safe configuration. Pressure is applied to the brake calipers through a hydraulic connection to the locomotive hydraulic system and controlled by a foot-operated master cylinder (CRWMS M&O 1998a, Section 7.3.9 and CRWMS M&O 1998b, Section 7.3.3.7). The locomotive parking brake is a spring-applied manual-release disc brake. The brake consists of an independent caliper mounted to operate on the disc common to the redundant brake system.

Dynamic braking, also known as regenerative braking, employs the use of the locomotive DC drive motors to control train speed on steep grades. The locomotive wheels are allowed to back-drive, or transfer mechanical power opposite to the normal direction, the transmission and drive motors. The de-energized motor armatures (rotor) are turned, creating an electric generator. The stator, or the non-rotating portion of the motor, is supplied with a current that generates a magnetic field. Eddy currents are induced in the rotors as they pass through this field, generating electrical power and resulting in a braking torque whose magnitude is a function of the excitation voltage of the stator coils (Air Brake Association 1975, Section II, pp. 19-22).

The power generated in dynamic braking is consumed in air-cooled resistor banks as heat. Extended-range dynamic braking may be included on the locomotive, allowing it to be used at

speeds as low as 4.8 km/hr (3 mph). Dynamic braking is ideal for holding speed constant while the locomotive descends the North Ramp and North Ramp Extension with the loaded transporter, but is not used to stop the train. The primary brake system should be used when attempting to slow down to a stop (CRWMS M&O 1998b, Section 7.3.3.7.4).

6.1.3 Sequence of Operations

As outlined in *Waste Emplacement/Retrieval System Description Document* (CRWMS M&O 2000c, p. 6) and *Waste Package Transport and Transfer Alternatives* (CRWMS M&O 2000b, Section 6.1.1), the process of WP emplacement follows a predefined sequence. Within the WHB, the WP is loaded in a horizontal position onto a WP pallet, which is designed to support the WP during transport and during the long-term emplacement. The WP pallet assembly is then loaded onto the transporter bedplate. The WP Transporter loading/unloading mechanism (rigid chain) draws the WP pallet assembly and bedplate into the shielded portion of the transporter and the transporter doors are closed. A single remotely controlled transport locomotive hauls the WP Transporter out of the WHB, where operators board the locomotive for manual operation. A second transport locomotive is attached to the opposite end of the WP Transporter from the original locomotive.

This dual-locomotive configuration ensures that there will be a locomotive at either end of the WP Transporter at all times during the North Ramp and North Ramp Extension descent. The second locomotive provides additional/redundant power and braking capacity, thereby providing a more reliable configuration.

The two locomotives move the transporter from the WHB, down the North Ramp or North Ramp Extension, and into either the East or West Main to the vicinity of the pre-designated emplacement drift. Near the emplacement drift entrance, one locomotive is uncoupled and parked nearby. This allows the unobstructed WP Transporter to be pushed into the emplacement drift turnout. The locomotive operators leave the locomotive(s). An operator located on the surface performs the remaining emplacement functions via remote control.

The transporter is moved partway into the emplacement drift turnout, and the transporter doors and the drift isolation doors are opened remotely. As shown in Figure 8, the emplacement drift transfer dock is designed so that the emplacement gantry rails straddle the WP Transporter as the transporter is pushed into the dock. This design feature allows the spring suspension within the transport trucks to decompress as the WP load is removed from the transporter deck. This design eliminates any requirements to maintain a constant height between the WP Transporter transfer deck and the emplacement drift transfer dock.

Once the transporter is docked, the transporter loading/unloading mechanism pushes the WP pallet assembly, which is being supported by the bedplate, out of the shielded portion of the transporter and onto the transfer deck. By straddling the WP Transporter, the emplacement gantry moves into position over the WP Pallet assembly with the gantry lifting lugs in the lowered position, engages the pallet lifting points, and raises the WP pallet assembly off the bedplate. The gantry carries the WP pallet assembly into the emplacement drift and stops at a pre-determined emplacement position. The WP pallet assembly is then lowered onto the emplacement drift transverse beams or other support system. The gantry disengages from the pallet and moves back to a waiting position at the emplacement drift transfer dock.

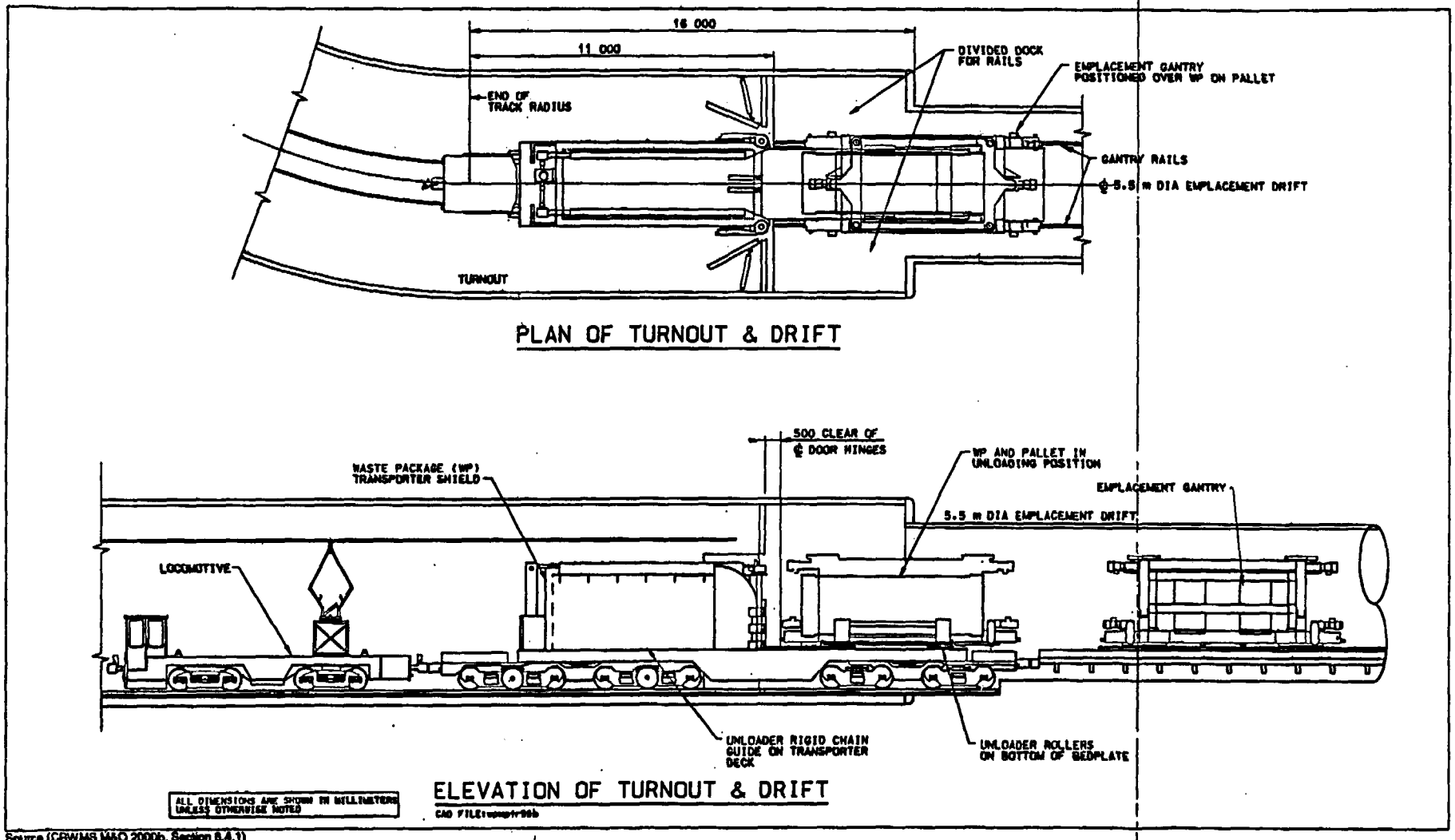

Source (CRWMS M&O 2000b, Section 6.4.1)

Figure 8. WP Transporter Interface at Emplacement Drift

INTENTIONALLY LEFT BLANK

The remote operator retracts the bedplate into the transporter. The transporter is partly pulled away from the drift entrance doors by the locomotive. The transporter and drift isolation doors are then closed. The transporter is pulled completely out of the emplacement drift turnout where the operators re-board and the second locomotive is re-coupled to the back of the transporter. The empty train is manually driven back to the WHB for another transport and emplacement operation (CRWMS M&O 2000b, Section 6.2.4; CRWMS M&O 2000c, p. 6; DOE 1998, Volume 2, Section 4.2.3.3).

6.2 DESCRIPTION OF SUBSURFACE RAIL SYSTEM

The subsurface rail system, also known as Subsurface Emplacement Transportation System, provides vehicle guidance from the WHB to the emplacement drifts by use of standard 115-lb AREA (American Railway Engineering Association) steel rail (DOE 1998, Volume 2, p. 4-60). As a Viability Assessment design, this rail size is valid for the SR Design. The system supports waste emplacement, waste retrieval, performance confirmation, closure, and maintenance operations. The rail system will also provide the electrical ground for DC overhead (catenary) power system in the main tunnels.

The existing ESF loop, encompassing the North Ramp, East Main Drift, and South Ramp, is located such that it may become an integral part of the potential repository. The ESF loop will be incorporated in the potential repository facility and used for repository access if determined appropriate. The gradients of the North Ramp –2.1486 percent, South Ramp –2.619 percent, Main Drift +1.3500 percent, and the large diameter of the ramps and mains makes them suitable for repository use (see Figure 4). The ESF drifts were excavated by a 7.62-m diameter TBM. Points along the ESF loop are called-out using Station numbers. The Station numbers represent the distance in meters along the ESF loop starting at the North Portal entrance (Sta. 00+00).

A deviation in line and grade occurred in the ESF as a result of a problem with TBM guidance. This occurred in the North Ramp between Station 00+60 and Station 01+08. The TBM trajectory was corrected to the –2.14862 percent grade at approximately Station 01+62.500 (see Figure 4). This deviation over the length of the North Ramp (2186.960 m) will not be assumed to be negligible. Therefore, slope calculations for the North Ramp will use –2.1486 percent grade from Station 01+62.50 to the start of the North Ramp Curve (Point B, Sta. 21+86.960) (Assumption 5.1).

The mains connect with the ramps and provide access throughout the potential repository at the emplacement level. The mains include the East Main, the East Main North Extension, the North Main, the West Main, and the Exhaust Main. The ramps and mains provide routes for travel within the subsurface area. The North Ramp Extension serves two purposes: (1) facilitates emplacement operation in the East Main North Extension during concurrent emplacement and development operations, and (2) as a by-pass route to the West Main to avoid interference with operations in the East Main or East Main North Extension. The North Ramp, East Main, and South Ramp are referred to as the ESF Loop when addressed collectively, and the ESF loop has been constructed. The South Ramp Extension, West Main, North Main, and East Main North Extension are referred to as the Perimeter Construction Loop when addressed collectively, and will be constructed as part of the potential repository (CRWMS M&O 1997a, Section 7.2.1).

During the initial stages of repository operation, construction efforts and emplacement operations will overlap. During this period, the repository will be divided into separated development and emplacement sides. On the development side, the South ramp will be the route for construction personnel, materials, equipment, and the muck handling system. On the emplacement side, the North Ramp will be the route for the locomotives and WP Transporter from the surface facilities to the repository. Personnel, materials, and other miscellaneous emplacement operations equipment will also use the North Ramp for access into the repository (CRWMS M&O 1997a, Section 7.2.1.1.2).

As shown in Figure 5, performance confirmation drifts will be installed above and below the repository block as part of the T.E.P. The first performance confirmation drift originates just prior to Point B from the North Ramp and is known as the Enhanced Characterization of the Repository Block. Two T.E.P. Observation drifts originate at Point F and travel above and below the north section of the repository block.

6.3 MAXIMUM SPEED DETERMINATION

The maximum runaway speed of the WP Transporter and the locomotives within the North Ramp is determined under three primary conditions: frictionless, standard rolling resistance, and standard braking. The braking is discussed in Section 6.3.3. Determining the maximum runaway speed for a worst-case runaway scenario initiating in the North Ramp and continuing down the North Ramp Extension Curve, through the North Ramp Extension, and down the North Main Curve is considered unrealistic. As will be shown in Section 6.4.3, a runaway transporter will tip-over in the 305-m radius curves before reaching the end of the downward grade. Therefore, speed calculations are performed for four runaway scenarios (refer to Figure 5 for location call outs):

Scenario 1. A runaway within the ESF loop initiating at Point A (Sta. 01+62.500) and proceeding through the North Ramp Extension Curve to Point D. Section 6.4.3 shows that tip-over at Point D is highly probable.

Scenario 2. A runaway initiating at an arbitrary point prior to entering the North Ramp Extension Curve (Point B) so that the speed exiting the North Ramp Extension Curve is 10 percent less than the calculated tip-over speed of 31.85 m/s (71.25 mph), which is approximately 28.67 m/s (64.1 mph). The transporter and locomotives proceed down the North Ramp Extension to the estimated transporter tip-over location, as described in Section 6.4.3. This location is where, through a 305-m radius S-curve, the North Ramp Extension curves intersect the East Main North Extension (between Points G and I).

Scenario 3. A runaway with an initial velocity of 8 km/hr (2.222 m/s, 4.97 mph) initiating at the start of the North Ramp Extension Curve (Point C) and continuing to the intersection between the North Main and the Exhaust Main (Point K).

Scenario 4. A runaway within the ESF loop initiating at Point A with an initial velocity of 8 km/hr (2.222 m/s, 4.97 mph). The runaway continues to Point B (see Figure 9) and proceeds through the North Ramp Curve to Point M. Section 6.4.3 shows that tip-over between Point B and M is highly probable. Figure 9 provides the reader with a visual reference of the 305-m radius North Ramp Curve at Point B.

Figure 9. North Ramp Curve - Point B (Sta. 21+86.960)

6.3.1 Frictionless Conditions

The calculation of runaway speeds for the frictionless condition is a conservative approach and develops an upper bounding limit for runaway speed. For the frictionless condition, the transporter final speed determination is not a function of train mass, but is purely a function of slope and distance. Figure 10, which is based on the data in Table 3, presents the grade, lengths, elevation changes, and other pertinent data used in runaway Scenario 1.

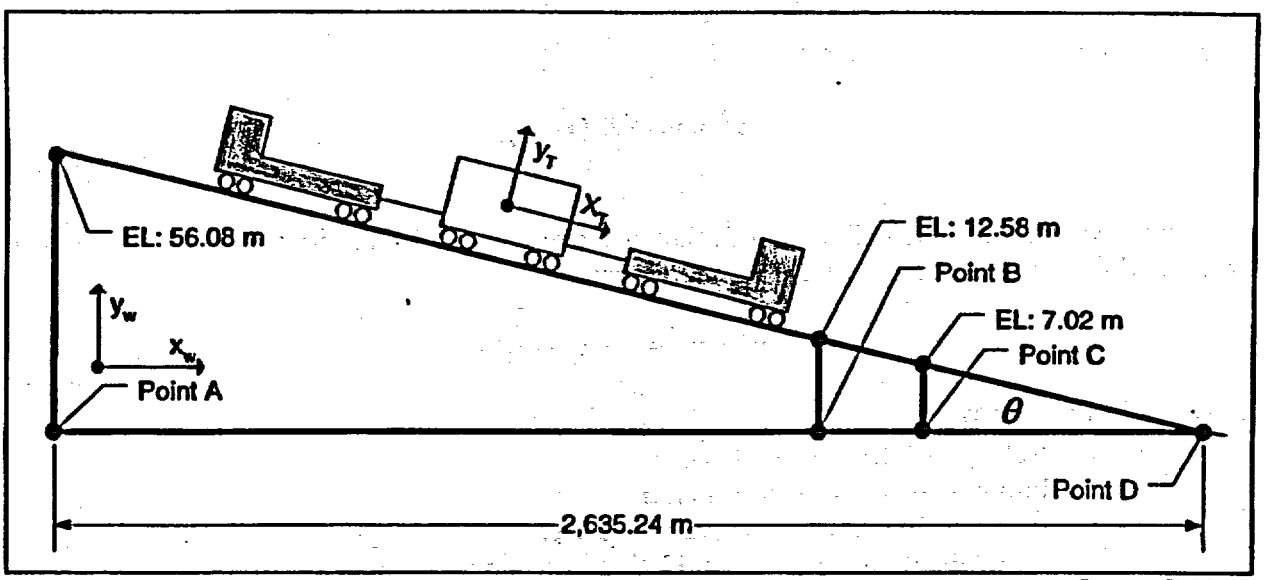

Source: Table 3

Figure 10. North Ramp Grade for Scenario 1

From the fundamental equation of motion for a body under constant acceleration (gravity), a velocity equation can be derived for the frictionless condition (Avallone and Baumeister 1987, p. 3-12):

$$x - x_0 = v_0 t + \tfrac{1}{2} a t^2 \qquad \text{(Eq. 4)}$$

where:

- x = Final position
- x_0 = Initial position
- v_0 = Initial velocity
- t = Time
- a = Acceleration (Gravity)

Differentiating Equation 4 with respect to time gives:

$$v = \frac{dx}{dt} = \frac{d}{dt}(x_0 + v_0 t + \tfrac{1}{2} a t^2) = v_0 + at \qquad \text{(Eq. 5)}$$

Substituting for the value t into Equation 5:

$$x - x_0 = \tfrac{1}{2}(v_0 + v)\left(\frac{v - v_0}{a}\right) = \frac{v^2 - v_0^2}{2a} \qquad \text{(Eq. 6)}$$

and rearranging Equation 6, gives:

$$v^2 = v_0^2 + 2a(x - x_0)$$

(Eq. 7)

Using the velocity equation (Equation 7) shown above to solve for the frictionless condition, we can rewrite the equation for the transporter case as:

$$v_T^2 = v_{To}^2 + 2a(x_T - x_{To})$$

(Eq. 8)

where (see Figure 10):

v_T = Velocity of the transporter
v_{To} = Initial velocity of the transporter
x_T = Position along x-axis relative transporter coordinate system
x_{To} = Initial Position along x-axis relative transporter coordinate system

Substituting for the change in position of the transporter (Δx_T), Equation 8 can be expressed as:

$$v_T^2 = v_{To}^2 + 2a(\Delta x_T)$$

(Eq. 9)

The total position change of the transporter can be rewritten in world coordinates:

$$v_T^2 = v_{To}^2 + 2a\sqrt{y_w^2 + x_w^2}$$

(Eq. 10)

where (see Figure 10):

x_w = Position along x-axis in the absolute world coordinate system
y_w = Position along y-axis in the absolute world coordinate system

The total acceleration (a) applied to the transporter in the relative x direction is found by taking the sinusoid of the slope (θ):

$$v_T^2 = v_{To}^2 + 2g \sin\theta\sqrt{y_w^2 + x_w^2}$$

(Eq. 11)

where (see Figure 10):

θ = Slope of incline (grade) in degrees, where

$$\theta = \tan^{-1}\left(\frac{\text{Vertical Change in Elevation}}{\text{Horizontal Change in Distance}}\right)$$

a = Acceleration due to gravity (g = 9.80665 m/s^2)

Rearranging Equation 11 provides the velocity equation for the frictionless condition:

$$v_T = \left[v_{To}^2 + 2g \sin\theta \sqrt{y_w^2 + x_w^2} \right]^{\frac{1}{2}}$$

(Eq. 12)

For Scenario 1, the maximum speed calculated under frictionless conditions occurs at the end of the North Ramp Extension Curve (Point D), as seen in Figure 5, and any decelerations from the curve are ignored. If the train is stopped at Point A (Sta. 01+62.500), the maximum frictionless velocity up to Point B (Sta. 21+86.960) can be found using Equation 12 as:

$$v_T = \left[(0\ \text{m/s})^2 + 2(9.80665\ \text{m/s}^2) \sin\left(\tan^{-1} \frac{43.50\ \text{m}}{2.02493\times10^3\ \text{m}} \right) \sqrt{(43.50\ \text{m})^2 + (2.02493\times10^3\ \text{m})^2} \right]^{\frac{1}{2}}$$

$$v_T = 29.21\ \text{m/s}\ (65.33\ \text{mph})$$

(Eq. 13)

Because of the slope change from –2.14862 to –2.06 percent at Point B, Equation 12 must be calculated for the distance between Point B and Point D. From Table 3, the elevation change and plan distance is 610.779 m and 12.58 m, respectively. The initial velocity used in Equation 14 is calculated in Equation 13 above.

$$v_T = \left[(29.21\ \text{m/s})^2 + 2(9.80665\ \text{m/s}^2) \sin\left(\tan^{-1} \frac{12.58\ \text{m}}{610.779\ \text{m}} \right) \sqrt{(12.58\ \text{m})^2 + (610.779\ \text{m})^2} \right]^{\frac{1}{2}}$$

$$v_T = 33.17\ \text{m/s}\ (74.19\ \text{mph})$$

(Eq. 14)

From the same initiation point (Point A), a train traveling at a maximum normal operating speed of 8 km/hr (Criteria 4.2.3) versus a train that is stopped at Point A (0 km/hr), the frictionless velocities for Scenario 1 are very similar. The frictionless velocity at Point D for an 8 km/hr (2.222 m/s) initial speed is be found using Equation 12, as:

$$v_T = \left[(2.222\ \text{m/s})^2 + 2(9.80665\ \text{m/s}^2) \sin\left(\tan^{-1} \frac{43.50\ \text{m}}{2.02493\times10^3\ \text{m}} \right) \sqrt{(43.50\ \text{m})^2 + (2.02493\times10^3\ \text{m})^2} \right]^{\frac{1}{2}}$$

$$v_T = 29.29\ \text{m/s}\ (65.52\ \text{mph})$$

(Eq. 15)

Again, because of the slope change from –2.14862 to –2.06 percent at Point B, Equation 12 must be calculated for the distance between Point B and Point D. The initial velocity used in Equation 16 is calculated in Equation 15 above.

$$v_T = \left[(29.29\ \text{m/s})^2 + 2(9.80665\ \text{m/s}^2) \sin\left(\tan^{-1} \frac{12.58\ \text{m}}{610.779\ \text{m}} \right) \sqrt{(12.58\ \text{m})^2 + (610.779\ \text{m})^2} \right]^{\frac{1}{2}}$$

$$v_T = 33.24\ \text{m/s}\ (74.34\ \text{mph})$$

(Eq. 16)

It is important to reiterate that the final velocity of the WP Transporter is not sensitive to the initial velocity, as shown above. Initial velocities of 0 km/hr and 8 km/hr (2.222 m/s) result in similar final velocities, 33.17 m/s and 33.24 m/s, respectively.

6.3.2 Standard Rolling Resistance Conditions

During the descent of a loaded transporter down the North Ramp and the North Ramp Extension, frictionless conditions are unrealistic and only provide an upper bounding limit as a worst case scenario. Frictional losses are present in many forms. The most prevalent sources of frictional losses are due to rolling resistance, aerodynamic drag, and, to a lesser extent, curve resistance. At low speeds, rolling resistance is dominant. As speeds increase, aerodynamic drag becomes the predominate source of frictional loss. Interestingly, curve resistance is a function of the curve radius and not velocity, as described in Section 6.3.2.2. As mentioned in Assumption 5.15, any increase in rolling resistance due to ram effect is assumed negligible.

6.3.2.1 Rolling Resistance

To reduce overall transportation cost (i.e., reduce train resistance), the railroad industry has performed numerous rail efficiency studies. From these studies, empirical rail-resistance data have been collected and resistance equations have been fitted to the data to describe rolling resistance mathematically. With known conditions of speed and railcar parameters, resistance on straight track can be predicted with reasonable accuracy. The most widely accepted formula for rolling resistance was developed by W.J. Davis (Air Brake Association 1998. pp. 235-239). According to *Marks' Standard Handbook for Mechanical Engineers* (Avallone and Baumeister 1987), the following equation, based on the Davis formula, has been used extensively for calculating freight-train resistances on straight track at speeds up to 17.88 m/s (40 mph). (Avallone and Baumeister 1987, Equation 11.2.11, p. 11-42)

$$R = 1.3W + 29n + 0.045Wv + 0.0005Av^2 \qquad \text{(Eq. 17)}$$

where:

- R = Train resistance (lb/car)
- W = Weight per car (tons)
- v = Train speed (mph)
- n = Number of axles
- A = Train cross-sectional area (ft^2)

The expression $1.3W + 29n$ represents bearing resistance, $0.045Wv$ represents wheel-flange resistance, and $0.0005Av^2$ represents aerodynamic drag (Air Brake Association 1998, pp. 235-239).

As speeds exceed 17.88 m/s (40 mph), *Marks' Standard Handbook for Mechanical Engineers* (Avallone and Baumeister 1987, p. 11-42) states that actual resistance values for interchange service fall below the calculations based on the above formula. Modifications to Equation 17 have been made for these increased speeds. The two equations shown below compensate for the increased speed, known as the Tuthill (Avallone and Baumeister 1987, Equation 11.2.12, p. 11-42) and Canadian National Railway (CNR) (Avallone and Baumeister 1987, Equation 11.2.13, p. 11-42) modifications, respectively.

$$R = 1.3W + 29n + 0.045Wv + 0.045v^2 \quad \text{TUTHILL}$$

(Eq. 18)

$$R = 0.6W + 20n + 0.01Wv + 0.07v^2 \quad \text{CNR}$$

(Eq. 19)

For comparison, the three resistance equations (Equations 17, 18, and 19) applied to the WP Transporter are shown in Figure 11 for speeds up to 35.76 m/s (80 mph), a weight of 400 MT (441 tons), and a cross–sectional area of 11.941 m^2 (128.5 ft^2). The cross-sectional area is estimated using Figure 2. The area of the body is estimated by using the height from top-of-rail to the bottom of the crown and the width of the transporter, not including the door hinges, or 2.907 m × 2.940 m = 8.547 m^2. The area of the crown is determined by:

$$\frac{\pi d^2}{4} \times \frac{1}{2} = \frac{\pi (2.940\,\text{m})^2}{8} = 3.394\,\text{m}^2$$

(Eq. 20)

Adding the two areas results in a total cross-sectional area of 11.941 m^2 (128.5 ft^2) OK

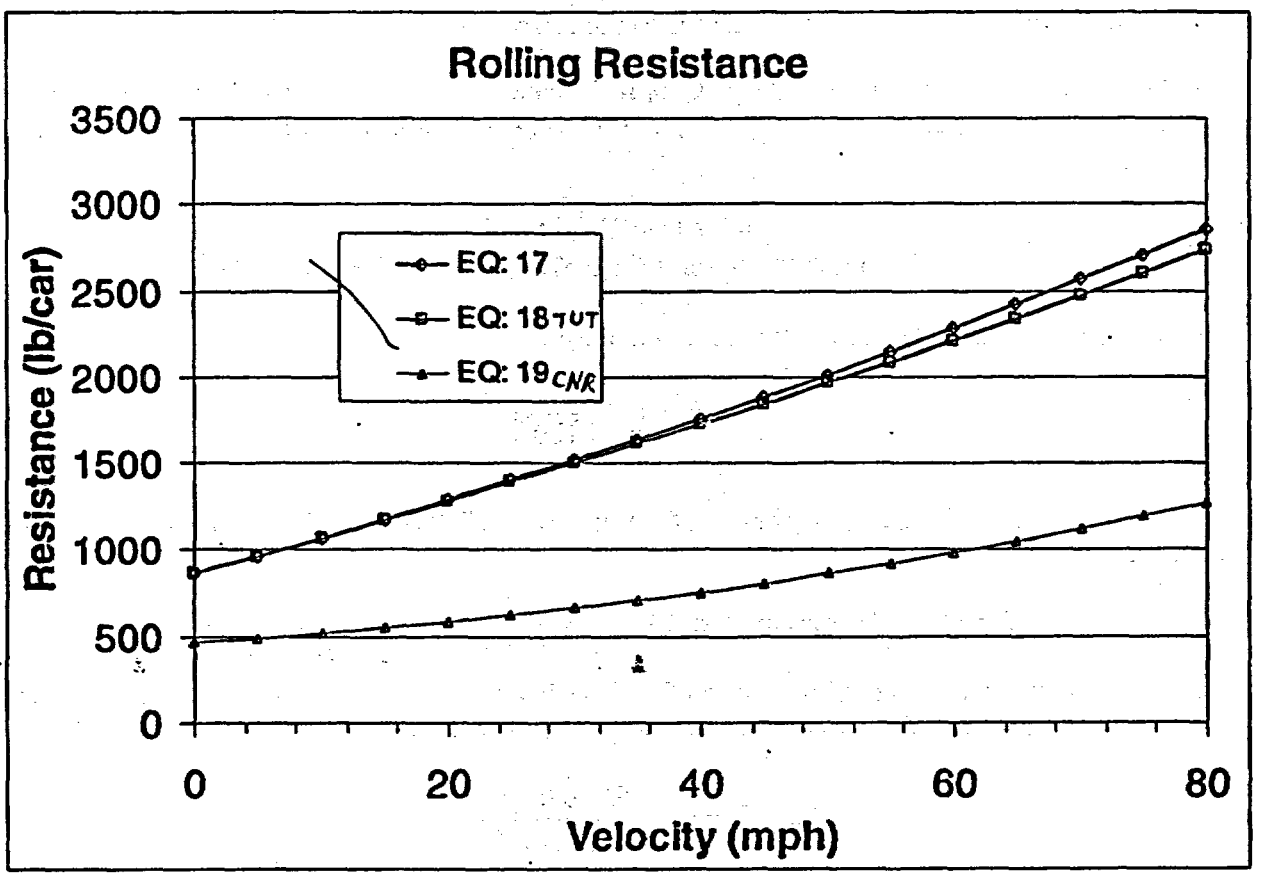

Source: Attachment III - Resistance

Figure 11. Rolling Resistance

Goodman Equipment Corporation (Goodman) developed a general "rule-of-thumb" rolling resistance value for use in sizing locomotives. Goodman suggests using 30 lbs of resistance for every ton of gross railcar weight if the rail car utilizes bronze bearings, or 20 lbs/ton for roller bearings (Goodman Equipment Corporation 1971a, p. 1). This method, however, does not account for the aerodynamic drag associated with faster train speeds. The frictional force used by Goodman is much larger in magnitude than the previous methods (Equations 17 through 19) and, therefore, results in slower calculated train velocities.

6.3.2.2 Curve Resistance

Additional rolling resistance results from curves in the rail, such as the North Ramp Curve. The wheels on standard railroad trucks are fixed to their axles, meaning both wheels must rotate at the same speed. In rounding a curve, the outer wheel must travel a slightly longer distance than the inner wheel. This is due to the inner rail having a slightly smaller radius than the outer rail. Because the outer wheel must travel a farther distance then the inner wheel, there is a tendency for one of the two wheels to skid, thereby creating additional rolling resistance in the curve. The sharper the curve, the greater this resistance becomes.

Curve resistance (R_c) and the effect of varying degrees of curvature on train resistance has been determined by tests. It has been found that one degree of curvature offers the same resistance to train movement as a 0.05 percent grade (Air Brake Association 1998, p. 239).

Grade resistance (R_g) is approximately 20 lb_f resistance for each ton of weight for each percent grade. For example, on a 1 percent grade, a 2000 lb (1 ton) railcar will have a grade resistance determined by:

$$R_g = \text{Railcar Weight} \times \sin(\theta)$$
$$= 1 \text{ ton} \times 2000 \text{ lb/ton} \times \sin(0.5729) = 19.99 \text{ lb} \approx 20 \text{ lb} \quad \text{(Eq. 21)}$$

where θ is the slope of the incline (grade) in degrees:

$$\theta = \tan^{-1}\left(\frac{1\%}{100}\right)$$

As stated above, resistance per degree of curvature is (R_c/θ_c) (Air Brake Association 1998, p. 239):

$$(R_c/\theta_c) = 0.05 \times 20 \text{ lb}_f/\text{ton} = 1 \text{ lb/ton for each degree of curvature}$$

Therefore, with each degree of curvature (θ_c), there is one pound of rolling resistance for every ton of railcar weight. A degree of curvature is defined as (Air Brake Association 1998, p. 239):

$$\theta_c = \frac{5{,}730 \text{ ft}}{\text{Curve Radius (ft)}} \quad \text{(Eq. 22)}$$

The degree of curvature (θ_c) applicable to the SR Site Layout (305 m) is:

$$\theta_c = \frac{5{,}730\,\text{ft}}{305\,\text{m} \times 3.2808\,\frac{\text{ft}}{\text{m}}} = 5.7262 \text{ degrees}$$

(Eq. 23)

Converting resistance per degree of curvature is (R_c/θ_c) to metric:

$$R_c/\theta_c = 1\frac{\text{lb}_f}{\text{ton}} \times \frac{4.448\,\frac{\text{N}}{\text{lb}_f}}{0.9071\,\frac{\text{MT}}{\text{ton}}} = 4.9033\frac{\text{N}}{\text{MT}}$$

$$= 8\frac{\text{lb}}{\text{TON}} \times \frac{4.448}{.9071} = 3.922831\frac{N}{MT}$$

(Eq. 24)

Therefore, the rolling resistance (R_c) due to the 305-m curve is:

$$R_c = \theta_c \times R_c/\theta_c = 5.7262° \times 4.9033\frac{\text{N}}{\text{MT}} = 28.078\frac{\text{N}}{\text{MT}}$$

$$= 5.7262° \times 3.9228 = 22.4629\frac{N}{MT}$$

(Eq. 25)

Goodman Equipment Corporation also developed a "rule of thumb" for rolling resistance within a curve that is used in locomotive sizing. The wheel base is found in Figure 3. The curve resistance, according to Goodman, is found using Equation 26 (Goodman Equipment Corporation 1971a, p. 1), where:

$$R_c = \frac{400 \times \text{wheelbase (ft)}}{\text{radius of curve (ft)}} = \frac{400 \times 6\,\text{ft}}{305\,\text{m} \times 3.2808\,\frac{\text{ft}}{\text{m}}} = 2.398\frac{\text{lb}_f}{\text{ton}} = 11.758\frac{\text{N}}{\text{MT}}$$

(Eq. 26)

The curve resistance using Equation 26 (Goodman) is less than that calculated using Equation 25 (Air Brake Association). The Goodman curve resistance is intended to be combined with the Goodman Equipment's rolling resistance of 20 lbs/ton. The rolling resistance Goodman suggests is much larger in magnitude and, as described in Section 6.3.2.3, is discarded as an accurate means of determining rolling resistance. Therefore, the curve resistance found in Equation 24 will be used in subsequent calculations.

6.3.2.3 Velocity Determination

The frictional force equation (Equation 17) from *Marks' Standard Handbook for Mechanical Engineers* (Avallone and Baumeister 1987, Equation 11.2.11, p. 11-42) combined with the curve resistance (Equation 24), as applicable, is herein considered as "standard rolling resistance."

The velocity determination using standard rolling resistance is derived from the physical laws of conservation of work and energy. The net work (W_{net}) must equal the change in energy, whether it is potential energy (PE) or kinetic energy (KE).

$$W_{net} = \Delta KE + \Delta PE$$

(Eq. 27)

where potential and kinetic energy are described as:

$$\Delta PE = mgh$$

(Eq. 28)

where:

m = Mass
g = Gravitational acceleration (9.80665 m/s^2)
h = Elevation change (height)

and,

$$\Delta KE = \frac{1}{2} m(v_1^2 - v_2^2)$$

(Eq. 29)

where:

m = Mass
v_1 = Initial train velocity
v_2 = Final train velocity

Substituting the formula for potential and kinetic energy (Equations 28 and 29, respectively) into Equation 27 gives:

$$W_{net} = \frac{1}{2} m(v_1^2 - v_2^2) + mgh$$

(Eq. 30)

Then, the net work (W_{net}), which is determined by the resistance force (F) over a distance (Δs), is substituted into Equation 30, which gives:

$$F\Delta s = \frac{1}{2} m(v_1^2 - v_2^2) + mgh$$

(Eq. 31)

Rearranging Equation 31 to solve for the final velocity (v_2) results in:

$$v_2 = \sqrt{\frac{-2}{m} F\Delta s + 2gh + v_1^2}$$

(Eq. 32)

Figure 12 shows the velocity for runaway Scenario 1 as a function of position for a train starting from 8 km/hr (2.222 m/s 4.97 mph) for frictionless, standard, and Goodman friction conditions. Scenario 1, as described in Section 6.3, is a runaway initiated at Point A (Sta. 01+62.500) and traveling through the North Ramp Extension Curve, and ending at Point D.

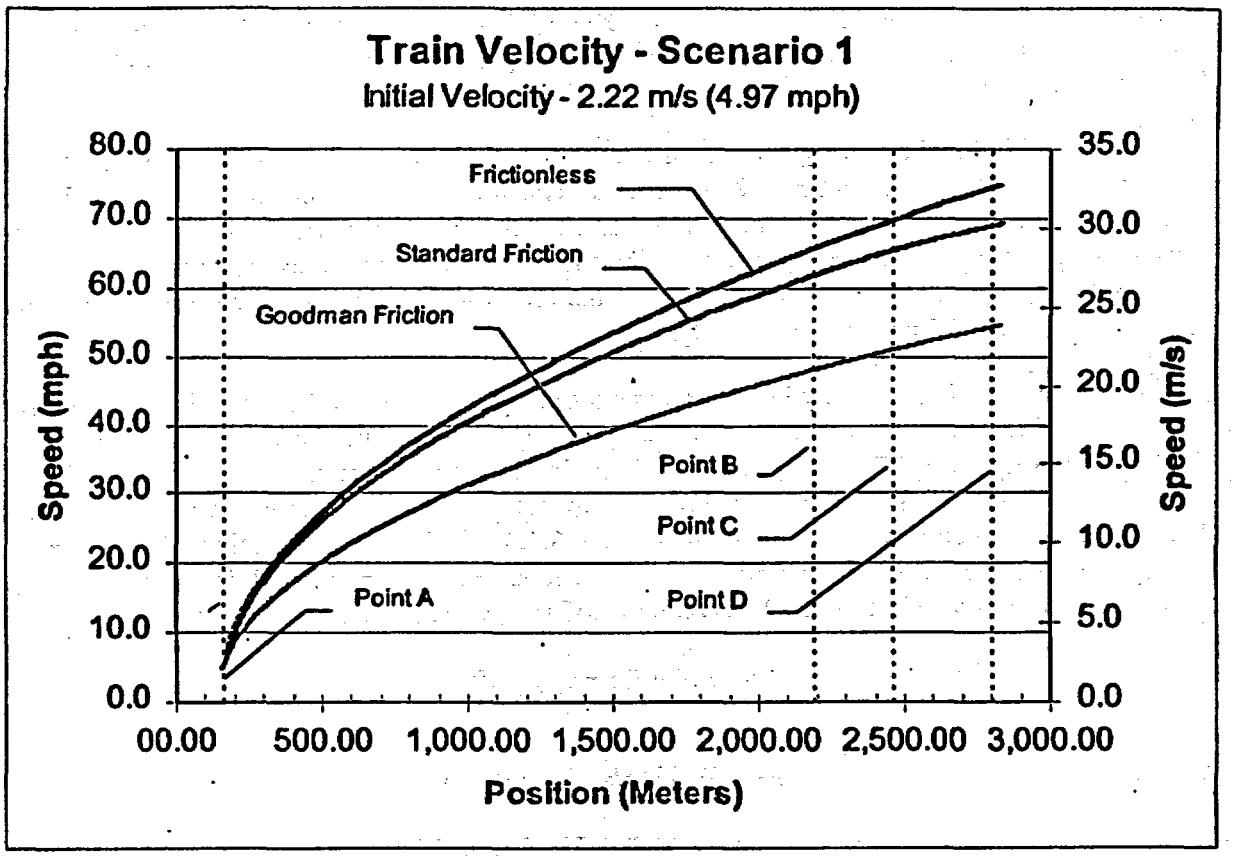

Source: Attachment III - Scenario 1

Figure 12. Velocity vs. Position for Runaway Scenario 1

Train velocities are calculated from the starting position of Station 01+62.500 (Assumption 5.1) for starting speeds of 0 m/s and 8 km/hr (2.222 m/s) under frictionless, standard rolling resistance, and Goodman's "rule-of-thumb" resistance method, and are presented in Table 5.

Table 5. Calculated Train Velocity for Scenario 1

	Standard Resistance		Goodman Resistance		Frictionless	
	Initial Speed: 0 km/hr	Initial Speed: 8 km/hr (2.22 m/s)	Initial Speed: 0 km/hr	Initial Speed: 8 km/hr (2.22 m/s)	Initial Speed: 0 km/hr	Initial Speed: 8 km/hr (2.22 m/s)
Point B	27.53 m/s (61.58 mph)	27.61 m/s (61.76 mph)	21.35 m/s (47.77 mph)	21.47 m/s (48.02 mph)	29.21 m/s (65.34 mph)	29.29 m/s (65.52 mph)
Point C	29.13 m/s (65.16 mph)	29.21 m/s (65.34 mph)	22.62 m/s (50.59 mph)	22.73 m/s (50.83 mph)	31.00 m/s (69.35 mph)	31.08 m/s (69.52 mph)

Point D	30.75 m/s (68.78 mph)	30.82 m/s (68.94 mph)	24.15 m/s (54.02 mph)	24.25 m/s (54.25 mph)	33.17 m/s (74.20 mph)	33.25 m/s (74.37 mph)

Source: Attachment III - Table III-3

As shown in Table 5, rolling resistance, aerodynamic drag, and curve resistance will reduce the overall train velocity by 6.4 percent at Point C and by 7.9 percent at Point D compared to the frictionless condition.

Although the frictional runaway speeds for Scenario 1 do not exceed the tip-over velocity found in Section 6.4.3, they are within 3.2 percent of each other. Therefore, it is assumed that the transporter will tip at Point D. Also, due to the inflated estimate for frictional force, Goodman's resistance speeds are comparably slower. Like the frictionless case, these speeds are disputable and should not be used to make an accurate estimation of train velocity. Therefore, the standard resistance values will be used in this analysis.

Scenario 2 starts with a runaway initiation at an arbitrary point within the North Ramp. Contrary to Scenario 1, this scenario assumes that the runaway will negotiate the North Ramp Extension Curve without tip-over. The exact runaway initiation location is not critical. However, the exit velocity (v_e) of the WP Transporter from the North Ramp Extension Curve is assumed to be less than the tip-over velocity determined in Section 6.4.3. If it can be anticipated that the WP Transporter does not tip-over at a velocity 10 percent less than the estimated tip-over speed (v_{TO}), then the exit velocity (v_e) at Point D would be 28.67 m/s, which is determined by:

$$v_e \text{ (Point D)} = v_{TO} \times 90\% \quad \text{(Eq. 33)}$$

where: $v_{TO} = 31.85$ m/s (Section 6.4.3)

$$v_e = 31.85 \text{ m/s} \times 90\% = 28.67 \text{ m/s (64.1 mph)} \quad \text{(Eq. 34)}$$

Using Equation 32, the velocities for Scenario 2 are shown in Table 6 and Figure 13. The velocity entering the 305-m radius S-curve at Point G is above the estimated tip-over speed. Therefore, tip-over between Points G and H is likely for this scenario.

Table 6. Calculated Train Velocity for Scenario 2

Location	Velocity
Point D	28.67 m/s (64.1 mph)
Point E	33.99 m/s (76.0 mph)
Point F	34.34 m/s (76.8 mph)
Point G	35.61 m/s (79.6 mph)

Source: Attachment III - Table III-4

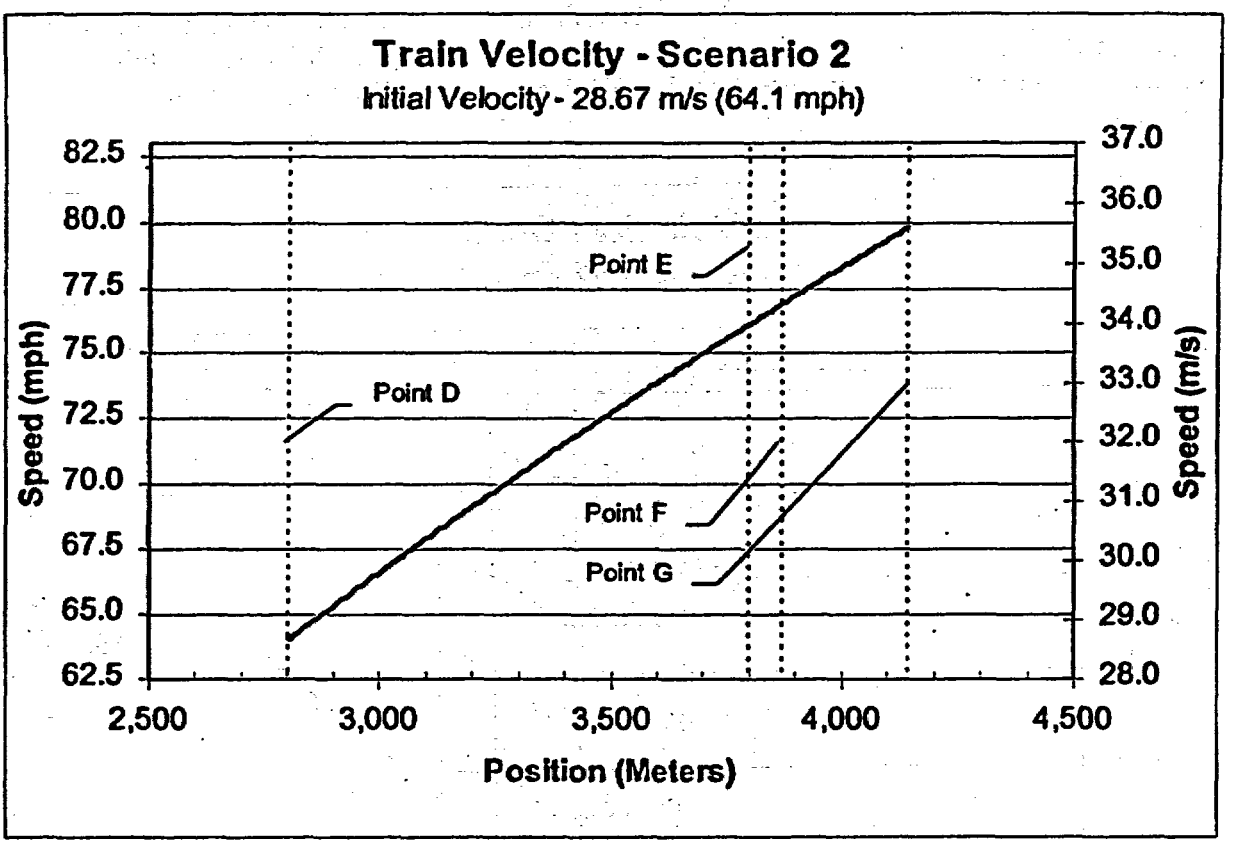

Source: Attachment III - Scenario 2

Figure 13. Velocity vs. Position for Runaway Scenario 2

Runaway Scenario 3 initiates at the top of the North Ramp Extension Curve (Point C). The runaway continues down the North Ramp Extension, through the S-curves (Points G and H) and intersection with the North Main. The runaway continues around the North Main curve to the low point at the intersection of the North Main and the Exhaust Main (Point K). The velocity of the train when the runaway starts is set at 8 km/hr (2.222 m/s, 4.97 mph). Using Equation 32, Table 7 and Figure 14 show the calculated transporter velocity at the starting point (Point C) and various other key points throughout the potential repository.

Table 7. Calculated Train Velocity for Scenario 3

Location	Velocity
Point C	2.22 m/s (4.97 mph)
Point D	10.63 m/s (23.8 mph)
Point F	22.33 m/s (50.0 mph)
Point G	24.37 m/s (54.5 mph)
Point H	24.92 m/s (55.7 mph)
Point J	26.47 m/s (59.2 mph)
Point K	28.47 m/s (63.7 mph)

Source: Attachment III -Table III-5

From Section 6.4.3, the tip-over velocity is estimated at 31.85 m/s (71.25 mph), which is approximately 11 percent greater than the maximum velocity at Point K for this runaway scenario. Therefore, it is estimated that the WP Transporter will not tip-over for this runaway scenario.

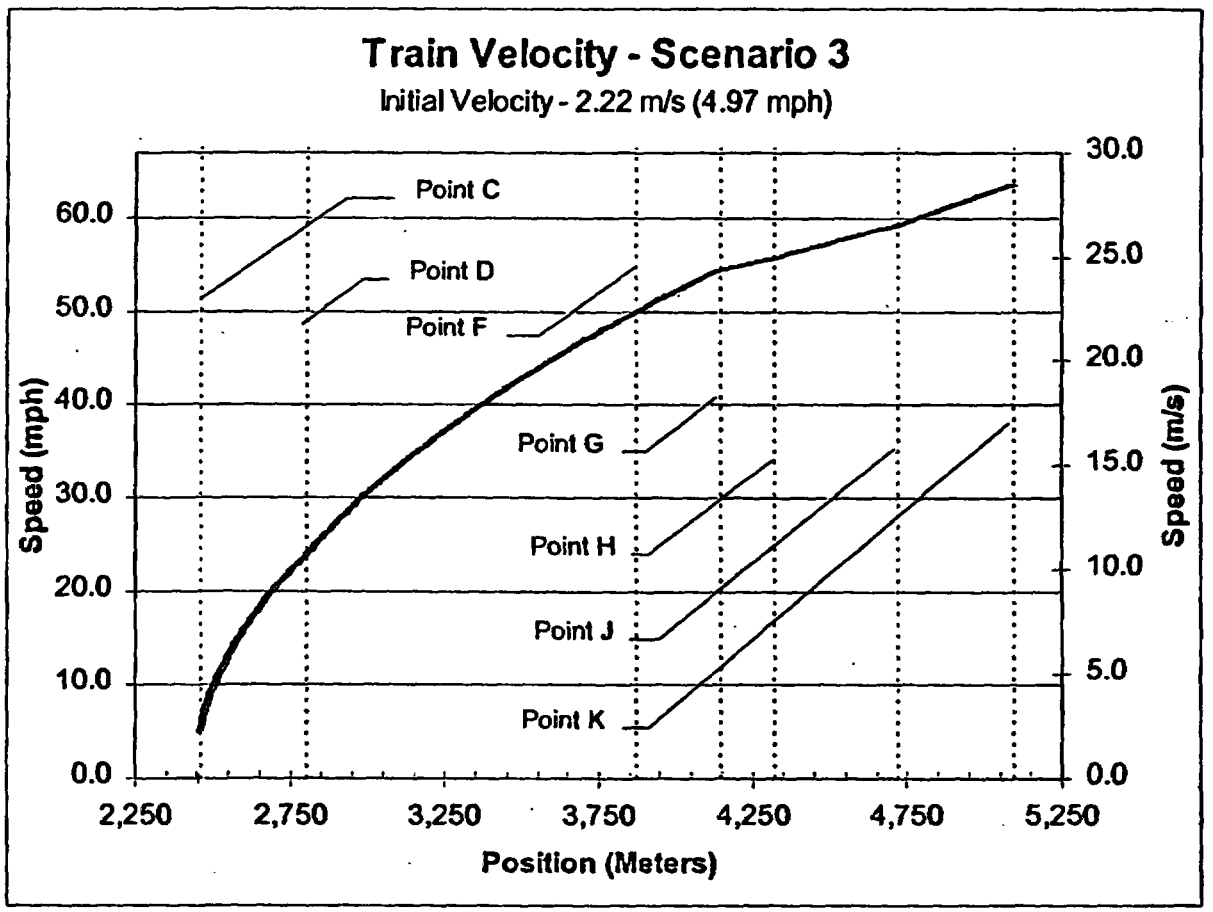

Source: Attachment III - Scenario 3

Figure 14. Velocity vs. Position for Runaway Scenario 3

Runaway Scenario 4 initiates at the top of the North Ramp (Point A) with a starting speed of 8 km/hr (2.222 m/s). The runaway continues down the North Ramp to Point B, which is the beginning of the North Ramp Curve, see Figure 9. The runaway continues around the North Ramp Curve to the intersection of the North Ramp Curve and the East Main (Point M). Using Equation 32, Table 8 and Figure 15 show the calculated transporter velocity at the starting point (Point A) and various other key points throughout the potential repository.

Table 8. Calculated Train Velocity for Scenario 4

Location	Velocity
Point A	2.22 m/s (4.97 mph)
Point B	27.61 m/s (61.8 mph)
Point M	30.67 m/s (68.6 mph)

Source: Attachment III - Table III-6

From Section 6.4.3, the tip-over velocity is estimated at 31.85 m/s (71.25 mph), which is approximately 3.7 percent greater than the maximum velocity at Point M for this runaway scenario. As stated for Scenario 2, it can be estimate that the WP Transporter will tip-over at a velocities within 10 percent of the estimated tip-over speed (v_{TO}). Therefore, the exit velocity (v_e) at Point M shows that the WP Transporter will tip-over.

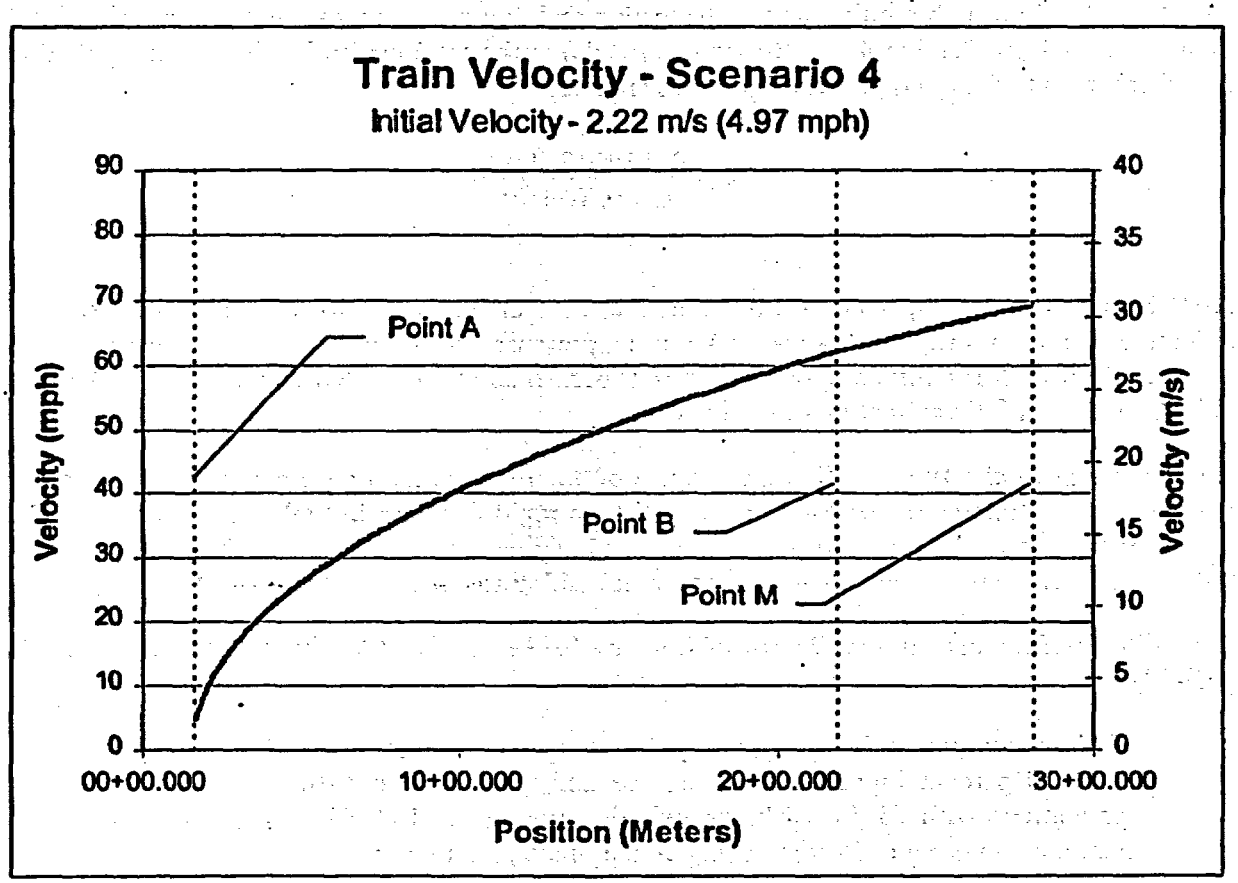

Source: Attachment III - Scenario 4

Figure 15. Velocity vs. Position for Runaway Scenario 4

6.3.3 Standard and Dynamic Braking Conditions

The desired effect of the entire brake system is to produce a retarding effect to control the WP Transporter and locomotive speeds. This speed control is especially necessary on the -2.14862 percent grade of the North Ramp. Retardation is simply the negative acceleration of

the train and is expressed in North America as miles per hour per second (mph/s). An equivalent metric unit is kilometer per hour per second (km/hr/s) or meters per second per second (m/s^2).

Calculation of the braking distance is based on many unknowns and variables that affect the overall braking efficiency and performance. Braking distance is a function of rolling, mechanical, curvature, and grade resistances, aerodynamic drag, the number of brake cylinders and their pressure and diameter, mechanical ratio of the brake levers and connections (brake rigging), brake rigging efficiency, coefficient of friction for the brake shoes/pads, and the gross weight of the loaded or unloaded railcar. Because of the complexity in determining actual braking distances, the Association of American Railroads (AAR) utilizes computer models to estimate the braking distance for a particular railcar.

For a commercial railcar brake system design to be approved for interchange service, the AAR and FRA mandate that the railcar meet all requirements of Standard S-401-99 of the AAR *Manual of Standards and Recommended Practices: Section E-Brakes and Brake Equipment* (AAR 1999). One such requirement is the testing and determination of the braking ratio (AAR Standard S-401-99, Section 4.0). Braking ratio (R_B) is the total net brake shoe force applied at the wheel tread to the rated gross weight of the railcar.

$$R_B = \frac{\text{Net Brake Force}}{\text{Gross Weight}} \qquad \text{(Eq. 35)}$$

AAR Standard S-401-99, Section 4.0, states that the net braking ratio for a 30-psi brake pipe reduction from an original 90-psi brake pipe pressure must be between 8.5 percent and 13 percent for high-friction composition brake shoes. It should be noted that a 30-psi brake pipe reduction is not a full application of the brakes.

It is important to clarify the definition and use of emergency braking on commercial railcar air brake systems. Emergency braking is actuated by a rapid decrease in brake pipe pressure. The control valve senses the rapid drop in pressure and applies air at full pressure from the reservoir to the brake cylinders thereby creating maximum braking force.

According to *Engineering and Design of Railway Brake Systems* (Air Brake Association 1975, p. II-13):

> "Freight equipment has emergency brake cylinder pressures and retardations about 20 percent higher than in service and encounters occasional emergency applications with 75-76 psi brake cylinder pressure and 60-62 percent gross or theoretical braking ratio when using 90 psi brake pipe pressure."

By using the braking ratio and the coefficient of friction for a high-friction composition brake shoe, one can determine a braking distance for the 13 percent and 60 percent braking ratios from the brake ratio equation (Equation 35).

The coefficient of friction (μ) for brake shoes/pads is required to be 0.38, the average of several static conditions tests (Section 4.3.1, AAR Specification M-926-99, Part 10.3). *Marks' Standard Handbook for Mechanical Engineers* (Avallone and Baumeister 1987, p. 11-35) provides a coefficient of friction of 0.30 as a conservative value for the dynamic coefficient of friction for high-friction composition brake shoes on steel wheels. As illustrated in *Engineering and Design of Railway Brake Systems* (Air Brake Association 1975, Figure. II-4), the coefficient of friction is a function of speed. The values for μ are approximately 0.5 near zero velocity and decay to 0.30 near 22.3 m/s (50 mph). The conservative value of 0.30 will be used as a lower bounding limit for this analysis.

Rearranging the brake ratio equation (Equation 35) and multiplying it by the coefficient of friction, one obtains the maximum and minimum brake retarding force in Newton's (N) (F_{Bmax} and F_{Bmin}) for the WP Transporter gross weight (W):

$$F_{B\max} = \mu R_B W = \mu R_B mg = 0.30 \times 0.60 \times 400\,\text{MT} \times 9.80665\ \text{m/s}^2 = 706{,}079\ \text{N} \quad \text{(Eq. 36)}$$

$$F_{B\min} = \mu R_B W = \mu R_B mg = 0.30 \times 0.130 \times 400\,\text{MT} \times 9.80665\ \text{m/s}^2 = 152{,}984\ \text{N} \quad \text{(Eq. 37)}$$

There is a concern that the brakes will "lock-up" the WP Transporter wheels. For this to happen, the maximum brake retarding force (F_{Bmax}) must be larger than the adhesion force (F_A) between the WP Transporter wheels and the rail. *Marks' Standard Handbook for Mechanical Engineers* provides a value 0.78 for the static coefficient of friction for dry, hard steel on hard steel (Avallone and Baumeister 1987, p. 3-26).

$$F_A = \mu W = \mu mg = 0.78 \times 400\,\text{MT} \times 9.80665\ \text{m/s}^2 = 3{,}059{,}675\ \text{N} \quad \text{(Eq. 38)}$$

This value for the adhesion force is significantly larger than the maximum brake retarding force. However, should the rail become greasy (spindle oil), the static coefficient of friction drops to 0.23 (Avallone and Baumeister 1987, p. 3-26).

$$F_A = \mu W = \mu mg = 0.23 \times 400\,\text{MT} \times 9.80665\ \text{m/s}^2 = 902{,}212\ \text{N} \quad \text{(Eq. 39)}$$

This value for the adhesion force for greasy rails is also greater than the maximum brake retarding force, therefore wheel "lock-up" should not occur.

It should also be clarified that these adhesion and brake retarding forces are for tread braking only. The use of the redundant disk brakes in combination with the tread brakes may cause wheel lockup. Further investigation is needed to determine the functions and conditions that each brake system (primary tread brake and redundant disk brake) will be employed.

For the determination of the distance required to stop the WP Transporter and locomotive train, only the tread brakes are used to show an upper bound on the stopping distance. The applied

brake retarding force multiplied by the distance traveled during the tread-brake application gives the total work done by the brakes. Using the conservation of work and energy equations (Equations 27 through 30), total distance traveled during braking can be determined for the entire train, i.e., the WP Transporter and both Locomotives.

To slowdown or stop a railcar, kinetic energy must be dissipated as heat. Recall from Section 6.3.2, the net work (W_{net}) must equal the change in energy, whether it is potential energy (PE) or kinetic energy (KE), or

$$W_{net} = \Delta KE + \Delta PE$$

(Eq. 27)

Substituting the formulas for kinetic and potential energy into Equation 27 gives:

$$W_{net} = \frac{1}{2} m(v_1^2 - v_2^2) + mgh$$

(Eq. 30)

where:

m = Mass
v = Train speed (Velocity)
g = Gravitational acceleration (9.80665 m/s^2)
h = Elevation change (height)

The average total of all retarding forces times the distance covered during the stop or slowdown equals the change in kinetic and potential energy. Therefore, the net work (W_{net}) is determined by multiplying the total resistance force (ΣF) over a distance (Δs). The rolling resistance and the tread brake retardation force comprise the total resistance force. To provide an upper bounding limit, any curve resistance and the retardation force from the redundant brakes are, for this analysis, ignored, i.e.,

$$\sum F \Delta s = \frac{1}{2} m(v_1^2 - v_2^2) + mgh$$

(Eq. 40)

The elevation change (h) during brake application is found by taking the sinusoid of the grade in degrees multiplied by the distance traveled. The final velocity (v_2) is assumed to be zero. The initial velocity (v_1) and the grade depend on the location where the brakes are first applied. For bounding purposes, assume a constant grade of –2.1486 percent through all stopping calculations.

$$\theta = \tan^{-1}\left(\frac{\%\text{Grade}}{100}\right) = \tan^{-1}\left(\frac{2.1486}{100}\right) = 1.2309^\circ \quad \checkmark$$

(Eq. 41)

$$h = \Delta s \times \sin(\theta)$$

(Eq. 42)

Rearranging the work equation (Equation 40) and substituting for the elevation change (Equation 42) gives:

$$\Delta s = \frac{m(v_1^2 - v_2^2)}{2[\sum F - mg\sin(1.2309)]}$$

(Eq. 43)

Using Equation 43, the stopping distance is calculated for all velocities up to 35 m/s, as shown in Figure 16.

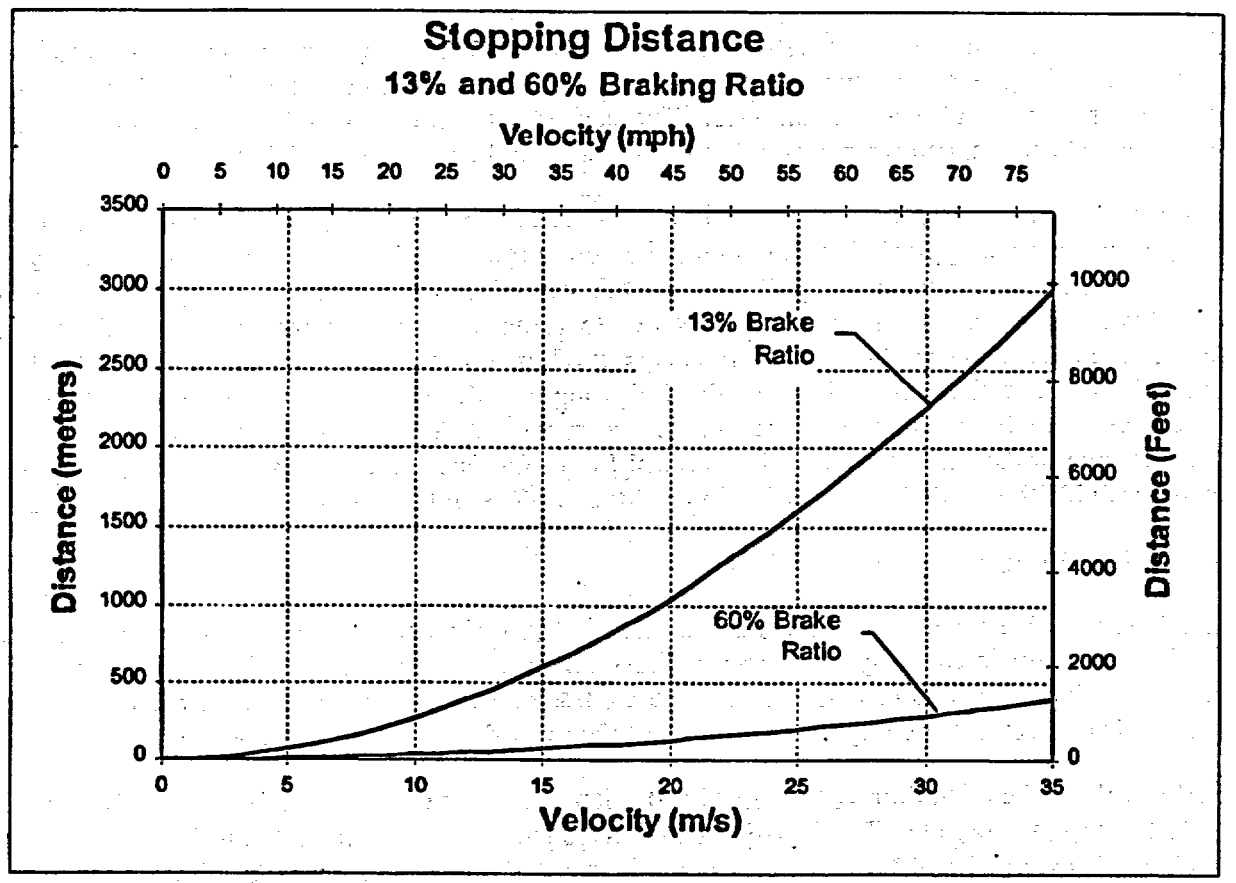

Source: Attachment III - Stopping Distance

NOTES: 1. The values represented in this figure use a –2.1486 percent grade as an upper bounding limit for stopping distances throughout the potential repository.
2. The stopping distances shown represent only tread braking by the two locomotives and the WP Transporter.

Figure 16. Stopping Distance

From an initial velocity of 8 km/hr (2.22 m/s or 4.97 mph), the WP transporter and two locomotives will take 13.5 m to stop at 30-psi brake pipe reduction (13 percent brake ratio) and

1.58 m at a full emergency brake application (60 percent brake ratio). At the estimated tip-over speed of 31.85 m/s (71.25 mph), the transporter will take 2,518 m (8,261 ft) and 321 m (1,054 ft) to stop under the 13 and 60 percent brake ratios, respectively (see Attachment III, Table III-9).

6.4 DERAILMENT AND TIP-OVER DETERMINATION

6.4.1 Description of Derailment Modes

The integrity of the rail and its related components have a significant effect on derailment. Any number of defects, wear patterns, or failures in the rail or its components (tie plates, fasteners, cross ties, ballast, and subgrade) could produce conditions favorable for a derailment. For example, Section 6.4.1.3 describes how worn railcar wheels and rails have a direct effect on the possibility for wheel-climb derailment. Other maintenance-related factors include track twist, rail shift, rail roll, track panel shift, etc.

Tie plates fixed to the cross tie restrain the rail laterally and distribute the vehicle loads onto the cross tie. Tie plates cant the rail inwards toward the gauge side for optimum locomotive, transporter, and/or rail car performance. The cant is set from 1:14 to 1:40, depending on the loads, vehicle speed, and service conditions (Avallone and Baumeister 1987, p. 11-41).

Fasteners fix the rail and tie plates to the cross ties. For the potential subsurface repository design application, typical fasteners could be screw-type or clip-type fasteners. Screw-type fasteners provide resistance to applied vertical forces while maintaining lateral support. Clip-type fasteners are used on concrete cross ties to provide a uniform resilient attachment and longitudinal restraint (Avallone and Baumeister 1987, p. 11-41). Cross ties distribute the load to the ballast under the ties and retain the rail gauge. Although ballast typically consists of limestone, granite, or slag, the SR subsurface repository design does not currently utilize conventional ballast or cross ties. The current SR Main Drift design uses concrete inverts that would provide the needed load distribution and the vertical and lateral restraint typical of ballast.

6.4.1.1 Rail Integrity and Profile

The integrity of the rails and the condition of the track (also known as track surface geometry) used in the emplacement system have a direct effect on the probability for derailment. Rail profile, track profile, and cross-level describe the track surface geometry and are each described below. The structural and physical condition of the track describes the rail integrity.

Rail profile is the elevation of the top-of-rail relative to a fixed reference line, typically top of ballast or top of subgrade. Track profile is the average elevation of the left and right rails, while track cross-level is the difference in elevation between the left and right rails. Track alignment, which is the direction or "route" of the track, and gauge, which is the distance between the two rails, are required to completely describe the track geometry. Track surface and alignment characteristics vary with distance along the track. Because of the nature of the track construction, track geometry variations can be repetitive or can be isolated, single events.

Improved rail inspections for defects have reduced the number of rail-integrity derailments in the commercial arena. In 1991-1992, derailments involving hazardous material spills caused by rail failure prompted the FRA to conduct an in-depth audit of existing rail inspection programs and

practices (DOT 1998, p. 21). Typical rail integrity failures are caused by the growth of internal defects within the rail, buildup of residual stresses, and crack initiation and growth. Internal defects are inclusions or imperfections within the rail typically caused by improper cooling or heat treating at manufacture. With repetitive loading, these small inclusions or imperfections can cause the initiation and propagation of cracks that result in the eventual failure of the rail.

A single large-amplitude track profile perturbation has less effect on derailment than a low amplitude repeated perturbation. Such repeated perturbations are associated with staggered rail, where sections of rail that are joined together in a staggered pattern along the length of the railroad rather than rail joints side-by-side. Half-staggered rail is assembled so that the sections of rail are joined opposite to the midpoint of the alternate section of rail. Although half staggered rail has better overall performance than non-staggered rail, half-staggered rail is known to initiate harmonics within the railcar suspension or structural frame. These harmonics may cause the railcar to roll, twist, or sway about its longitudinal axis, or cause the trucks to oscillate left and right along the railroad centerline, which is called hunting. These oscillatory conditions can result in the derailment of the railcar at relatively low speeds.

The FRA studied railcar harmonics and focused on the harmonic roll associated with railcars having a high center of gravity operating on half-staggered bolt-jointed rail of 11.9 m (39 ft) lengths. This scenario is characterized by a low speed 4.5-8.9 m/s (10-20 mph) derailment of a car having a truck-center spacing of less than 13.7 m (45 ft) (DOT 1998, p. 38). The construction method of the subsurface emplacement rail system, whether continuous-welded, bolt-jointed, or half-staggered bolt-jointed, has yet to be determined. Therefore, it is recommended that the transporter, with its short truck-center spacing (11.778 m or 38.6 ft) and relatively high center of gravity (2.123 m or 7.0 ft) (see Figure 2 and Figure 3), avoid operations in this 4.5-8.9 m/s (10-20 mph) regime on half-staggered rail.

6.4.1.2 Track Stability

The stability of the rail track has a direct effect on derailment. Rail shift, rail roll, and track panel shift all present possibilities for derailment. A gauge-widening derailment occurs when a rail shift or rail roll occurs as shown in Figure 17. Between 1993 and 1998, the number one cause of track-related derailments in interchange service in the United States was failure of track to maintain gauge due to missing or defective ties and fasteners (DOT 1998, p. 25).

Rail shift can be caused by large rail deflection and/or rail separation from the tie plate or cross tie. As the shift becomes large, the rail wheel is able to drop between the rails (Blader 1990, Section 1.2). This scenario can be envisioned with runaway Scenario 2 within the North Ramp Extension Curve. As large lateral loads are applied to the rail during a "moderate-speed" runaway, where speeds are high but tip-over is not imminent, the possibility of rail shift and rail roll derailment exists. Further investigation would be needed to predict such an event.

Rail roll occurs when the overturning moment created by large lateral forces between the rail wheel and the rail become large enough to roll the rail. Forces needed to roll are difficult to predict. A theoretical overturning moment calculation can be performed if rail fasteners are ignored. If "pull-out" forces of fasteners and rail twist forces can be predicted, a more accurate rail roll calculation can be performed.

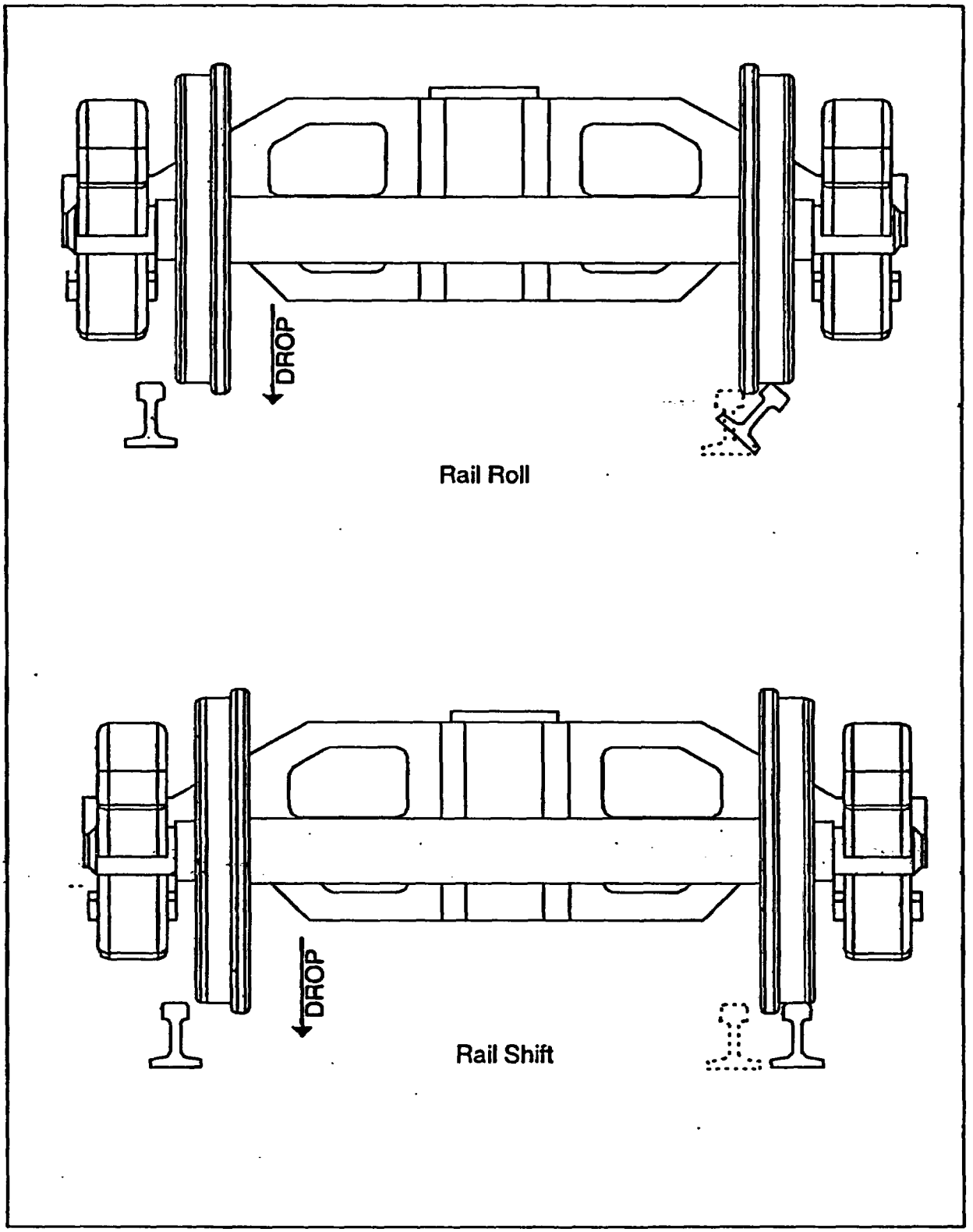

Figure 17. Gauge Widening Derailments

Track panel shift is the lateral deflection of the track, including the rails, tie plates, and ties, over the ballast. Although directional control of a railcar is not initially compromised, as speeds increase any shift of noticeable magnitude, on the order of an inch, is regarded as an incipient derailment (Blader 1990, Section 1.2). For the ramps and mains, the SR subsurface repository design is envisioned to utilize precast concrete inverts and 300-mm thick cast-in-place concrete lining (DOE 1998, Section 4.2.2.2). This will serve as both rail ties and ballast, thereby reducing the possibility for track panel shift.

6.4.1.3 Wheel Climb Derailment

Wheel climb derailment is the combined lateral and vertical departure of the rail wheel up onto the head of the rail, preventing the normal control of the wheel at the rail interface. This type of derailment occurs when the forward motion of a rotating wheel is combined with large lateral forces and often reduced vertical (weight) forces. The reduction of vertical forces is called wheel unloading and is usually induced by dynamic motions of the rail car. Such dynamic motions could be induced from harmonic roll or pseudo-statically in spiral or curve negotiation (Blader 1990, Section 1.2).

Large lateral forces can be caused by dynamic motions of the railcar during truck hunting, sudden and large braking applications, and by the effects of large forces at the coupler from pushing or pulling of the railcar while in a curve. Large lateral forces caused by braking within a curve are called buff forces and typically cause wheel climb on the outside rail. Large lateral forces caused by the pulling of a railcar through the curve are called draft forces and typically cause the wheel to climb the inside rail (DOT 1998, p. 45). Lubrication of the track reduces the possibility of a wheel climb derailment by reducing the coefficient of friction between the flange and the rail. However, lubrication of the rail also increases the chances of "wheel-lock" during heavy or emergency braking, as described in Section 6.3.3. The ratios of the lateral force to the vertical force (L/V ratios) are used in the creation of criteria indicative of incipient derailment.

6.4.2 Derailment Calculations

Due to the complexities at the wheel/rail interface, accurate derailment calculations cannot made at this time. The mathematical determination of an incipient derailment is extremely complicated and is a function of many variables and unknowns. However, a very conservative method is available for determining incipient wheel climb derailment conditions based on the vertical and lateral loads on any particular wheel. The ratio of lateral to vertical forces is known as the Nadal criterion (Blader 1990, pp. 44-46) and has been used throughout the railroad test community. The Nadal criterion is based on the assumption that a simple equilibrium of forces exists between the wheel and the rail at a single point of contact just prior to derailment (see Figure 18). This extremely simplified mathematical model of the wheel/rail interface is considered very conservative within the railroad community (Blader 1990, p. 44). The conservative nature of the Nadal criterion has prompted research activities to better describe and predict the wheel/rail interface just prior to derailment.

The AAR has performed numerous studies on derailment and derailment modes. The development of a test rail vehicle capable of creating controlled derailments of a single axle has provided the AAR with research into derailments. Known as the Track Loading Vehicle (TLV),

this test vehicle allows for fundamental research and investigation capabilities into some of the causes of derailment, as well as providing a means of checking and improving the derailment criteria currently in use, such as the Nadal criterion. Also, a software program called NUCARS (New and Untried Car Analytic Regime Simulation) has been developed to model and simulate rail and railcar dynamics. This software program has been used to model wheel/climb derailments (Blader 1990, pp. III–IV).

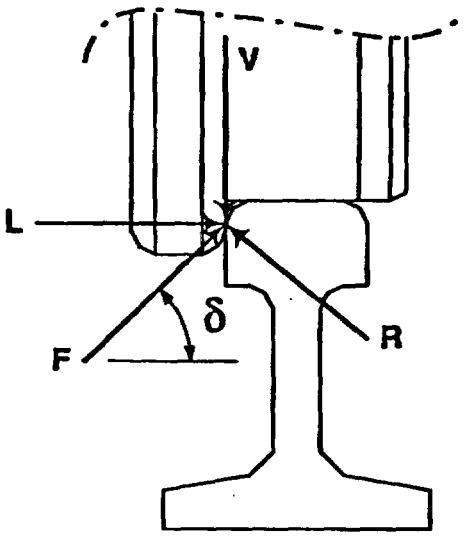

Figure 18. Wheel/Rail Forces at Incipient Derailment

From the curvature at the wheel flange and the rounding of the rail, an equivalent contact angle (δ) between the wheel/rail interface is presumed. The Nadal criterion is based on this presumption and that only a single point of contact exists between the wheel and rail at incipient derailment. As the wheel rotates, the lateral forces (L) push the wheel flange against the side of the rail causing friction at the rail/flange interface. Wheel climb derailment occurs when the lateral forces create enough friction to overcome the downward force (V), and the wheel is able to climb the rail.

The equilibrium equations for the vertical (V) and lateral (L) forces are:

$$L = R\sin(\delta) - F\cos(\delta)$$

(Eq. 44)

$$V = R\cos(\delta) + F\sin(\delta)$$

(Eq. 45)

The resistance force (F) is a function of the resultant force (R) and the coefficient of friction (μ) at the wheel/rail interface.

$$F = \mu R$$

(Eq. 46)

The Nadal criterion is the ratio of the lateral to vertical forces. Substituting the resistance force back into the Nadal equation, the resultant force drops out of the equation.

$$\frac{L}{V}=\frac{R\sin\delta-F\cos\delta}{R\cos\delta+F\sin\delta}=\frac{\sin\delta-\mu\cos\delta}{\cos\delta+\mu\sin\delta}$$

(Eq. 47)

The Nadal criterion is a function of equivalent flange angle (δ) and the coefficient of friction (μ) between the wheel flange and rail. Figure 19 shows the Nadal Criterion for various flange angles and friction values. Based on Exhibit 9 and the statement "Exhibit 9 shows the solution of this expression for a range of values, appropriate to normal railroad operations" from *A Review of Literature and Methodologies in the Study of Derailments Caused by Excessive Forces at the Wheel/Rail Interface* (Blader 1990, p. 46), flange angles are typically 70-80 degrees for new rails and wheels. The flange angle (δ) decreases as the rail and wheels wear, with 55 degrees showing severe wear. Characteristically, dynamic coefficients of friction (μ) for hard steel sliding on hard steel are approximately 0.42 (Avallone and Baumeister 1987, p. 3-26).

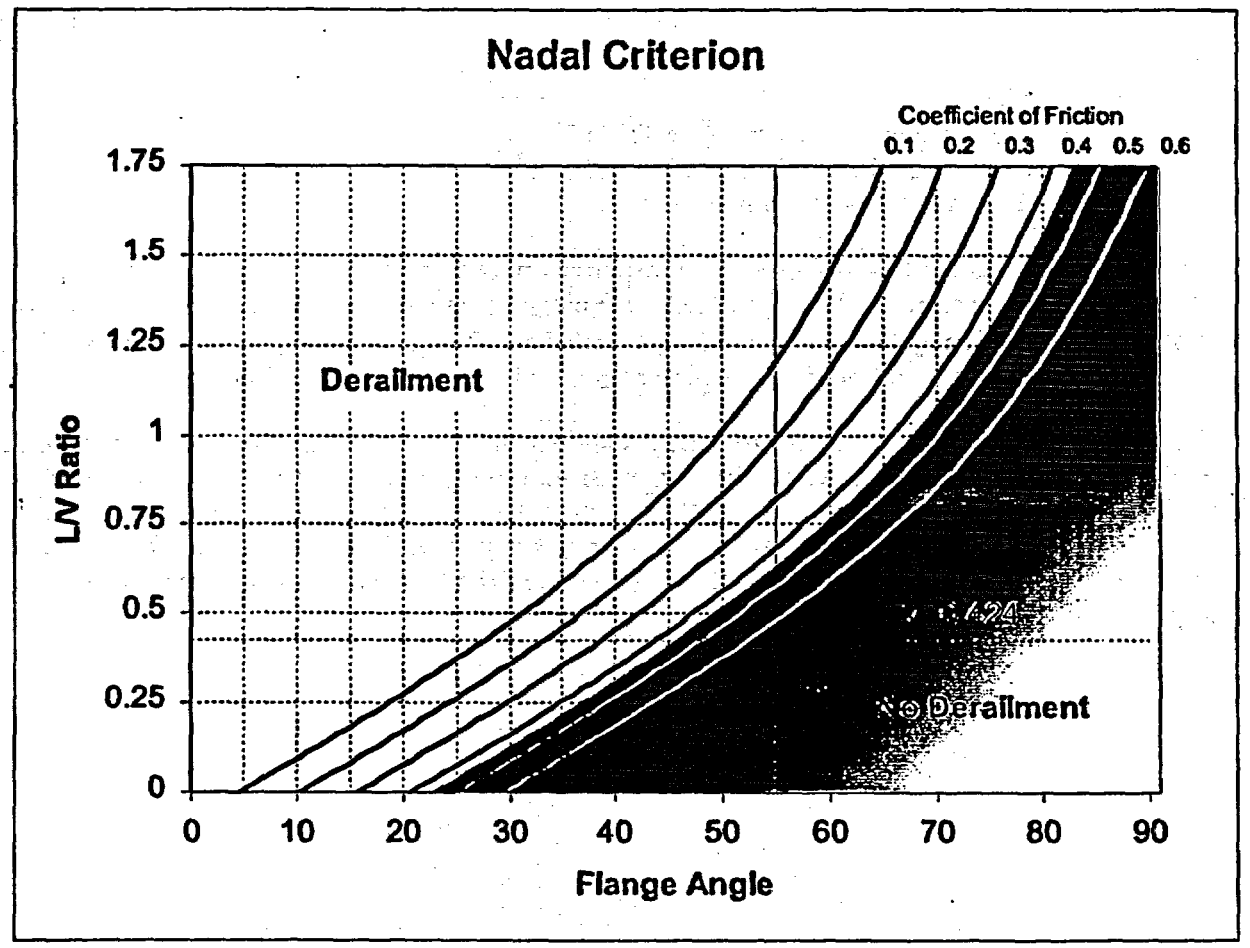

Source: Attachment III - Nadal Criterion

Figure 19. Nadal Criterion

The estimation of the L/V ratio for the WP Transporter would help determine if a derailment condition exists. The L/V ratio for the calculated speeds of Scenario 1 (Section 6.3.2.3) within the North Ramp Extension Curve is found by deriving the vertical and lateral forces induced as the transporter travels through the curve. The lateral force is based on the centrifugal force due to the velocity and curvature of the 305-m radius curve. The vertical force is simply the weight of the transporter, i.e.,

$$L = \frac{mv^2}{r} \qquad \text{(Eq. 48)}$$

$$V = mg \qquad \text{(Eq. 49)}$$

$$\frac{L}{V} = \frac{mv^2}{r} \times \frac{1}{mg} = \frac{v^2}{rg} = \frac{(30.82\ \text{m/s})^2}{(305\text{m})(9.80665\ \text{m/s}^2)} = 0.318 \qquad \text{(Eq. 50)}$$

where:

m = Mass
v = WP Transporter velocity (see Table 5)
g = Gravitational Acceleration (9.80665 m/s^2)
r = Radius of Curve (305 m)

Table 9 summarizes the L/V ratio for the transporter runaway scenarios at key points throughout the subsurface repository. The derailment conclusions are derived from Figure 19 for the coefficient of friction (μ) equal to 0.42 and rail/wheel flange angle (δ) at 55 degrees. The conclusion is for derailment only. Transporter tip-over is addressed in Section 6.4.3.

The L/V ratios for the transporter are low. As shown in Figure 19, the WP Transporter would derail only under a full runaway condition with extremely worn rails/wheels and very high wheel/rail coefficients of friction. It should also be noted that the Nadal criterion determination does not include dynamic effects such as hunting, sway, wheel unloading, or other dynamic phenomenon, such as seismic activity, that may increase the L/V ratio. This increased L/V ratio may increase the likelihood of a derailment.

Table 9. Anticipated L/V Ratio and Results

Runaway Scenario	Location	Velocity with Standard Rolling Resistance (Initial Velocity =8 km/hr)	L/V Ratio (Eq. 50)	Results ($\mu = 0.42$ $\delta = 55°$)
Runaway Scenario 1	Point C	29.21 m/s (65.34 mph)	0.285	No derailment
	Point D	30.82 m/s (68.94 mph)	0.318	No derailment
Runaway Scenario 2	Point D	28.67 m/s (64.1 mph)	0.275	No derailment
	Point G	35.61 m/s (79.6 mph)	0.424	No derailment
Runaway Scenario 3	Point G	24.37 m/s (54.5 mph)	0.199	No derailment
	Point J	26.47 m/s (59.2 mph)	0.234	No derailment
	Point K	28.47 m/s (63.7 mph)	0.271	No derailment
Runaway Scenario 4	Point B	27.61 m/s (61.8 mph)	0.255	No derailment
	Point M	30.67 m/s (68.6 mph)	0.314	No derailment

6.4.3 Tip-Over Calculations

The determination of tip-over will help establish safe operating speeds for the loaded WP Transporter. This will also provide maximum tip-over speed that can be used with the frictional runaway scenarios to determine if tip-over is possible.

For these calculations, the WP transporter is assumed to be a rigid body; i.e., there is no sway caused by compression of the springs within the transporter truck suspension and there is no tip-over of the WP, pallet, or bedplate within the WP transporter (Assumption 5.5)

The initial determination of tip-speed neglects the WP Transporter mass-moment of inertia so that an upper bounding limit for tip velocity can be established. In dynamic motion calculations, the mass moment of inertia increases the energy required to tip the WP transporter, thereby increasing the speed in the curve necessary for tip-over (Assumption 5.6).

The summation of the tip-over moments (M_{TO}) in the curve is used to determine the overturning speed. Determining the magnitude of the centrifugal force applied to the center of gravity of all the major components (i.e., WP transporter railcar, bedplate, pallet, and WP) will provide a method for determining the tip-over speed (v_{TO}),

$$\sum M_{TO} = 0 \qquad \text{(Eq. 51)}$$

$$\sum M_{TO} = \text{Weight} \times \text{Moment Arm} - \text{Centripital Acceleration} \times \sum \text{mass} \times \text{Moment Arm}$$

(Eq. 52)

$$\sum M_{TO} = 0 = mgL_1 - \frac{v_{TO}^2}{r} \sum mL_2$$

(Eq. 53)

where:

- m = Mass
- g = Gravitational Acceleration (9.80665 m/s^2)
- v_{TO} = Tip-Over Train Velocity
- L_1 = Horizontal distance from C.G. to rail
- L_2 = Vertical distance from C.G. to top-of-rail
- r = Radius of curve

Rearranging the equation to solve for tip-over velocity:

$$v_{TO} = \sqrt{\frac{mgL_1 r}{\sum mL_2}}$$

(Eq. 54)

Substituting the values from Table 2 and Figure 2 into Equation 54:

$\sum mL_2$ =	136.0 MT × 0.827 m	(Transporter Rail Car)
	10 MT × 1.588 m	(Bed plate/rollers)
	3 MT × 1.929 m	(Pallet)
	85 MT × 2.907 m	(WP)
+	153.4 MT × 2.875 m	(Shielding)
=	822.259 MT-m	

$$v_{TO} = \sqrt{\frac{(387.4\ \text{MT})(9.80665\ \text{m/s}^2)(0.720\ \text{m})(305\ \text{m})}{822.259\ \text{MT} - \text{m}}}$$

NOTE: The actual total weight of 387.4 MT is used, rather than the bounded 400 MT (see Criteria 4.1.4 and Assumption 5.16)

$$v_{TO} = 31.85\ \text{m/s}\ (71.25\ \text{mph})$$ ✓

(Eq. 55)

For Scenario 1, the frictional speed entering the North Ramp Curve at Point B is a maximum of 27.61 m/s as shown in Section 6.3.2.3. This is less than the tip-over speed of 31.85 m/s. However, as the transporter travels down the North Ramp Extension Curve, transporter speed will increase to a velocity (30.82 m/s) near the tip-over speed. Although the frictional runaway

speeds for Scenario 1 do not exceed the tip-over velocity, they are within 3.2 percent of each other. Therefore, it is assumed that the WP Transporter will tip at Point D.

Of the runaway scenarios selected for establishing the maximum runaway transporter speeds in Section 6.3.2.3, Scenario 2 achieves the highest speed, 35.60 m/s (79.6 mph). This speed was calculated at Point G, which is where the runaway encounters curves towards the intersection between the North Ramp Extension and the North Main. This speed exceeds the calculated tip-over speed of 31.85 m/s. Therefore, it is likely that the loaded transporter will tip-over during the defined runaway scenario.

6.5 IMPACT LIMITER EFFECTIVENESS AND JUSTIFICATION

Impact limiters are devices attached to the WP Transporter that would help absorb impact energy in the event of a collision. Currently employed on railroad and truck transportation packaging (casks) used during transportation of commercial spent nuclear fuel, impact limiters prevent damage or a breach of the cask in certain crash scenarios. Impact limiters are designed to crush upon impact and absorb a large portion of the impact energy. An impact limiter consists of an assembly made up of a shell covering energy-absorbing material. The shell primarily provides structural support, containment for the energy absorbing material, and protection against inadvertent crushing. The crushable material typically consists of plastic foam, metal honeycomb, wood, or any other crushable, energy-absorbing material (McConnell et al. 1996, Section 5.2.1).

The use of impact limiters on the ends of the emplacement equipment may not provide the same level of protection from front or rear end collisions. The worst case event is assumed to begin while the transporter is traveling down the North Ramp into the repository, and impacts a repository wall resulting in a breached WP.

Section 6.4.3 showed that the WP Transporter is likely to tip-over in a worst case runaway condition. As illustrated in Figure 20, the WP Transporter will not completely rotate onto its side within a 305-m radius curve. The WP Transporter side and top will impact the wall, not the front or rear. Therefore, impact limiters on the ends of the WP Transporter will provide negligible impact protection.

If a derailment occurred, and assuming the WP Transporter traveled straight after the derailment, the WP Transporter would strike the North Ramp Curve wall at a very shallow angle, approximately 6 degrees, as shown in Figure 21. Because of the shallow, oblique angle of contact with the drift, impact limiters on the ends of the WP Transporter would provide negligible impact protection in a derailment scenario.

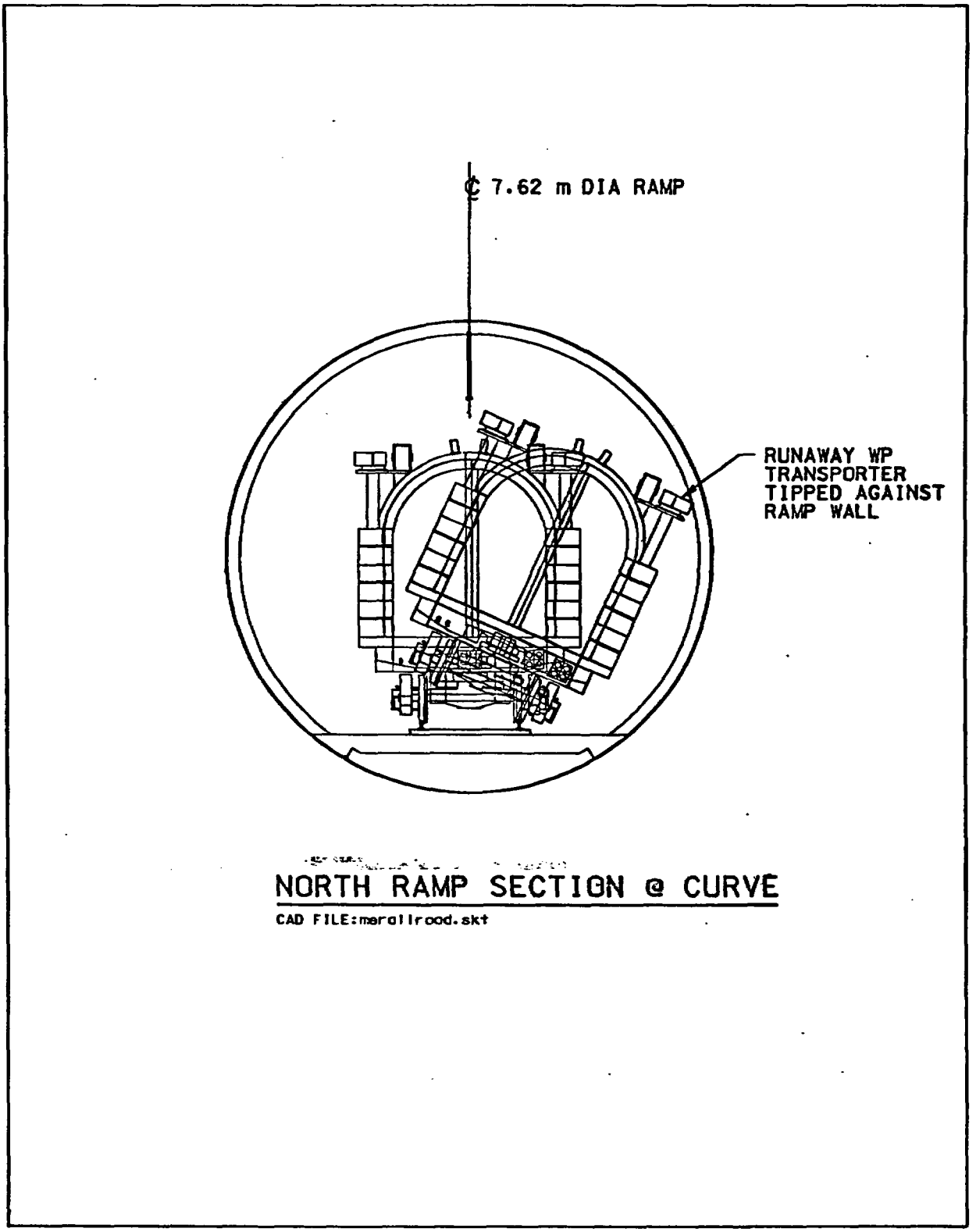

Figure 20. WP Transporter Tip-Over Scenario

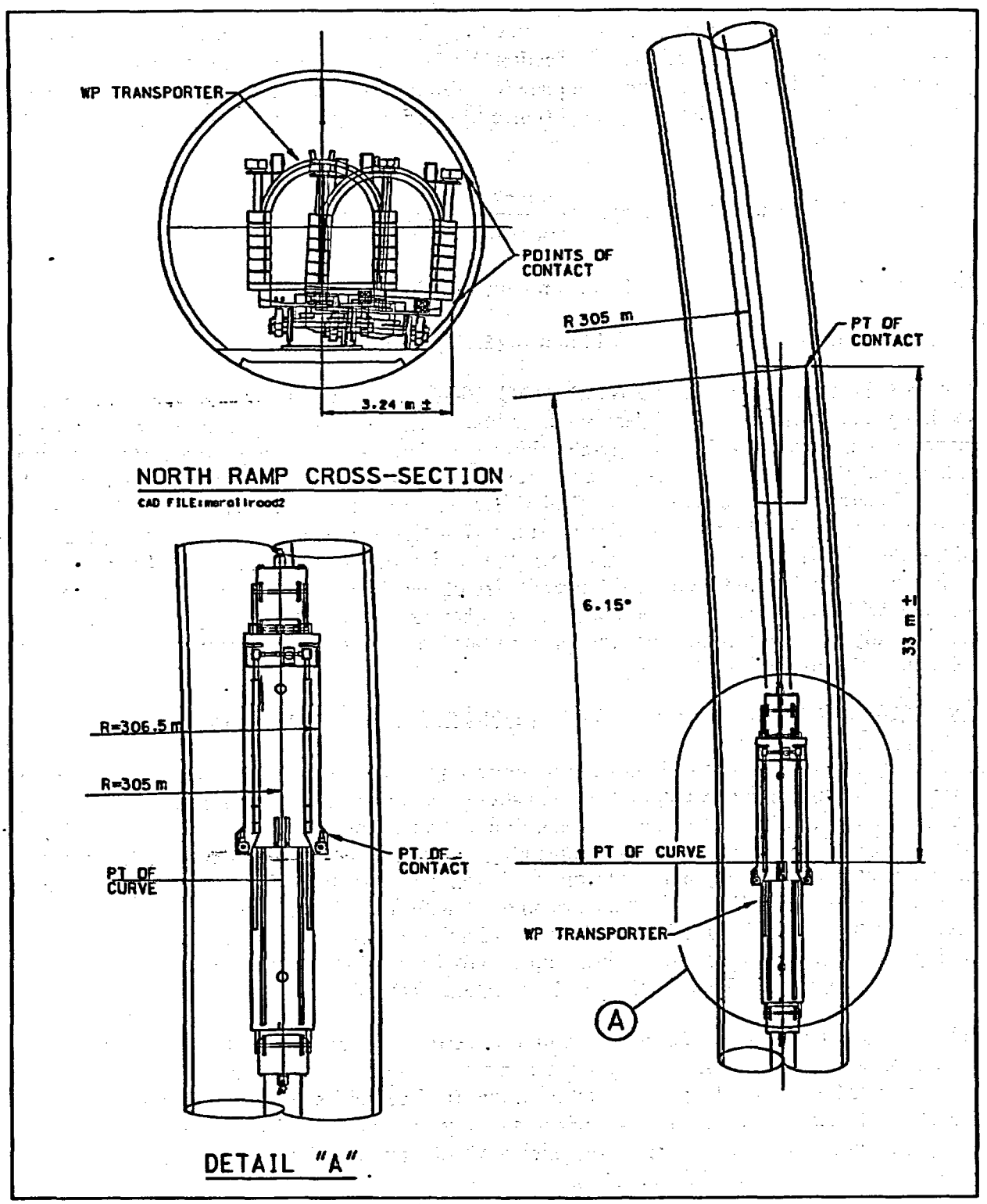

Figure 21. WP Transporter Derail Scenario

It should be noted that the dimensions presented in Figure 21 are preliminary, and are verified below in accordance with AP-SI.1Q, Section 5.1.1. The computer aided design software provides a level of accuracy deemed adequate for this analysis. The 6.15-degree angle of impact can be hand verified by calculating the distance traveled during a derailment, both horizontally and longitudinally.

Dermine the hypotenuse of the triangle : $\frac{306.47\ \text{m}}{\cos(6.15^\circ)} = 308.24\ \text{m}$

Horizontal travel: 308.24 m - 305 m = 3.24 m

Longitudinal travel: $308.24\ \text{m} \times \sin(6.15^\circ) = 33.0\ \text{m}$

The WP Transporter design (CRWMS M&O 2000b, Section 6.4.3.1) includes radiological shielding that consists of a stainless steel, carbon steel, and borated polyethylene composite. Incorporation of a crushable, energy-absorbing material, such as honeycomb metal, into the radiological shield composite design could reduce the effect of a collision or impact on the WP. As the innermost layer of the radiological shield, this impact limiter material would provide protection to the WP in all crash, derailment, and/or tip-over scenarios by protecting the WP within the WP Transporter. Although the incorporation of an energy-absorbing layer into the radiological shield would increase the overall size of the shielding, this concept would provide the WP with considerable impact protection, whereas a conventional impact limiter could provide only negligible protection, except in isolated instances such as alcove corners or rock columns at the divergence of drifts.

6.6 TRANSPORTER NORMAL OPERATING SPEED DETERMINATION

The determination of the maximum normal-operating transporter speed is based on industry practices, and, to a lesser extent, on the calculations made within this analysis. Based on mining locomotive manufacturer equipment, standard mine-industry practices utilize 16 km/hr (4.5 m/s or 9.9 mph) as a maximum standard operating speed for locomotive travel within a mine environment. Balco Inc., a manufacturer of trolley locomotives for the mining industry, manufactures a 60-ton Trolley/Battery Locomotive with a maximum speed range of 8 to 12.8 km/hr (5 to 8 mph) (Balco 1998, p. 1). Goodman Equipment Corporation, also a manufacturer of mining locomotives, lists standard operating speeds for mining locomotives above 15 tons at 16 km/hr (10 mph) (Goodman Equipment Corporation 1971b, p. 1).

Table 5 showed that the difference in initial velocity of a runaway had little effect on the maximum speed. The difference between a runaway initiated at 0 km/hr to one initiated at 8 km/hr (2.222 m/s or 4.97 mph) resulted in similar final velocities. Section 6.8 develops a FTA that showed that the probability of such a runaway is very low. The speeds at which the transporter will tip-over and the speed at which a wheel-climb derailment would occur are shown to be very high (Sections 6.4.2 and 6.4.3).

An area of concern is at low- to moderate-speed derailments caused by track defects as described in Section 6.4.1. It can be envisioned that a WP Transporter could derail at low speed and

impact with an immovable object or, a similar situation, where the lead locomotive derails and the WP Transporter impacts the locomotive. The WP shall be designed to withstand a 2.0-m drop onto the ends, or 2.4-m drop onto its side (Criteria 4.2.6)

Using the velocity equation derived in Section 6.3.1, the speed of a falling WP can be found for 2-m and 2.4-m drop heights,

$$v^2 = v_0^2 + 2a(x - x_0)$$

(Eq. 7)

Substituting the change in position (x - x_0) with the change in height (Δh) and the acceleration (a) with gravity (g) gives:

$$v^2 = v_0^2 + 2g(\Delta h)$$

(Eq. 56)

In addition, rearranging Equation 56 to solve for the final velocity (v), with the initial velocity (v_0) equal to zero. The acceleration (a) in Equation 7 is the acceleration of gravity (g) used in Equation 56.

$$v = [2g(\Delta h)]^{1/2} = [(2)(9.80665\ m/s^2)(2\ m)]^{1/2} = 6.263\ m/s$$

(Eq. 57)

$$v = [2g(\Delta h)]^{1/2} = [(2)(9.8066\ m/s^2)(2.4\ m)]^{1/2} = 6.861\ m/s$$

(Eq. 58)

Criteria 4.2.3 states that the WP Transporter speed shall be limited to 8 km/hr (2.22 m/s or 4.97 mph). Although the system description document from which this criteria is referenced does not provide any basis for this speed, based on the above calculations, 8 km/hr is 2.82 times slower than an equivalent 2-m design basis WP drop height.

The initial revision of this analysis (CRWMS M&O 2000e, Section 6.6) resolved TBV-252 at 8 km/hr. This revision is consistent with the previous, in that the maximum transporter speed of 8 km/hr (2.222 m/s or 4.97 mph) is adequate, based on:

- 2-m WP drop height Safety Factor of 2.82
- Mining-Industry standard of 16 km/hr or less for mining locomotives
- Relatively high speeds needed for tip-over and wheel-climb derailments
- Recommendation that the WP Transporter, with its short truck-center spacing (11.778 m or 38.6 ft) and relatively high center of gravity (2.122 m or 6.96 ft), avoid operations in the 4.5-8.9 m/s (10-20 mph) regime, as described in 6.4.1.1.

6.7 UNCONTROLLED DESCENT MITIGATION

Although the WP transporter and the locomotives all have redundant fail-safe brake systems that provide retarding force by using different braking methods, which prevents CCFs, there are still concerns with runaway conditions caused by probabilistically low brake failure(s). Two additional alternative methods are presented for the mitigation of a WP Transporter runaway.

6.7.1 Magnetic Track Brakes

Magnetic track brakes are a brake system that provides an additional braking force independent of the disk or wheel brakes. Typically installed on the railcar trucks, the track brakes can only be used in an all-or-nothing scenario. These brake systems are often deployed for providing emergency brake effort or for supplemental braking when there is poor wheel-to-rail adhesion conditions. Magnetic track brakes are capable of providing railcar deceleration rates on the order of 2.46 m/s^2 to 3.58 m/s^2 (5.5 to 8.0 mph/s) (Air Brake Association 1975, p. V-22).

When magnetic track brakes are applied, spring-activated/pneumatic-return cylinders lower two rows of permanent or electromagnetic magnets onto each rail. The magnetic attraction between the magnet and the railhead creates a frictional force in the opposite direction of movement. The amount of magnetic attraction between the railhead and the magnet dictates the amount of friction generated. Electromagnetic track brakes have the advantage of being able to adjust the amount of attraction between the railhead and the magnet. The adjustment is made by varying the amount of current supplied to the electromagnets. The friction created provides significant retardation force transmitted to the railcar truck and is capable of stopping the railcar. Upon completion of the emergency or supplemental braking, air is supplied to the pneumatic cylinders that pull the magnets off the railhead and retract the system to its stowed position.

This configuration provides braking force immediately after air is released from the supply line. Whether air pressure is released purposely or by a brake-line failure, this system would provide fail-safe emergency braking.

6.7.2 Car Retarders

Railcar retarders are commonly used in modern commercial rail yards, especially large classification hump yards. Retarders are incorporated into the rail system rather than the railcar itself (see Figure 22). The retarders provide retarding force to the wheels of railcars to slow them as they pass through the retarder. A classification hump yard is a large rail yard used for separating trains into groups and sorting the groups for reassembling train sets. Railcars are pushed up a hill (hump) by a locomotive, uncoupled, and then rolled downhill into remotely controlled sorting tracks.

The commercial railcar to be sorted is "bled off," allowing the air contained within the railcars' reservoirs, brake cylinders, control valves, and train line to escape into the atmosphere, thereby releasing the brakes. As described in Section 6.1.1.1, commercial railcars utilize compressed air from a reservoir to apply the brakes.

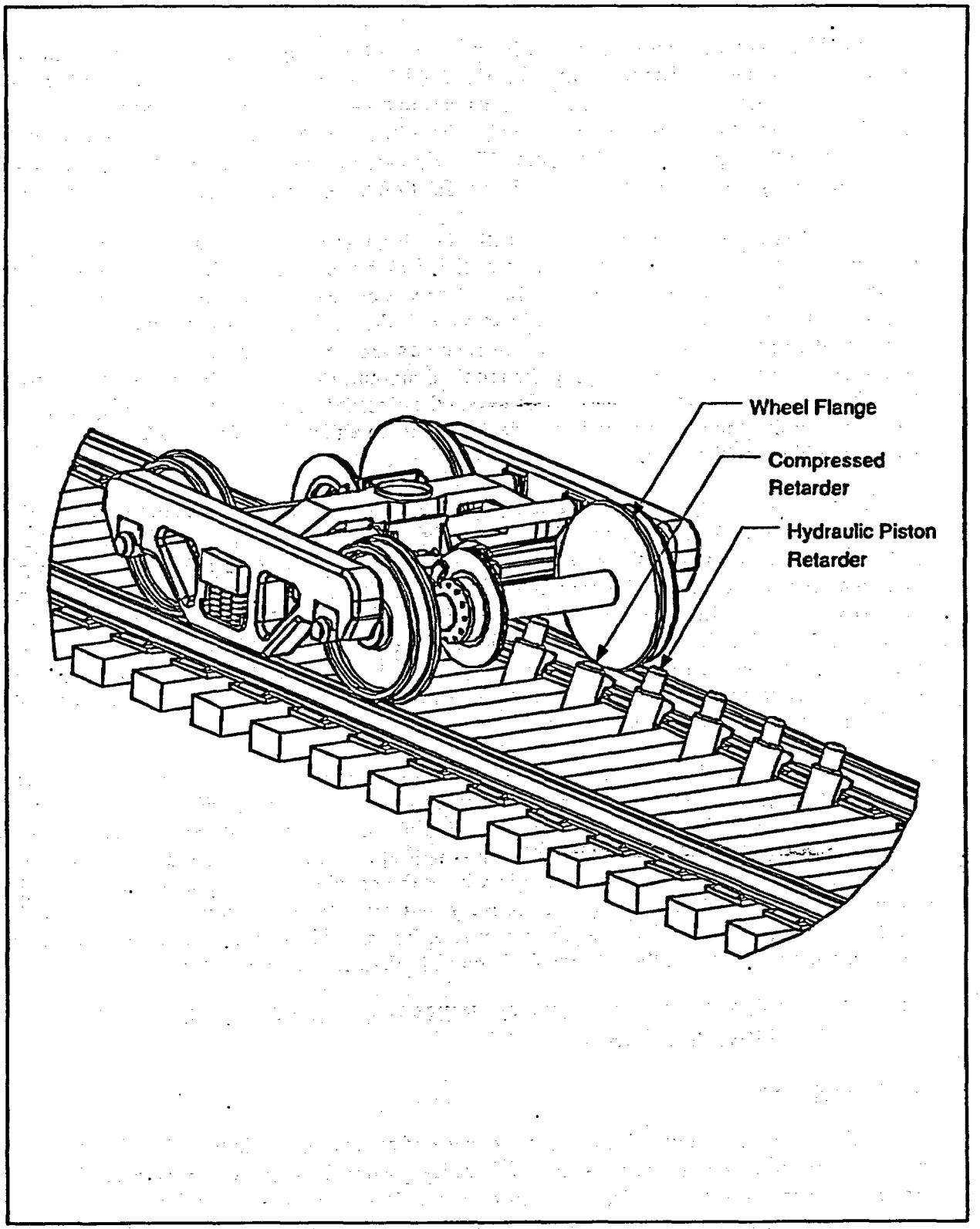

Figure 22. Hydraulic Piston Retarder

The "bled-off" commercial railcar, as it is pushed over the hump by the locomotive, can now be considered a runaway. The runaway railcar's speed is controlled by a series of retarders. These retarders are located at key track locations throughout the classification yard. The master retarder, located at the yard's hump, provides the initial retarding force to the wheels of the cars as they leave the high point of the hump. The retarders in each section of track again retard the cars so that they run into a predetermined classification track at a predetermined rate of speed.

Two major types of retarders are currently in use: wheel clamp and hydraulic piston-type retarders. Wheel clamp retarders are part of the track system and produce friction by clamping to both sides of each rail wheel. As the railcar wheels travel through the retarder, the force applied to the sides of the wheel in conjunction with the coefficient of friction create a retarding force used to reduce railcar speed. These retarders are an active system where electronically controlled pneumatic cylinders apply the required amount of force to the wheel clamps to slow the railcar smoothly and accurately. However, these retarders are often very noisy and require clearance for the pneumatic cylinders underneath and on either side of the track – which may not be compatible with the concrete invert design.

The hydraulic piston-type retarders are passive energy-absorption systems similar in function to a shock absorber. A series of retarder pistons are installed vertically to the insides of the both rails so that the rail wheel flange depresses the hydraulic piston (see Figure 22). Each piston contains precision control valves, hydraulic fluid, and nitrogen gas at pressure. The precision control valves are calibrated during manufacture for speed control in the range of 0 m/s to 5 m/s (0 mph to 11 mph). For railcars travelling above the control speed, kinetic energy is extracted as each wheel depresses the piston. For railcars traveling below the control speed, negligible energy is extracted. The absorbed kinetic energy is dissipated as heat by the retarder piston (Attachment I and Ultra Dynamics 1997).

As a common piece of rail equipment, either or both types of retarders could be installed at key positions throughout the North Ramp and the Mains. A series hydraulic piston-type retarders equally spaced at a determined distance would provide an additional method for slowing the locomotives and WP transporter and maintain speeds at or below the maximum normal operating speed. Correctly sized and spaced retarders have the capability of stopping a WP Transporter without braking capability, thereby effectively and reliably preventing a runaway condition. Further investigation into the possible use of retarders should include a failure-effects analysis, such as, but not limited to, the effects of a jammed hydraulic-piston retarder.

6.8 ESTIMATES OF FREQUENCY OF RUNAWAY USING ACTUARIAL DATA AND FAULT TREE ANALYSIS

6.8.1 Objective

The definition of a Category 2 DBE is a sequence of events that leads to a significant release of radioactivity to the environment with a probability greater than one in ten thousand in the time period before permanent closure. For a preclosure period of nominally 100 years (Assumption 5.13), the average annual probability of occurrence (frequency) of such an event sequence must exceed 1.0×10^{-6} per year to be considered a credible DBE (4.2.13). If the frequency is less than 1.0×10^{-6} per year, then the event sequence is considered "beyond design

basis." One goal of the MGR is to eliminate all credible scenarios with the potential for significant release of radioactivity. The present analysis examines potential design features that will ensure that a transporter runaway is beyond design basis.

Several prior studies have been performed with the objective of screening out a transporter runaway as a potential DBE. Those studies (summarized in Section 6.8.2) were based on (1) adaptations of actuarial data on accidents from commercial railway and mining accidents, or (2) based on FTAs. None of the prior studies were able to show with high confidence that the runaway could be dismissed as beyond design basis. The present analysis builds on the prior analyses of actuarial data and fault tree models to examine the possibility of incorporating potential design alternatives to reduce the frequency of a transporter runaway to below the threshold of 1.0×10^{-6} per year.

The present analysis presents two approaches: (1) a re-analysis of probabilities derived from actuarial data with application; and (2) modification of the fault tree models for both the initiation frequency and the conditional probability of the failure to stop.

6.8.2 Background: Results of Prior Analyses

The process for identifying the list of DBEs for a facility like the MGR is a systematic search and screening process to ensure completeness and conservatism. A preliminary hazards analysis (CRWMS M&O 1997c, Section 7.2.3.1.2, p. 70) identified an uncontrolled descent of a transporter train as a potential DBE since runaways have occurred in railway and mining operations. Several follow-on analyses investigated the frequencies of such events and concluded that the runaway event could not be screened out as beyond design basis. The following subsections summarize the approaches and results of those studies.

6.8.2.1 Application of Actuarial Data

Summary of Results of Prior Studies–When available and relevant, actuarial data on accidents provide a good basis for screening potential accident frequencies. Since the MGR design and operations are first-of-a-kind, there is no existing event database that is specific to, or directly applicable to, the MGR. Therefore, inferences are made from other industries that use railcars and locomotives to haul heavy loads. *DBE/Scenario Analysis for Preclosure Repository Subsurface Facilities* (CRWMS M&O 1997c) describes four such analyses conducted for the MGR.

One prior study examined data for mine hauling accidents and NRC road and rail transportation accidents. From this data, the frequency of a MGR runaway was estimate to be in the range of 3.84×10^{-4} per year to 3.00×10^{-3} per year (CRWMS M&O 1997c, Section 7.2.5.3, p. 99).

A second prior study reported in *DBE/Scenario Analysis for Preclosure Repository Subsurface Facilities* (CRWMS M&O 1997c, Section 7.2.5.3, p. 98) examined accident data for commercial railways for events involving speeds greater than 16.1 km/hr (10 mph). The accident rate per mile traveled was screened to include only events that involve loss of speed control related to human or mechanical failures and judged to represent the MGR operations. That study estimated the frequency of runaways on the North Ramp to be 5.4×10^{-5} events per year. This frequency was viewed as being "borderline incredible" noting that the MGR train will incorporate

safeguards on operations that should reduce the frequency by one or two orders of magnitude (CRWMS M&O 1997c, Section 7.2.5.3, p. 98).

DBE/Scenario Analysis for Preclosure Repository Subsurface Facilities (CRWMS M&O 1997c, Section 7.2.5.3 p. 102) performed new analyses of accident data for commercial trains from the Department of Transportation-FRA for the period 1995 through 1996. The data presented the contributions from various causal factors and accident rates per mile. The event occurrence rates were adjusted for the MGR to reduce the contributions of certain causal factors that do not apply to the MGR because of the different environments, operational restraints, inspection, and maintenance of tracks and vehicles. The results give a range of 7.75×10^{-5} to 9.95×10^{-5} per year as the frequency for runaway on the North Ramp.

DBE/Scenario Analysis for Preclosure Repository Subsurface Facilities (CRWMS M&O 1997c, Section 7.2.5.3 p. 103) also analyzed accident data for mining locomotives as reported by the British Health and Safety Executive for the period 1986 through 1988. The data presented the contributions to the total accident rate from various types of accidents, such as derailment at switches (21%), derailment on track (36%), collisions (36%), and runaway (21%). The raw data were adjusted for applicability to the MGR to reduce the contributions of certain causal factors and accident types based on assumed environments, operational restraints, inspection, and maintenance of tracks and vehicles for the MGR. The result gives 3.24×10^{-4} per year as the frequency for runaway.

The summary of four estimates from actuarial data gives a probability for runaway in the range of 7.75×10^{-5} to 4.71×10^{-3} per year (CRWMS M&O 1997c, Section 7.2.5.3, p. 104). The median value is given as 6.04×10^{-4} per year and is greater than the threshold value of 1.0×10^{-6} per year.

Insights Derived from Prior Studies–The actuarial data for railway and mining locomotive accidents show that a runaway is a very unlikely event for manually controlled systems, but is not sufficiently unlikely to be regarded a beyond design basis for the MGR. An examination of the actuarial data (CRWMS M&O 1997c, Attachment I, Tables I-5 and I-7) indicate that the accident data represents a composite of human- and hardware-caused runaways. The data cited exclude environmentally caused events that were screened out from the source data as being inapplicable to the MGR operating conditions (CRWMS M&O 1997c, Section 7.2.5.3, pp. 101-103). Depending on which data set is used, it is observed that a reduction in the initiation frequency by factors ranging from about 50 to approximately 600 would lower the runaway frequency to 1.0×10^{-6}. The median frequency of 6.04×10^{-4} per year, derived from the prior evaluations, requires a factor of 1.70×10^{-3} to lower the runaway frequency to 1.0×10^{-6}.

A breakdown of the causal factors of railway runaway in the commercial railway data (CRWMS M&O 1997b, Attachment I, Table I-5) shows that about 48 percent are human-caused, 49 percent are hardware caused, and the remainder due to locomotive fires. Similar breakdowns of runaway causes in the mining locomotive data that are potentially applicable to the MGR (CRWMS M&O 1997b, Attachment I, Table I-7) indicate a split of about 68 percent human-caused and 32 percent hardware-caused.

Given the high reliability that is achievable with electronic controls and/or interlock systems, it can be postulated that design features could be provided in the instrumentation and controls for

the WP Transporter and locomotives. Such control systems would virtually eliminate human-initiated runaways. Further, incorporating redundant and diverse design elements in the hardware portions of the brake system(s) could significantly reduce the likelihood of hardware-initiated runaways. The potential effects of such design features are discussed below.

Demonstration of Runaway Frequency Reduction Using Actuarial Data–A median value of 6.04×10^{-4} per year for transporter runaway was derived from actuarial data. As indicated above, about half of the runways may be attributed to human-caused events and half to hardware-caused events, i.e., about 3.02×10^{-4} per year for either event. This section will demonstrate how potential design features might achieve the target frequency of less than 1.0×10^{-6} per year.

It is proposed (Assumption 5.9) that design features would reduce the likelihood of driver error. Such design features could include electronic interlocks that prevent the train operator from descending the North Ramp unless service and/or dynamic brakes are actuated. Another proposed design feature could be an alarm that alerts the operator if the trains speed reaches the maximum normal operating speed.

For such electronically controlled design features, a single channel solid-state logic module was estimated to have a failure probability of 1.65×10^{-6} per demand (e.g., CRWMS M&O 1997b, Attachment III, Item 10). With such a design, the human contribution to runaway frequency could be reduced from about 3.02×10^{-4} per year to about 4.98×10^{-10} per year (i.e., $3.02\times10^{-4} \times 1.65\times10^{-6}$). That is, a runaway would require a human error in combination with the failure of at least one highly reliable electronic device. Adding these types of design features could essentially eliminate the human contribution to the runaway probability.

mix units

The residual runaway frequency would be attributed to hardware failures with a frequency of about 3.02×10^{-4} per year. It is evident that additional design features, such as component or subsystem redundancy within the hardware design, could likewise drive the residual frequency to below 1.0×10^{-6} per year. The FTA described in the following sections explores ways to reduce the hardware and the human contributions to runaway frequency.

6.8.2.2 Summary and Results from Previous Fault Tree Analyses

Two FTAs have been performed (CRWMS M&O 1997c and CRWMS M&O 1997b) to estimate the frequency of transporter runaway. These analyses are summarized below and are used as a basis for the present analysis.

6.8.2.2.1 Fault Tree Analysis for DBE Screening Analysis

In *DBE/Scenario Analysis for Preclosure Repository Subsurface Facilities* (CRWMS M&O 1997c, Section 7.2.5.3 p. 104), an FTA was developed to (1) provide an estimate that was independent of the actuarial data, and (2) provide a structure to examine how design and operational features might provide defense-in-depth that can prevent or mitigate a runaway. The fault tree quantification used generic failure rate data for components and human error rates to provide a "bottom up" synthesis of the frequency of runaway. The model included potential human errors and potential mechanical, electronic, and software systems failures.

The top event of the fault tree "Runaway occurs on North Ramp" was developed through an AND gate having input events "Runaway Initiated" and "Fail to Slow or Stop Before Derail or Collision." The frequency of the runaway (top event) is calculated as the product of the frequency of the event "runaway initiated" and the conditional probability of "fail to stop or slow..." given a runaway is initiated. The fault tree model was developed to a level of system decomposition that was appropriate for the level of design detail that was available. The failure to slow or stop was estimated to range from 2.5×10^{-3} to 5.0×10^{-2} per demand (CRWMS M&O 1997c, Section 7.2.5.3, p. 108), and was shown to be dominated by the human error contribution.

The frequency of runaway was quantified for three cases:

- Brake control and actuation system having redundant channels (5.7×10^{-4} per year)
- Brake control and actuation system having non-redundant channels (8.2×10^{-4} per year)
- Actuation system that can be operated only by the on-board drivers; i.e., having no capability for intervention by control-room operators (1.1×10^{-2} per year) (CRWMS M&O 1997c, Attachment XVI, p. XVI-1).

Based on the analysis of the first two cases, it was concluded that the model could provide results that agree reasonably well with the estimates based on actuarial data, and that the runaway could not be screened out of the DBE list. It was noted, however, that the case without control room intervention (which is similar to commercial rail and mining operations represented by the actuarial data) predicted a runaway frequency that is two orders of magnitude greater than the actuarial data. This suggests that the fault tree model, wherein the probability of a runaway is dominated by human error, is conservative. unrealistically conservative?

6.8.2.2.2 Fault Tree Analysis for Logic Model Demonstration

Application of Logic Diagrams and Common-Cause Failures to Design Basis Events (CRWMS M&O 1997b) presents another FTA of the transporter train runaway that is somewhat more detailed than that presented in *DBE/Scenario Analysis for Preclosure Repository Subsurface Facilities* (CRWMS M&O 1997c). That analysis was developed to illustrate the application of fault-tree methods. The basic fault tree model is similar to that described in Section 6.8.2.2.1 and Assumption 5.7. The approach is described in some detail because this fault-tree model is used as the baseline for the new analyses described in Section 6.8.3.

A key feature of *Application of Logic Diagrams and Common-Cause Failures to Design Basis Events* (CRWMS M&O 1997b) was to illustrate how potential CCFs can be included in fault tree models. The analysis used the "beta-factor" method for quantifying the probabilities of CCFs (CRWMS M&O 1997b, Section 3.2.1 p. 12). The fault tree model indicates potential CCFs within and between the three vehicles of a transporter train. The hierarchy of CCFs was identified as:

- "Intra-vehicle" – defined as CCFs of components/systems that are located in one locomotive, or in the transporter, such as the concurrent failure of two brake-release air cylinders, or concurrent failure of two channels of an electronic control system

- "Like-vehicle" – defined as CCFs of components/systems that are located in different locomotives (e.g., concurrent failures of all brake cylinders in both locomotives)

- "All-vehicle" – defined as concurrent failures of all brake cylinders in the two locomotives and the transporter.

The various CCFs may be attributed to errors in manufacturing, installation, maintenance or testing. The beta-factor assumes that a certain fraction of documented failure rates for individual components/systems are attributed to CCFs. As documented in *Application of Logic Diagrams and Common-Cause Failures to Design Basis Events* (CRWMS M&O 1997b, Section 3.2.2 p. 15), three values of beta-factors, 0.1, 0.01, and 0.001, were assumed to represent the respective intra-, like-, and all-vehicle CCFs. The beta factors are applied to the total failure rate for one component or train of a redundant system.

The top-level fault tree model in *Application of Logic Diagrams and Common-Cause Failures to Design Basis Events* (CRWMS M&O 1997b) is used as the starting point in the present study and is termed the baseline. The top event is "Runaway Occurs on the North Ramp" which is developed through an AND gate having input events "Runaway Initiated" and "Failure to Apply Brakes After Runaway Initiation."

At the time of that analysis, no details were available on the control system design for driving or braking the locomotive, nor for the on-board or central control room. Available information consisted of analyses of concepts of operations for transporting and emplacing WPs that debated the advantages and disadvantages of manual versus automatic control, and concepts for providing communication links between the central control room and the locomotives while underground. Further, there were no details regarding the mechanical or electrical design of the braking systems for the locomotives or transport car. Available information was limited to principles of operation such as having a "fail-safe" brake and application of proven braking technology typical of mining and/or commercial rail locomotives. As a consequence, the FTA had to make numerous assumptions, generally biased toward conservatism, to explore whether or not a potential runaway event is credible and, if so, to identify potential vulnerabilities in the conceptual design or operations.

The results of the previous FTA indicate that the estimated frequency of runaway is very low, but not less than 1.0×10^{-6} per year. Further, the previous FTA indicated that the likelihood of a runaway was dominated by human errors. The present analysis re-visits these FTAs to explore potential design solutions that can eliminate runaway as a credible accident for the MGR.

Tree in Ref. →

Fault Tree for Initiation of Runaway–The quantification of the frequency of "Runaway Initiated" (top event INIT_RA, CRWMS M&O 1997b, Att. I) implicitly includes the maloperation of the dynamic brakes. The failure to actuate the dynamic brakes on the locomotive is treated as part of the initiation (i.e., the driver inadvertently disables the dynamic brakes). Dynamic brakes are not modeled in the "fail to apply brakes after runaway initiation" since the dynamic brakes are not intended for emergency stops.

Need this R.L. for Tree

The frequency of the initial operator error is calculated as the product of the frequency of the initial error at 4.56×10^{-1} per year times the probability of failure to recover (0.5 per opportunity),

seems really high!

seems high

giving 2.28×10^{-1} per year (CRWMS M&O 1997b, p. 43). The sub-tree for "Runaway Initiation" includes contributions from failures of electrical system (2.51×10^{-4} per year), control system (7.52×10^{-5} per year), and communications system (7.52×10^{-5} per year). CCFs of the assumed redundant channels of the control and communications systems are included in the estimate of event frequencies. The sum of the contribution from the hardware failures is 4.01×10^{-4} per year. The initiating event frequency is assessed to be 2.28×10^{-1} per year, and is dominated by human error.

In Section 6.8.3.1, the effects of incorporating one or more electronic systems to prevent or reduce the likelihood of human initiation of runaway are examined by modifying the fault tree model.

Need Ref. for Tree →

Fault Tree for Failure to Stop a Runaway–The fault tree for the event "Failure to Apply Brake After Runaway Initiation..." (top event NOSTOP, CRWMS M&O 1997b, Att. II) is developed through an OR gate to the events (1) "Human Operators Fail to Apply Service Brakes"; (2) "Failure of Service Brake Hardware – All Three Vehicles" (i.e., due to independent failures and combinations of "intra-vehicle" and "like-vehicle" CCFs); and (3) "CCF of Service Brakes in All Three Vehicles" (i.e., representing the "all-vehicle" CCFs). The probability of human error is the joint probability that the on-board drivers and control room operators fail to act. The probability of event NOSTOP is assessed to be 2.58×10^{-3} per demand (value of NOSTOP.CAF, CRWMS M&O 1997b, Att. V). In that model, the failure to apply brakes is dominated by the human error probability.

The probability of hardware failures that contribute to the probability of event NOSTOP was calculated to be 8.10×10^{-5} per demand (value of the top event named NOSTOPHW.CAF, CRWMS M&O 1997b, Att. V). The probability of NOSTOPHW.CAF is dominated by two causes: the independent failure of the air-brake control valves in both locomotives (2.69×10^{-5} per demand) and the CCF of the two valves at 5.19×10^{-5} per demand.

Section 6.8.3.2 discusses the effects of incorporating one or more electronic systems to reduce the probability of the failure of human operators to stop the runway and incorporation of other potential design concepts to reduce the probability of hardware failures.

Need Ref For Tree →

Fault Tree for Runaway Event–The frequency of the top event "Runaway Occurs on the North Ramp" was calculated to be 5.88×10^{-4} per year (the product of events INIT_RA and NOSTOP). This value is very similar to that reported in Section 6.8.2.2.1 and is more than two orders of magnitude above the threshold for credible DBEs. To achieve a frequency of 1.0×10^{-6} per year or less, a reduction factor of at least 1.70×10^{-3} is required (1.0×10^{-6} per year divided by 5.88×10^{-4}).

.228 × 2.58 E-3 ✓

The FTA (CRWMS M&O 1997b) also provides sensitivity analyses for some alternative models of the failure to apply brakes, as summarized below.

1. Reduced redundancy of intra-vehicle brake components. This modification insignificantly increased the probability of hardware failure, from 8.09×10^{-5} to 8.16×10^{-5} per demand and did not affect the frequency of runaway that was dominated by human error probability.

2. Using a single locomotive. This resulted in a significant change to 5.28×10^{-3} per demand in the hardware contribution, dominated by the failure of the single brake control valve. This change brought the hardware contribution to the same order of magnitude as the human error contribution and doubled the frequency of runaway.

3. Adding a redundant brake control valve to one locomotive in a one-locomotive train. Including CCF effects, the probability of hardware failure dropped to 5.46×10^{-4} per demand. This resulted in a small increase in runaway frequency relative to the baseline case.

4. Adding redundant brake control valves to a two-locomotive train. Including CCF effects of intra- and inter-locomotive, the probability of hardware failure is 5.22×10^{-5} per demand, which is a small improvement over the baseline case with virtually no effect on the runaway frequency that was dominated by human error probability.

Based on prior FTAs and sensitivity studies, it was concluded that the transporter runaway could not be screened on a frequency basis.

6.8.3 Fault Tree Analysis of Runaway Frequency Using Alternative Designs

As noted in Section 6.8.2.2.1, the results of the previous fault-tree analysis predicted a runaway frequency of 5.88×10^{-4} per year. This suggests that some design alternative must be provided to bring the frequency to $1.0\square10^{-6}$ per year or lower. The analysis considers several design alternatives that either reduce the likelihood of initiating a runaway or reduce the probability of failing to stop a runaway.

The present analysis builds on the models and insights gained from the prior studies (Assumption 5.7) to provide a preliminary evaluation of the following design alternatives (Assumption 5.9):

- Enhanced on-board systems.
  - Electronic interlock (or permissive) to ensure that dynamic brakes are engaged or service brakes are set in a drag mode before an operator can start the train down the North Ramp.
  - Alarm to alert operator when train speed exceeds normal operating range or the train is accelerating.
  - Automatic actuation of service brakes to control normal descent, with human drivers and operators providing backup actuation.
  - Automatic actuation of emergency brakes, with human drivers and operators providing backup actuation.
  - Redundant and diverse brake systems on transporter car: A hydraulic-operated disk brake system provides backup to the air-release brakes on the locomotives and transporter car.

- Redundant and diverse hydraulically actuated disk brake caliper systems on locomotives (in addition to dynamic braking system).

- Out-board system: A track-mounted speed retarder system that maintain the speed of an unbraked train to a predetermined maximum (well below the critical derailing speed) before the train enters a curve.

The evaluation of the effect of each alternative (or combination of alternatives) was based on a quantification of new fault trees that represent, respectively, the event "Runaway Initiated" (top event labeled "INIT_ALT" in Figure 23 and "Failure to Apply Brakes After Runaway Initiation" (top event labeled "NOSTOP" in Figure 24 or "NOSTOP_k" in Figure 25 through Figure 27, where *k* represents a design alternative). Each of the new fault trees is based on the prior analysis presented in *Application of Logic Diagrams and Common-Cause Failures to Design Basis Events* (CRWMS M&O 1997b, Att. I and II, respectively)

6.8.3.1 Evaluation of Design Alternative to Reduce the Frequency of Initiation

Figure 23 displays a fault tree model for the initiation of a runaway. The top event is labeled "INIT_ALT" and is a modification of the fault tree for top event "INIT_RA" (CRWMS M&O 1997b, Att. I). The top event is resolved through an OR gate so that the top event occurs when either one or both of two input events occur. One input event is "Runaway Initiated by Human Error" (HUM_ALT) and the other input event is "Runaway Initiated by Hardware Failures and Failure of Automatic Speed Controller" (INIT_HWC). The fault tree for INIT_ALT incorporates three potential electronic features that could be incorporated into the design. The first is an interlock (or permissive) that requires that dynamic or drag brakes be engaged before the human operator is allowed to initiate the train's descent. The second is an alarm that alerts the on-board and control-room operators if the train speed exceeds the maximum permissible operational limit, or is accelerating while on the down grade. Finally, the third is an automatic speed controller or brake actuation system that applies service brakes when the speed approaches the maximum speed for normal descent. The latter is assumed (Assumption 5.11) to be independent of the alarm to the operators in this fault tree model.

Sub-tree HUM_ALT–The event HUM_ALT has three inputs via an AND gate. All three events must occur before a runaway is initiated by a human operator. One input event in "Runaway Condition Created–Initial Human Error" (INITIALHE) that was defined in the original fault tree as a composite of several potential ways to initiate a runaway in a manually controlled system for driving the train and for applying brakes. This composite operator error was included the failure to engage the dynamic brake. The event INITIALHE was estimated to have a frequency of 0.456 per year (CRWMS M&O 1997b, Att. III) and was the dominant contributor to the frequency of runaway in the prior analysis.

.228

Another input event to HUM_ALT is the event "Failure of Interlock–No Descent Without Dynamic Brake" (INTERLOCK). This event represents the addition of a postulated design feature that assumes (Assumption 5.9) that the descent will be controlled, with gravity being the primary motive force. If a dynamic or regenerative brake is incorporated in the design, the proposed interlock will ensure that that brake system is actuated. (If dynamic brakes are not incorporated, then operating procedures are expected to require that the service brake be set to

provide some prescribed amount of drag during the descent, pulsed if necessary to prevent heat-up and brake fade.) This interlock will ensure that the human cannot drive the train down the ramp in an uncontrolled or hazardous manner. The probability of failure was estimated to be the same as other single-channel solid-state logic modules applied in the prior FTA, with a value of 1.65×10^{-6} per demand (see Table 10) (CRWMS M&O 1997b, Att. III, Item 10).

The second postulated design feature assumes that an alarm will be provided to alert the onboard and control-room operators if the train speed exceeds the normal operating limit, or the train is accelerating (Assumption 5.9). The influence of this design feature is represented in the third input to the AND gate to event INIT_ALT as the event "Initial Human Error Not Recovered in Time to Prevent Runaway" (RECOV_ALT). This event replaces the event RECOVER in the original INIT_RA fault tree that represented a non-alarmed situation (CRWMS M&O 1997b, Att. I). The event RECOV_ALT is resolved via an OR gate to represent the two possible failure situations: (1) event OP_ALARM which represents the failure of the operators to respond to the alarm and take correct and timely actions to stop the runaway, and (2) the event OP_ALFIL which represents the situation where the alarm system fails AND the operators fail to diagnose the situation in time to take action to stop the runaway. A probability of 1.0×10^{-4} is assigned to event OP_ALARM based on estimates of human error probabilities (HEPs) in response to a single alarm (Swain and Guttmann 1983, Table 20-23). The event ALARM, "Alarm System Fails," is assigned a value of 5.5×10^{-7} (1.0×10^{-6}/hr × 0.55 hr) exposure duration during descent. Alarm failure rates are per *Generic Component Failure Database* (Eide and Calley 1993). Given that the alarm has failed, a conditional probability of operator failure to recover of 0.5 is assigned to event OP_NOALARM and is the same value assigned to event RECOVER in the original fault tree (CRWMS M&O 1997b, Att. I). The probability of event RECOV_ALT is approximately 1.0×10^{-4}. If the alarm feature is not provided, the value of RECOV_ALT would be approximately 0.5.

× 45 t event / yr

Table 10. Definition, Probabilities, and Bases for Basic Events Shown in Fault Trees

Event Name	Type of Event	Probability	Description	Basis
AUTODET	Basic	1.82×10^{-7}	Failure of Automatic Speed & Brake Actuation System to Apply Service Brakes	Assumption 5.11
BKVALV1	Basic	5.19×10^{-3}	Control Valve Fails to Release Air Pressure in Brake Line of Locomotive 1 and Transporter	CRWMS M&O 1997b, Att. III, p. 2
CCBCYLAL	Basic	1.04×10^{-7}	CCF of Brake Cylinders on All Vehicles (Air Brake System)	CRWMS M&O 1997b, Att. III, p. 2
CCFALL	Undeveloped	3.60×10^{-6}	CCF Brake Mechanisms All Vehicles (Air Brake System)	Summary of sub-tree in CRWMS M&O 1997b, Att. II, p. 2; probability based on dominant basic event (CCSPRGALL)
COM_CRLOCO	Undeveloped	0.00	Failure of Communications Link: Main CR to Train	Shown as undeveloped event in CRWMS M&O 1997b, Att. III, p. 3. Not quantified; shown for completeness

(Per demand)

(1.7E-3 in 1997c)

Event Name	Type of Event	Probability	Description	Basis
CR_OPFAIL	Basic	5.00×10^{-2}	Control Room Operator Fails to Detect, Diagnose, & Apply Service Brake	CRWMS M&O 1997b, Att. III, p. 3
HARDWR	Undeveloped	8.09×10^{-5}	Failure of Service Brake Hardware – All Three Vehicles (Air Brake System)	Summary of tree in CRWMS M&O 1997b, Att. II, p. 3; Quantified from NOSTPHW.CAF in CRWMS M&O 1997b, Table V-1
HARDHYD	Basic	5.19×10^{-3}	Failure of Hydraulic Disk Brakes on Transporter	Assumption 5.12
OB_DRIVER	Basic	5.00×10^{-2}	On-Board Driver Fails to Apply Service Brakes	CRWMS M&O 1997b, Att. III, p. 4
NOSTOP_R	Undeveloped	2.58×10^{-3}	Failure to Apply Brakes After Runaway Initiation	Summary of top event NOSTOP per CRWMS M&O 1997b, Att.II, p. 1
RETARD	Basic	Goal of 1.70×10^{-3},	Failure of Hydraulic Retarders to Slow Train	See text, Section 6.8.3.4
INIT_RA	Top	2.28×10^{-1}/yr	Runaway Initiated	CRWMS M&O 1997b, Att. I
INIT_ALT	Top	7.38×10^{-10}/yr	Runaway Initiated	Proposed design alternatives incorporated into fault tree, Assumption 5.9
HUM_ALT	Sub-tree	7.52×10^{-11}/yr	Runaway Initiated by Human Error	Includes credit for interlock and alarms; Assumption 5.9
INITIALHE	Undeveloped	0.446/yr possible error	Runaway Condition Created – Initial Human Error	Based on baseline model in logic study CRWMS M&O 1997b
RECOV_ALT	Sub-tree	1.00×10^{-4}	Initial Human Error Not Recovered in Time to Prevent Initiation	Includes credit for alarm to alert operator; Assumption 5.9
OP_ALARM	Basic	1.00×10^{-4}	Operator Fails to Respond to Alarm	Human error probability, Swain and Guttmann 1983, Table 20-23
ALARM	Basic	5.5×10^{-7}	Alarm System Fails	Section 6.8.3.1
OP_NOALARM	Basic	0.5	Operator Fails to Diagnose and Respond in Time	Section 6.8.2.2.2
INIT_HWC	Sub-tree	6.62×10^{-10}/yr	Runaway Initiated by Hardware Failure and Failure of Automatic Speed Controller	Assumption 5.8
AUTSPD1	Basic	1.65×10^{-6}	Failure of Automatic Speed Controller or Service Brake Actuator	Assumption 5.8 and auto speed; based on a single-channel system.
INIT_HDW	Sub-tree	4.01×10^{-4}/yr	Runaway Initiated by Hardware Failure	Based on baseline model in logic study
INICONTR	Undeveloped	7.52×10^{-5}/yr	Malfunction in Computerized Control System	Based on baseline model in logic study
INITCOMM	Undeveloped	7.52×10^{-5}/yr	Runaway Initiated by Malfunction in Communication System	Based on baseline model in logic study
INELECT	Undeveloped	2.51×10^{-4}/yr	Runaway Initiation – Malfunction in Electric System	Based on baseline model in logic study
INTERLOCK	Basic	1.65×10^{-6}	Failure of Interlock: No Descent Without Dynamic Brakes	Assumption 5.8 and auto speed; based on a single-channel system.

The calculated frequency of the event HUM_ALT with all three design features is evaluated to be 7.52×10^{-11} per year. Although such a low frequency estimate may be viewed with suspicion since the model is based on preliminary and incomplete design data, it nevertheless illustrates that the likelihood of the human initiation of a runaway can be reduced substantially below the conservative value presented in the original analysis. Alternatively,

- If the operator alarm feature is not provided, the frequency of HUM_ALT would increase to about 3.76×10^{-7} per year; or
- If the interlock feature is not provided, the frequency of HUM_ALT would increase to about 4.46×10^{-5} per year.

Both results are significantly less probable than the value of 0.228 per year that was used in original analysis (CRWMS M&O 1997b, Att. I).

Sub-tree INIT_HWC–The event "Runaway Initiated by Hardware Failure and Failure of Automatic Speed Controller" (INIT_HWC) is developed as an AND gate having two inputs. The input INIT_HDW represents, through an OR gate, three ways by which malfunctions in electrical, manually actuated electronic control, or control-room-to-locomotive communications system could initiate a runaway independent of operator actions. As illustrated in Figure 23, the frequency of event INIT_HDW is estimated to be 4.01×10^{-4} per year. In the prior FTA (CRWMS M&O 1997b, Att. I), these three potential initiators were input directly to the event INIT_RA through an OR gate. They were evaluated to be less likely initiators than the human caused runaway in that analysis. Given the low value that appears achievable for the frequency of HUM_ALT, as described above, the hardware contribution to runaway initiation would now be the dominant contributor.

If an independent automatic speed control system were incorporated into the design, the hardware contribution could be reduced. The event AUTSPD1 represents this design feature as the second input to the AND gate of event INIT_HWC. A failure probability of 1.65×10^{-6} per demand is assigned to the event AUTSPD1. This is the value used in the prior fault tree models and elsewhere in the present analysis as a representative value for a single-channel solid-state logic module (see Table 10).

The calculated frequency of the event INIT_HWC is 6.62×10^{-10} per year. Although such a low frequency estimate may be viewed with suspicion since the model is based on preliminary and incomplete design data, it nevertheless illustrates that the likelihood of runaway due to malfunctions in electronic or electrical systems can be reduced substantially below the conservative value presented in the prior studies.

Top-event INIT_ALT–The frequency for the event "Runaway Initiated" (INIT_ALT) is the sum of the frequencies of the events HUM_ALT and INIT_HWC. The frequency is 7.38×10^{-10}, with the major contribution being from the hardware failures. As noted above, such low values must be used with caution since they are based on incomplete design information, but they do support the position that both human- and hardware-caused initiators can be made very unlikely.

The sensitivity of results to the postulated design features are summarized in Table 11. It is noted that the effect of using none or only one of the potential design alternatives is the following:

- If none of the alternatives are provided, the frequency of HUM_ALT would be about 0.228 per year, as would the event INIT_HUM, and would dominate the top event INIT_ALT frequency of about 0.228 per year. This is the baseline case.

- If only the operator alarm is provided, the frequency of HUM_ALT would be about 4.56×10^{-5} per year and hardware failures would dominate the top event INIT_ALT frequency of about 4.47×10^{-4} per year;

- If only the interlock is provided, the frequency of HUM_ALT would be about 7.52×10^{-7} per year and hardware failures would dominate the top event INIT_ALT frequency of about 4.02×10^{-4} per year;

- If only the automatic speed controller is provided, the frequency of INT_HWC would be about 4.01×10^{-4} per year, but event HUM_ALT would be about 0.228 per year and would dominate the top event INIT_ALT frequency of about 0.228 per year.

It is observed that the most effective way to reduce the frequency of initiation is to reduce the probability of human error.

Table 11. Results of Fault Tree Analysis for Frequency of Initiation

Design Feature for Aiding Operator	INIT_HUM (events per year)	INIT_ALT, No Speed Controller (events per year)	INIT_ALT, With Speed Controller (events per year)
Manual Control (Baseline)	0.228	0.228	0.228
Alarm, No Interlock	4.56×10^{-5}	4.47×10^{-4} (1)	4.56×10^{-5} (2)
Interlock, No Alarm	7.57×10^{-7}	4.02×10^{-4} (1)	7.53×10^{-7} (2)
Interlock + Alarm	7.57×10^{-11}	4.01×10^{-4} (1)	7.37×10^{-10} (2)

6.8.3.2 Evaluation of Design Alternative to Reduce the Probability of Failure to Stop

As a baseline for the evaluation of design alternatives, a simplified version of the fault tree for the top event "NOSTOP" was derived from the detailed fault tree presented in *Application of Logic Diagrams and Common-Cause Failures to Design Basis Events* (CRWMS M&O 1997b, Att. II). The failure logic for the top event, as established in *Application of Logic Diagrams and Common-Cause Failures to Design Basis Events* (CRWMS M&O 1997b, Att. II), is that the brakes on all three vehicles (both locomotives and the WP Transporter) have to fail concurrently during the time that the train is descending the North Ramp.

The simplified fault tree is shown in Figure 24. The details of the original tree, which has multiple levels of logic gates and runs for 19 pages, have been suppressed below the first or second level of logic gates, and the diagram now fits on one page. The legend shown in Figure 27 explains the symbols used in all of the fault trees presented in this section.

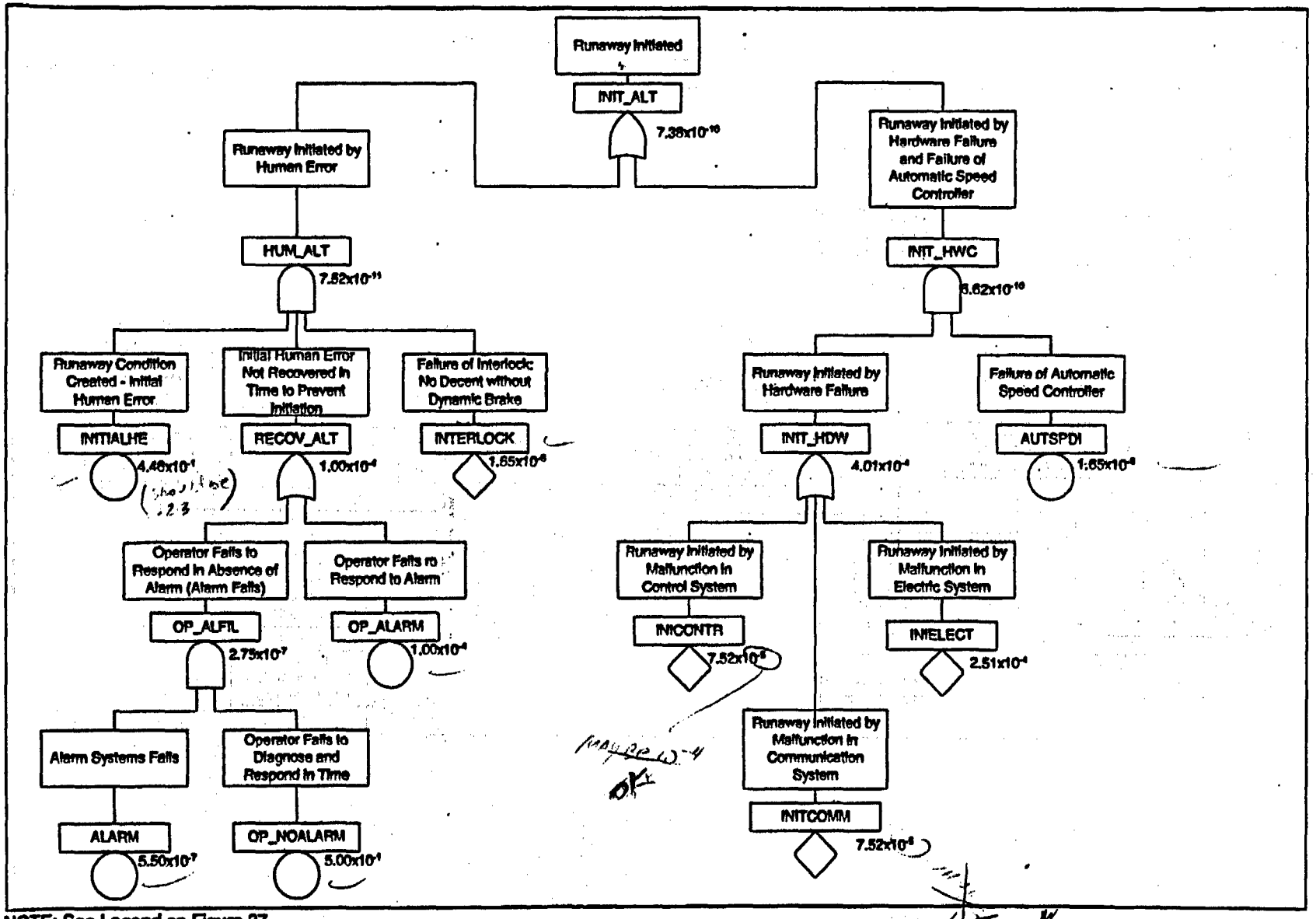

NOTE: See Legend on Figure 27

Figure 23. INIT_ALT – Runaway Initiated

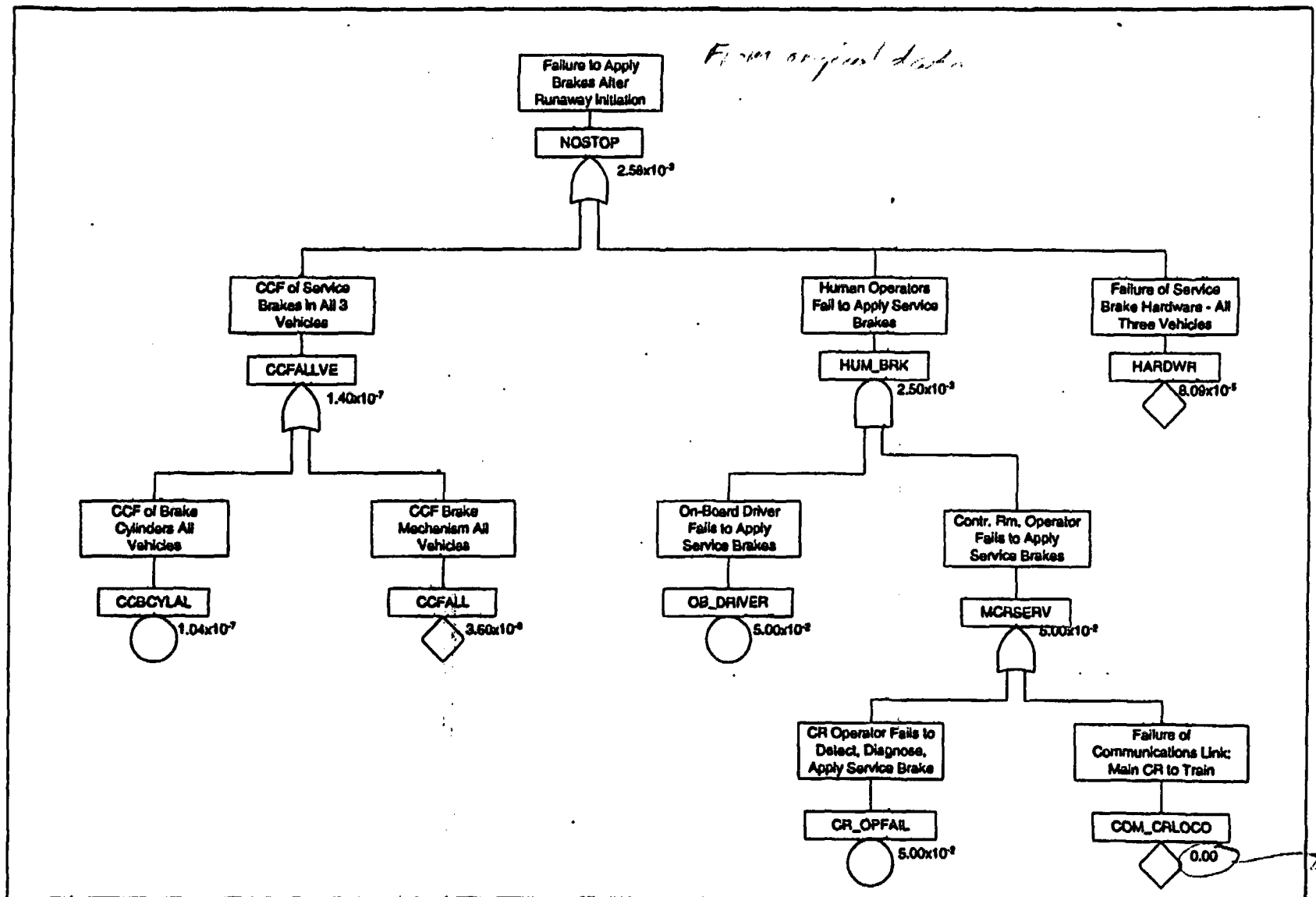

NOTE: See Legend on Figure 27

Figure 24. NOSTOP Baseline

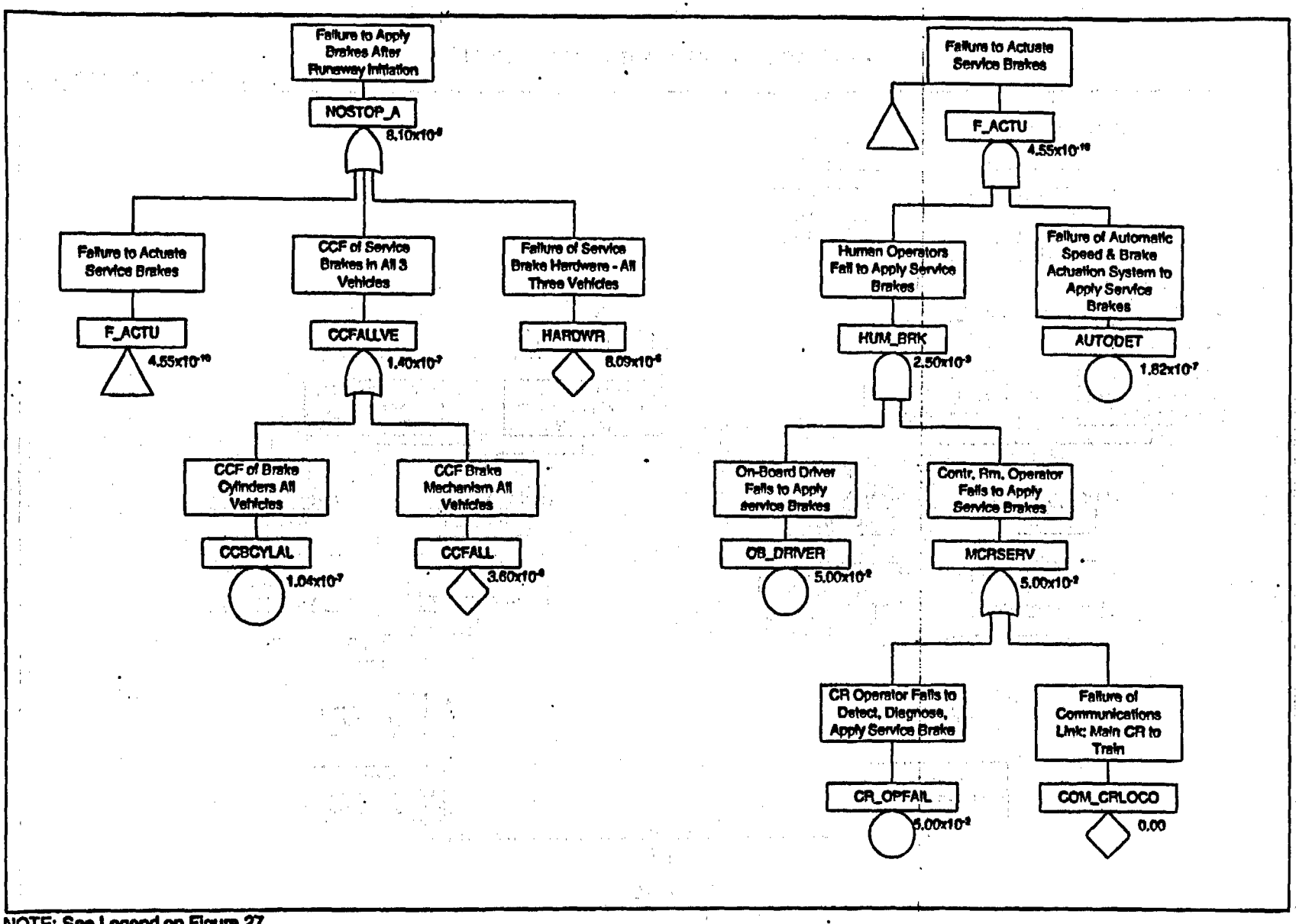

NOTE: See Legend on Figure 27

Figure 25. NOSTOP_A with Automatic Brake Actuation

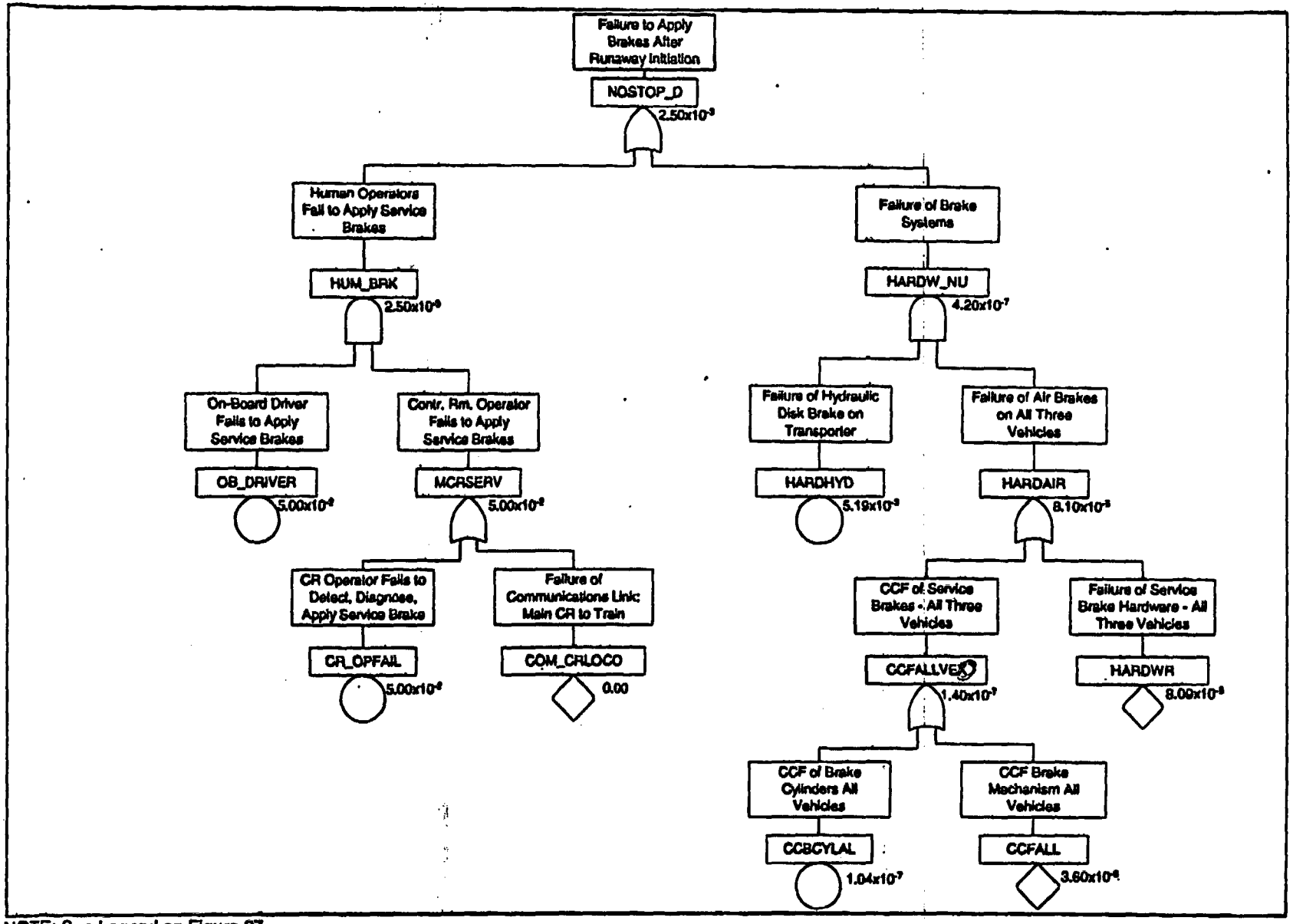

NOTE: See Legend on Figure 27

Figure 26. NOSTOP_D with Hydraulic Disk Brakes

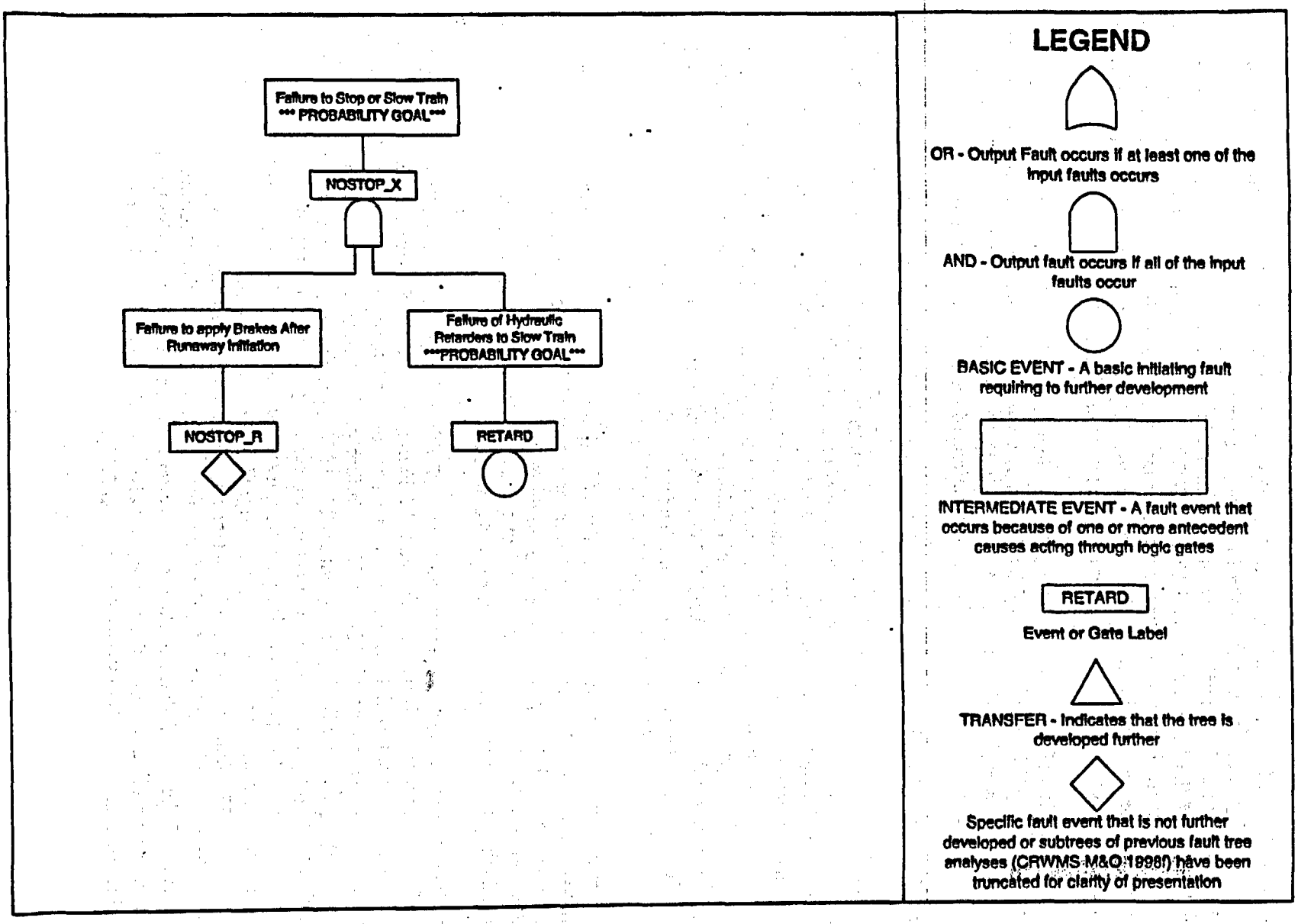

Figure 27. NOSTOP_X with Hydraulic Retarders

The definitions of the events represented by the basic, undeveloped, and intermediate events (represented by logic gates) are shown in the text boxes in Figure 24. The values and bases for the basic events and undeveloped events are shown in Table 10. For the present analysis, the probabilities of the basic events and CCFs (CRWMS M&O 1997b, Att. III) are shown in the fault tree figures. The probabilities were propagated up through the various gates by hand calculations (i.e., adding inputs to OR gates and multiplying inputs to AND gates). The values for the baseline evaluation are shown in the gate labels in Figure 24.

The quantification of the top event NOSTOP is shown to be 2.58×10^{-3}, and is the value presented for NOSTOP.CAF in *Application of Logic Diagrams and Common-Cause Failures to Design Basis Events* (CRWMS M&O 1997b, Att. V, p. V-1). The evaluations of the design alternatives, described in later sections, are based on modifications of the baseline fault tree.

6.8.3.2.1 Fault Tree Analysis of Automatic Emergency Brake Application

The probability of the top event NOSTOP is shown to be 2.58×10^{-3} (NOSTOP.CAF, CRWMS M&O 1997b, Att. V, p. V-1). Inspection of the cut sets listed in *Application of Logic Diagrams and Common-Cause Failures to Design Basis Events* (CRWMS M&O 1997b, Att. V, p. V-2) shows that the probability of NOSTOP is dominated by the failure of both the on-board drivers and control room operators to react to the runaway and apply the service brakes. The probability of that event HUM_BRK, "Human Operator Fails to Apply Service Brakes," was estimated to be 2.5×10^{-3} per demand in the original FTA. When the human error contribution was suppressed in a sensitivity study, the contribution from hardware failures only was shown to be 8.09×10^{-5} (NOSTOPHW.CAF, CRWMS M&O 1997b, Att. V, p. V-1).

Rather than rely on human response to detect and react to an excess speed condition, an alternative design would add instrumentation and control logic to the locomotive systems to sense runaway and to apply emergency braking using the service brake system and/or a dedicated emergency brake system (Assumption 5.11). The drivers and operators would provide diverse backup to the automatic detection and actuation.

To model the modified system, a new fault tree is developed (top event named "NOSTOP_A") in Figure 25. In the new fault tree, the F_ACTU ("Failure to Actuate Service Brakes") is an AND gate that has the event HUM_BRK ("Human Operators Fail to Apply Service Brakes") as one input and a new event labeled AUTODET ("Failure of Automatic Speed and Brake Actuation System to Apply Service Brakes"). Event HUM_BRK represents the failure of human operators to provide backup actuation should the automatic system fail. Event AUTODET represents the effects of failure of the proposed design alternative. The event AUTODET includes only the detection and logic hardware that outputs a signal to the brake control system. It is assumed (Assumption 5.11) that the automatic detection system has two-channel redundancy and is subject to both independent and CCF of the two channels. Since the electronic systems and components of the speed-detection/actuation system are expected to be similar to the control system in the baseline system, the value 1.82×10^{-7} per demand is used as an estimate of the probability of event AUTODET (see Assumption 5.11).

The probability of F_ACTU in Figure 25 is the product of probabilities of AUTODET and HUM_BRK, which gives about 4.54×10^{-10} ($1.82\times10^{-7} \times 2.5\times10^{-3}$). The gate HARDWR is assigned the probability of 8.09×10^{-5} per demand based on the value of NOSTOPHW.CAF (CRWMS M&O 1997b, Att. V), which represents the hardware contribution. From Figure 25, it can be seen that the probability of the top event (labeled NOSTOP_A) is about 8.10×10^{-5} with the dominant contributors being hardware failures (event HARDWR plus a small contribution of 1.40×10^{-7} from the CCF event CCFALLVE, "CCF of Service Brakes in All 3 Vehicles").

The frequency of runaway is re-evaluated to be 1.84×10^{-5} per year as the product of the original initiation frequency INIT_RA (2.28×10^{-1}/yr) and the probability of NOSTOP_A (8.09×10^{-5}). It should be noted that if the waste package emplacement rate is changed from 456 to 524 per year, the frequency of runaway becomes 2.11×10^{-5} (1.84×10^{-5} per year × 524/456). This evaluation indicates that it may not be possible to drive the event frequency to below the 1.0×10^{-6} per year threshold for DBEs by the addition of an automatic emergency brake actuation system alone, since in this evaluation of a single design alternative, the frequency of initiation due to human error remains high.

6.8.3.2.2 Fault Tree Analysis of Redundant and Diverse Brakes on Transporter Car

This potential design modification was suggested in *Waste Package Transporter Design* (CRWMS M&O 1998a, Section 7.3.9). The redundant system is a hydraulically actuated disk brake system, with disks mounted on two axles of the transporter (see Assumption 5.9). Brakes are applied by the positive motion of hydraulic cylinders. The hydraulic master cylinder and control are located on the primary and secondary locomotives. Because the system works on a different principle than the air-release primary service brake and uses fluid lines and controls that are separate from the primary brake system, it is diverse and essentially redundant to the primary system.

To evaluate the effect of the proposed design alternative, a new fault tree was developed for the top event "NOSTOP_D," as shown in Figure 26. The fault tree was structured to evaluate the effect of using disk brakes on the transporter. The fault tree shown in Figure 26 features the following:

- Event HARDW_NU ("Failure of Brake Systems) is input to the top event NOSTOP_D.
- HARDW_NU is an AND gate with the inputs:
  - A new event HARDHYD "Failure of Hydraulic Disk Brakes on Transporter."
  - A new OR gate HARDAIR "Failure of Air Brakes on All Three Vehicles."
- The inputs to HARDAIR are the original events HARDWR (8.09×10^{-5}) and CCFALLVE (1.40×10^{-7}), which represents the CCF of the air brake systems and does not include any failures of the hydraulic disk brake system.

To evaluate the effect of using the hydraulic system, the probability of event HARDHYD is estimated to be about 5.19×10^{-3} per demand, the same as the event SBTRANSP ("Failure to Apply Service Brake Transporter") of the original NOSTOP fault tree (see Figure 24). Since there are no design details, it is assumed in Assumption 5.12 that the failure modes and

probabilities of the two kinds of mechanical systems are similar, but independent. The failure of the single airline control valve was the dominant independent failure at 5.19×10^{-3} per demand (see Table 10 and Assumption 5.12). It is assumed (Assumption 5.12) that a control valve in a hydraulic brake system will have a similar failure probability as its counterpart valve in the air brake system.

The event HARDW_NU is evaluated to be about 4.20×10^{-7} per demand ($8.10\times10^{-5} \times 5.19\times10^{-3}$). In actuality, it is unlikely that a failure probability lower than 1.0×10^{-6} per demand can be achieved even with a diverse and redundant brake system because some other failure mode, previously negligible and not modeled, may become important and dominant. The fault tree of Figure 26 does not model any CCFs that are common to both the hydraulic and air systems. This ignores a small contribution to the expected failure probability for the hardware, but this effect is not important, as noted below..

The effect of adding a diverse, redundant, hydraulic brake system to the two locomotives, as well as to the transporter car, would show a similar reduction in the probability of failure of the mechanical portions. Further, if the hydraulic brake of the primary locomotive is interconnected to and actuates that of the transporter car, the effect is one of having two diverse and fully redundant service brake systems: air and hydraulic. The hydraulic brake system is subject to intra-system CCFs, similar to those modeled for the air brakes in Figure 25. As noted above, the probability of failure of the air brake hardware was estimated to be 8.1×10^{-5} per demand. The probability of concurrent failure of the two systems, including their respective intra-system CCFs, but no inter-system CCFs, is estimated to be the product of the respective probabilities as 7.2×10^{-9} per demand, i.e., $(8.1\times10^{-5})^2$. It is possible that some inter-system CCF mode may be identified that would cause concurrent failure of both the air and the hydraulic brake systems, and would increase the probability above the 7.2×10^{-9}. However, the net probability should remain sufficiently low.

Evaluation of the top event NOSTOP_D gives a probability of 2.58×10^{-3} and is dominated by the event HUM_BRK, the failure of the humans to actuate the brakes. Therefore, reducing the probability of hardware failures alone will not be effective in reducing the probability of NOSTOP_D and the frequency of a runaway is not reduced. Therefore, there appears to be no advantage of using the diverse brake system, by itself, unless the contribution from human error is significantly reduced.

6.8.3.2.3 Fault Tree Analysis of Combined Alternatives: Automatic Actuation and Diverse Brake System

Table 12 summarizes the probabilities for the baseline NOSTOP and the alternatives NOSTOP_A and NOSTOP_D. The value for NOSTOP_A is the least (8.10×10^{-7}), but is too high to reduce the frequency of runaway to less than 1.0×10^{-6} per year. Therefore, the FTA was extended to evaluate the effect of combining the effects of the automatic actuation and using diverse brakes on the transporter. In this case, the probability of NOSTOP would be evaluated as the sum of two very small probabilities, F_ACTU (4.55×10^{-10}) from Figure 25. and HARDW_NU (4.20×10^{-7}) from Figure 26. As shown in Table 12, the sum is about 4.20×10^{-7} per demand, which is dominated by hardware failures. The estimated frequency of runaway becomes 9.59×10^{-8} per year; i.e., the product of the initiation frequency INIT_RA (2.3×10^{-1}/yr)

and the probability of failing to stop of 4.20×10^{-7} per demand. It should be noted that if the emplacement rate is changed from 456 to 524 per year, the frequency of runaway becomes 1.10×10^{-7} (9.59×10^{-8}/yr × 524/456). This frequency is well below the cutoff of 1.0×10^{-6} per year for credible events. If a redundant and diverse disk brake system is added to both locomotives, the probability of HARDW_NU would be even less. Although other failure modes, which are not included in the present analysis, may be discovered in analyses of actual system designs, it appears feasible to incorporate design features into the design of the transporter train brake, control, and communications systems. These design features will ensure that the frequency of a runaway (uncontrolled descent) is less than 1.0×10^{-6} per year, even when the frequency of initiation remains at 2.3×10^{-2} per year; i.e., without design alternatives to reduce the human errors in initiation.

Table 12. Results of Fault Tree Analyses for Failure to Apply Emergency Brakes

Design Feature for Applying Emergency Brakes	Top Event Name	Top Event Probability per demand	Comment
Manual Actuation, Air Brake Only (Baseline)	NOSTOP	2.58×10^{-3}	Dominated by human error
Automatic Actuation, Air Brake Only	NOSTOP_A	8.10×10^{-6}	Dominated by hardware failures
Manual Actuation, Air Brake + Hydraulic Disc Brake	NOSTOP_D	2.50×10^{-3}	Dominated by human error
Automatic Actuation, Air Brake + Hydraulic Disc Brake	No fault tree, sum of F_ACTU + HARDW_NU	4.20×10^{-7}	Dominated by hardware failures

6.8.3.3 Effects of Combining Design Alternatives to Reduce Initiation and Automatic Actuation of Brakes

The prior sections have examined the effects on runaway frequency that may be achieved by reducing the frequency of initiation or on reducing the probability of failure to stop, i.e., the failure to actuate emergency brakes in a timely fashion. This section evaluates the effects of combining one or more design alternatives as summarized in Table 13.

The first row of Table 13 is the baseline case that features manual control of the descent, including the operation of dynamic brakes or modulated service brakes, and manual actuation of emergency brakes. The frequency of runaway is shown to be 5.88×10^{-4} per year.

The second row of Table 13 illustrates the effect of adding just an alarm to alert the operators to excess speed or acceleration, but maintaining the manual control and manual emergency brake actuation. The frequency of runaway is reduced to 1.18×10^{-7} per year and is much less than the threshold of credibility of 1.0×10^{-6} per year.

The third row of Table 13 illustrates the effect of adding just an interlock that prevents the operators from descending the ramp unless dynamic brakes are engaged (or service brakes set to a pre-determined drag resistance). Otherwise, control remains manual and emergency brake

actuation is manual. The frequency of runaway is reduced to 1.95×10^{-9} per year and is significantly less than the threshold of credibility of 1.0×10^{-6} per year.

The fourth row of Table 13 illustrates the effect of adding both an alarm to alert the operators to excess speed or acceleration but maintaining manual control, and an automatic emergency brake actuation. The frequency of runaway is reduced to 3.69×10^{-9} per year and is significantly less than the threshold of credibility of 1.0×10^{-6} per year.

The fifth row of Table 13 illustrates the effect of adding both an interlock to the dynamic brakes, and an automatic emergency brake actuation. The frequency of runaway is shown to be the exceedingly low value of 6.13×10^{-11} per year. With such a low value, it is possible that some other mechanism for initiating and/or enabling a runaway will be revealed as being more likely.

The evaluations of Table 13 do not include the effects of redundant and diverse hydraulic disk brakes on reducing the probability of failure to stop. NOT TRUE, Per last row (7).

Throughout the present analysis, it is reiterated that reducing the probability of human error can be an effective way to eliminate the transporter runaway event as a credible accident for the MGR. This analysis has demonstrated several potential design alternatives that appear capable of achieving this objective. As the designs of the transporter train and its control and safety systems evolve, fault-tree analysis or other techniques need to be applied to ensure that the frequency of an uncontrolled descent remains less than 1.0×10^{-6} per year.

Table 13. Estimates of Runaway Frequency for Several Alternative Design Features

Design Features	Initiation Frequency per year	Probability of Failure to Stop per demand	Frequency of runaway per year	
Manual control and manual emergency brake application (Baseline)	0.228	2.58×10^{-3}	5.88×10^{-4}	
Alarm on speed, no interlock, manual emergency brake application.	4.56×10^{-6}	2.58×10^{-3}	1.18×10^{-7}	OK
Interlock on dynamic brake, manual emergency brake application.	7.57×10^{-7}	2.58×10^{-3}	1.95×10^{-9}	OK
Alarm on speed, no interlock, automatic emergency brake application.	4.56×10^{-6}	8.10×10^{-4}	3.69×10^{-9}	OK
Interlock on dynamic brake, automatic emergency brake application	7.57×10^{-7}	8.10×10^{-4}	6.13×10^{-11}	OK
Manual control and automatic emergency brake application (air-brake only)	0.228	8.10×10^{-4}	1.85×10^{-4}	
Manual control and automatic emergency brake application (redundant air-& hydraulic brakes)	0.228	4.20×10^{-7}	9.59×10^{-8}	OK 9.59×10^{-8}

6.8.3.4 Fault Tree Analysis of Rail-Mounted Speed Control System

An alternative to improving the reliability of the on-board systems and/or the human operators is to use some external means to slow or stop a train. Among the possible concepts is the hydraulic

speed retarder system described in Section 6.7.2. A series of hydraulic devices are mounted along critical portions (or all) of the rails of the North Ramp. The hydraulic devices are designed, manufactured, and calibrated such that a train rolling over each device at a speed below the pre-set speed feels virtually no retardation. A train having a speed above a pre-set speed, however, must expend kinetic energy to pass over each of the hydraulic units. Every wheel on the entire train on both rails receives some retardation. With a sufficient number of retarders per unit length of rail, a train on the grade of the North Ramp can be made to roll with a constant speed without application of any on-board brakes. The total number of retarders and their spacing have to be determined for the specific weights of the transporter train, the number of wheels, and the speed desired. This section addresses the effect on preventing the transporter runaway event or making it sufficiently unlikely to be considered beyond design basis.

As described, the hydraulic retarder units are essentially passive devices that do not require actuation by operator or electronic control systems. Further, the units do not require any active support systems such as electrical power. Each unit is self-contained and has active components and fluids inside (e.g., hydraulic capsule, precision control valves, oil, and nitrogen gas) that can fail and result in loss of function. The units have to be adjusted or calibrated to achieve a specified design speed. As for any mechanical device, each retarder units is subject to both independent and CCFs of the mechanisms. The vendor recommends a periodic maintenance schedule based on utilization or time; this schedule appears to be aimed at avoiding wear-out failures. No information is available from the vendor regarding the random failure rate experienced in the field.

A fault tree representation that includes the effect of the external system is shown in Figure 27. The top event NOSTOP_X is represented as an AND gate having the inputs NOSTOP_R (which is shown as an undeveloped event to represent an evaluation of the top event NOSTOP in Figure 27) and a new event RETARD (i.e., "Failure of Hydraulic Retarders to Slow Train"). The probability of NOSTOP from the original analysis is 2.58×10^{-3} and was shown to be dominated by human error. The probability of RETARD requires a new calculation and several assumptions not used in the previous analyses. As noted in, the performance goal for RETARD is a failure probability less than 1.70×10^{-3} per demand.

? Based on 5.88×10^{-4} runaway data (Baseline)

In the design specification for the retarder track segment(s), it will be required to have some number N of retarder units to ensure that the train will maintain some desired design speed of V_D, say 8 km/hr (2.22 m/s or 4.97 mph). However, the critical speed for tip-over in the North Ramp Extension Curve, V_C, is shown in Section 6.4.3 to be 31.85 m/s (71.25 mph) and is much greater than V_D. This means that only a certain number (K where $K < N$), of the units have to be functional to provide the safety function; i.e., limit the speed to V_C at the entrance to the curve. Between inspections and repair, several units of the total N may fail to function from both independent and common-cause events. The number K is termed the "success criterion" for the array of retarder units as this is the minimum number of functioning units required to ensure the speed does not exceed V_C. Once K is specified on the basis of slowing requirements, the minimum number of installed retarder units, N_{Min}, is determined from the probability requirements; i.e., that the probability of failure be 0.0017 per demand. It should be noted that the number of installed retarder units may be greater than N_{Min} in order to achieve the design speed V_D.

The fundamental model for computing the value of RETARD is to calculate the probability of failure of a system in which K out of N must function for success. The fundamental model computes the cumulative probability of having $(N\text{-}K)$ or more failures in a binomial failure model where q is the probability that any retarder unit is unavailable (failed) when needed. When N is large (i.e., > 10), the cumulative binomial distribution can be approximated by a normal distribution having a mean and standard deviation. For a given q and a given K, the problem becomes that of determining N such than the probability of having more failures than $(N\text{-}K)$ is 0.0017. This probability model addresses independent failures only. CCFs can be added to the model as discussed at the end of this section.

The function NORMDIST built into Microsoft Excel gives the cumulative probability versus the number of standard deviations beyond the mean number of failures. Therefore, the problem becomes that of finding N_{Min} such that the cumulative probability of $(N_{Min}\text{-}K)$ is less than 0.9983 (i.e., the complement of 0.0017). It is noted that the cumulative distribution reaches 0.9983 at 2.93σ beyond the mean and 0.9987 at 3.0σ. For convenience, the 3.0σ criterion will be applied in the analysis.

The relationship between the parameters becomes:

$$(N-K) = \mu + 3.0\sigma = N \times q + 3.0\sqrt{N \times q} \qquad \text{(Eq. 59)}$$

where:

μ = Statistical mean ($\mu = N \times q$)

σ = Statistical standard deviation ($\sigma = \sqrt{N \times q}$)

The problem is to find N for a given K and q. The solution is by trial-and-error. For illustration, two values of K are used: 100 and 200.

Three values of q are used in the sensitivity study: 0.5, 0.1, and 0.006.

- The values of 0.5 and 0.1 are selected on the following basis:

  1. The manufacturers recommended replacement interval as the lessor of 5 years or 1.5-2 million cycles. The utilization rate for each retarder unit during MGR operations in which about 500 emplacement trips per year are made during the peak years indicates that the refurbishment will be time-limited; i.e., replaced after 5 years. It is assumed (Section 5.12) that the effective failure rate, λ_E, is 0.2 per year (100 percent fail in 5 years) although the random failure rate, λ_R, for such units is expected to be significantly less (see the next bullet).

     grossly conservative

  2. The average unavailability of the device is calculated as $q_{Avg} = \frac{1}{2}\lambda_E \tau$, where τ is the inspection/repair interval. If no inspections or refurbishments are made within the recommended period, the average probability of a unit being unavailable is 0.5; i.e., [½×0.2×5]. This would not be an acceptable situation, but is evaluated to determine its effect on performance. If inspection and repair are made every year, on the other hand, the average unavailability of each unit is approximately $q_{Avg} = 0.1$, i.e., ½×0.2×1.

- The value of 0.006 is selected on the following basis:

  1. It is noted that manufacturers' recommendations for replacement provide a margin to the time or condition when wear-out failures (end of useful life) are expected to begin. Prior to reaching the point of incipient wear-out conditions, the unit failure rate λ_R, due to random failure, is usually small.

  2. Failure rate data for hydraulic actuators gives a mean of 0.29 per million hours and a 60 percent-confidence range of 0.057 to 0.88 per million hours (Arno 1981, p. 24). For a mission time of 5 years, the unavailability [$q_{Avg} = \frac{1}{2}\lambda_E \tau$] of any retarder unit ranges from 0.0012 to 0.0192, with a mean of 0.006. In the sensitivity analysis, it is assumed (Assumption 5.10) that the random failure rate for a retarder unit is similar to that of the generic hydraulic actuator to contrast the results to the baseline FTA. Table 14 summarizes the results of the sensitivity study.

Table 14. Number of Total Retarder Units Required to Meet Probability Goal

K, Minimum Number of Functioning Retarder Units	Average Unavailability Factor q_{Avg} for Each Retarder Unit		
	0.5	0.1	0.006
100	270	123	103
200	495	239	205
300	714	354	306

The first column lists the number of retarder units required to ensure the speed does not exceed V_C. The entries in each row indicate the minimum number of installed retarder units to achieve a failure probability $\leq 1.7\times10^{-3}$ per demand as a function of the unit unavailability factor, q_{Avg}. The results demonstrate that it is feasible to use an array of retarder units to achieve the probability goal, even for relatively high unavailability of individual units. For example, in the case of q_{Avg} of 0.5 (undesirable), the array must have more than twice the number of units required to ensure the critical speed V_C is not exceeded; i.e., $N \geq 270$ for $K = 100$, $N \geq 495$ for $K = 200$, and $N \geq 714$ for $K = 300$. For the case of $q_{Avg} = 0.1$, N must exceed K by about 20 percent to achieve the probability goal. For the case of $q_{Avg} = 0.006$, N must exceed K by about 3 percent.

CCFs can be included in the model to give more conservative requirements for the number of installed units and for unit unavailability. If a simple beta-factor model is applied, the unit unavailability factor is the only parameter to be controlled, since in the beta-factor model all of the installed units are unavailable on demand. This is a useful CCF scoping model for systems having a few redundant units (e.g., 2 to 4), but is viewed as too conservative (and even unrealistic) for a system having 10 or more redundant units. Since the retarder array is expected to have hundreds of units, the beta-factor method is not appropriate except as a conservative basis for a scoping analysis.

In the beta-factor model (CRWMS M&O 1997b, Section 3.2.1), the failure rate for CCFs is assumed to be a fraction of the total failure rate for one unit. For the scoping analysis of the

hydraulic retarders, β is assumed to be 0.1 (Assumption 5.10) so that $\lambda_{CCF} = 0.1\lambda_R$ and $q_{CCF} = \frac{1}{2}\lambda_{CCF} \times \tau$, which is applied to the entire system of N units, irrespective of the value of N. The performance goal for q_{CCF} is 1.7×10^{-3} per demand. Using the value $\lambda_R = 0.29$ per million hours gives $\lambda_{CCF} = 0.029$. Assuming an inspection time $\tau = 5$ years (43,800 hours) gives $q_{CCF} = 6.4\times10^{-4}$ per demand which is better than the goal of 1.7×10^{-3} per demand. This analysis indicates that the system failure probability of a retarder system should be acceptable if the unit failure rate is at least as low as for typical hydraulic units, even under the assumption of CCF of the entire array.

Inasmuch as the analyses have shown that the frequency of runaway can be brought to less than 1.0×10^{-6} per year using reliable electronic interlocks, alarms, and/or automatic brake actuation systems, the track-mounted speed retarder system is unlikely to be necessary, but could provide defense-in-depth.

INTENTIONALLY LEFT BLANK

7. CONCLUSIONS

The maximum speed determined for a runaway WP Transporter and two locomotives under frictionless and standard rolling resistance conditions was high. From Scenario 1, an uncontrolled descent that initiates near the top of the North Ramp (Point A) would likely result in the WP Transporter tipping over within the North Ramp Extension Curve. The maximum runaway speeds of 33.25 m/s and 30.82 m/s for frictionless and standard rolling resistance conditions are within 10 percent of the tip-over speed of 31.85 m/s (71.25 mph) and, therefore, it can be estimated that the WP Transporter will tip-over within the North Ramp Extension Curve.

For Scenarios 2, 3, and 4, only standard rolling resistances were used to determine the maximum runaway speed. Scenario 2 initiates at an arbitrary point along the North Ramp. From this point, the WP Transporter is able to negotiate the North Ramp Extension Curve, and exits the curve (Point D) at a speed below the tip-over speed. The transporter continues down the North Ramp Extension, a –2.06 percent downward grade, and tips over in the 305-m radius S-curve (Point G) at a speed of 35.61 m/s.

Scenario 3 initiates from Point C with an initial velocity of 8 km/hr. The WP Transporter is below the tip-over speed as it travels through the 305-m radius S-curve located between Point G and Point I. The transporter remains below the tip-over speed as it travels down the North Main Curve to Point K. At this point, the downward grade transitions to a positive grade. The transporter reaches a maximum velocity of 28.47 m/s, which is below the tip-over speed.

Scenario 4 initiates from Point A with an initial velocity of 8 km/hr. The WP Transporter is below the tip-over speed as it travels through Point B, just prior to entering the 305-m radius North Ramp Curve. The transporter remains below the tip-over speed at 30.67 m/s (68.6 mph) as it travels down the North Ramp Curve to Point M. However, the runaway speed and the tip-over speed (31.85 m/s) are within 10 percent and, therefore, it can be estimated that the WP Transporter will tip-over within the North Ramp Curve.

Therefore, Scenarios 1, 2, and 4 involve speeds fast enough for tip-over. It was found that tip-over would occur in the 305-m radius curves at slower speeds than derailment. Section 6.4.2 introduced the Nadal criterion as a simplified method for determining derailment speeds. For all four runaway scenarios, derailment would only occur when the rails are severely worn and there is a high coefficient of friction between the wheel flange and the head of the rail.

Although the findings of this analysis are accurate for the inputs and the assumptions made, for subsequent use, further refinements of this analysis are needed as the baseline design evolves to reduce uncertainties related to the emplacement system. The design of the WP Transporter, Subsurface Layout (TBV-4208), and the WP (TBV-246), all have a direct effect on the maximum attainable speed, tip-over calculations, and derailment determination.

It is also recommended that a higher fidelity model of the WP Transporter design be developed to provide a more accurate representation of the dynamic effects of the WP Transporter. Runaway, derailment, and tip-over speed calculations should incorporate the mass moment of inertia and the changes in center of gravity location during railcar tilting, rocking, and swaying

about the suspension system. This would provide a more accurate dynamic analysis of the WP Transporter.

The effects of the locomotives at either end of the WP Transporter have not been investigated in the derailment, tip over, and collision scenarios and, therefore, should be included in future investigations as well. In addition, because of the complexities at the wheel/rail interface, accurate derailment calculations were not made. However, a general and conservative estimate was made using the Nadal criterion for maximum speeds in the 305-m radius curves for incipient derailment.

Due to the large radius of the 305-m radius curves within the subsurface, conventional impact limiters on the ends of the WP Transporter would have negligible energy-absorbing effectiveness should a derailment or tip-over occur (see 6.4.2 and 6.4.3). From this, it is recommended that further investigation is needed into the use of energy-absorbing materials within the WP Transporter radiological shielding. This type of impact limiter could provide WP protection in multiple crash and/or impact scenarios.

The utilization of non-failsafe disc brakes for the WP Transporter and the locomotives presented in Sections 6.1.1.1 and 6.1.2.1 needs further investigation. The justification for or against the use of fail safe or non-failsafe disc brakes for secondary or redundant brake systems has yet to be performed.

Criteria 4.2.3 states that the WP Transporter speed shall be limited to 8 km/hr (2.22 m/s or 4.97 mph). Although the related System Description Document does not provide any basis for this speed, based on the calculations discussed in Section 6.6, 8 km/hr is 2.82 times slower than an equivalent 2 m design basis WP drop height.

The initial revision of this analysis (CRWMS M&O 2000e, Section 6.6) resolved TBV-252 at 8 km/hr. This revision is consistent with the previous, in that the maximum transporter speed of 8 km/hr (2.222 m/s or 4.97 mph) is adequate, based on:

- 2-m WP drop height Safety Factor of 2.82
- Mining Industry standard of 10 km/hr or less for mining locomotives
- Relatively high speeds needed for tip-over and wheel-climb derailments
- Recommendation that the WP Transporter, with its short truck-center spacing (11.778 m or 38.6 ft) and relatively high center-of-gravity (2.122 m or 6.96 ft), avoid operations in the 4.5-8.9 m/s (10-20 mph) regime, as described in Section 6.4.1.1.

The TBVs identified in Sections 4 and 5 are carried through to the outputs of this analysis as outlined in Table 15. This document may be affected by technical product input information that requires confirmation. Any changes to the document that may occur as a result of completing the confirmation activities will be reflected in subsequent revisions. The status of the input information quality may be confirmed by review of the Document Input Reference System database.

Table 15. TBD and TBV Information and Impacts

TBx Number	Description	Impact
TBV-245	Maximum WP Lift Heights of 2 m in vertical orientation and 2.4 m in a horizontal orientation	The maximum WP drop height has an effect on the justification for the maximum normal-operating speed of the transporter as presented in Section 6.6.
TBV-246	Waste Package Characteristics	Variations in Waste Package weight and size have an impact on the runaway, braking, derailment, and tip-over determinations presented in Sections 6.3.2.3, 6.3.3, 6.4.2, and 6.4.3, respectively
TBV-253	305-m Minimum Radius – Subsurface Waste Emplacement Transportation System Curvatures	The rail curve radius has a direct impact on rolling resistance, derailment, and tip-over calculations presented in Sections 6.3.2.2, 6.4.2, and 6.4.3, respectively.
TBV-274	Track Gauge for Surface Facilities, ramps Main Drifts, and turnouts	Track gauge has a direct affect on derailment and tip-over calculations presented in Sections 6.4.2, and 6.4.3 respectively.
TBV-308	Waste Package Weight-Uniformly Distributed	The uniformity of the WP weight has a direct affect on the tip-over calculations presented in Section 6.4.3.
TBD-330	The minimum number of WPs that the system shall be designed to recover	The number of WPs for recovery has a direct affect on the estimates of frequency of runaway presented throughout Section 6.8
TBV-690	Preclosure period (from beginning of repository operations to permanent closure) is assumed to be 100 years	The preclosure period has a direct affect on the estimates of frequency of runaway presented throughout Section 6.8
TBV-3130	Use of hydraulic disk brakes on transporter car as diverse, redundant backup to air-operated brakes	The use of hydraulic disk brakes has a direct affect on the braking calculations presented in 6.3.3, and the estimates of frequency of runaway presented throughout Section 6.8
TBV-3133	Assumptions on design and operations of braking, control, and communications systems of locomotives and transporter car as bases for fault-tree model	This assumption a direct affect on the estimates of frequency of runaway presented throughout Section 6.8
TBV-3138	Establishes bases for using beta-factor model for probability of CCFs.	The beta-factor model has a direct affect on the estimates of frequency of runaway presented throughout Section 6.8
TBV-3142	Failure rate for hydraulic actuator (surrogate for failure rate for rail-car speed retarder unit)	The failure rate for a hydraulic actuator has a direct affect on the estimates of frequency of runaway presented throughout Section 6.8
TBD-3936	Annual throughput for the Waste Handling Systems	The throughput of WPs has a direct affect on the estimates of frequency of runaway presented throughout Section 6.8
TBV-4208	Three-dimensional representation of the subsurface facility planning layout. This information is the output of the *Site Recommendation Subsurface Layout* (CRWMS M&O 2000d, Attachment II) and is used as inputs for the numerical representation of the Subsurface Layout (see Sections 4.1.2 and 4.1.5).	The subsurface layout has a direct affect on the entire analysis, including, but not limited to, runaway speeds, tip-over, derailment, stopping, and runaway probability.

7.1 CONCLUSIONS OF FAULT TREE ANALYSES

Although the design status of the mechanical, control and instrumentation systems of the WP transporter train are in various stages of conceptual design, it is possible and necessary to estimate the likelihood of potential accident scenarios such that, as the designs mature, provisions can be made to eliminate or reduce the probability of undesired events. To be considered incredible or "beyond design basis," the frequency of a potential accident sequence must be less than 1.0×10^{-6} per year.

Previous studies have estimated the frequency, or annual probability of occurrence, of a runaway transporter train. Estimates from actuarial data for commercial railway accidents and commercial mining accidents indicate that the median frequency of a runaway (adjusted for MGR operational conditions) is in the range of 7.75×10^{-5} per year to 4.71×10^{-3} per year (see Section 6.8.2.1). Previous FTAs of the conceptual transporter train and associated brake, control, and communications systems estimate the frequency of runaway to be about 5.88×10^{-4} per year (see Section 6.8.2.2.2), which is in good agreement with the actuarial data.

The prior evaluations of actuarial data and FTAs indicate that reducing the event frequency by a factor of about 1.70×10^{-3} would drive the event to the "beyond design basis" regime. The present analysis indicates that it appears to be feasible to achieve this reduction factor by applying one or more design alternatives. For example, the analyses demonstrates that electronic interlocks, alarms, and automatic brake actuation systems can significantly reduce the probability of human errors that contribute to both initiation of runaway and to the failure to stop a runaway. Further, the analyses indicate that speed retarder units mounted on the rails of the North Ramp can also reduce the frequency of an uncontrolled descent to less than 1.0×10^{-6} per year. Although the present analysis does not address uncertainty factors in the estimate of probabilities, considerable conservatism was employed in prior analyses and in the present study.

The present analysis has modified prior fault tree models to assess the effect of various postulated design features. Design features were included that reduce the likelihood that human operators or hardware can initiate a runaway. To calculate the frequency of a runaway event, the frequency of the initiating event is multiplied by the probability of failure to stop. These design features are:

1. An electronic interlock that prevents the operator from starting the train down the ramp without having dynamic brakes (or drag brakes) engaged.

2. An alarm to alert the operators when the speed of descent is too high or the train is accelerating, and

3. An automatic application of service brakes to maintain the speed within the normal operating range.

Whereas the original analysis predicted an initiation frequency of 0.228 per year, the FTA indicated that Alternatives 1 or 2, above, could reduce the frequency of human initiation to 7.57×10^{-7} and 4.56×10^{-5} per year, respectively. Using Alternative 3 alone would not

significantly reduce the frequency of initiation of 0.228 per year. However, when used in combination with either Alternative 1 or 2, the contribution from hardware becomes insignificant and the frequency of runaway initiation is 7.57×10^{-7} and 4.56×10^{-5} per year, respectively (see Table 11).

The original fault tree evaluated the probability to stop a runaway to be 2.58×10^{-3} per demand. Multiplying this probability by the initiation frequencies discussed above, gives 1.95×10^{-9} per year ($7.57\times10^{-7} \times 2.58\times10^{-3}$) and 1.18×10^{-7} ($4.56\times10^{-5} \times 2.58\times10^{-3}$) per year, respectively. The FTA indicates that either of these design alternatives, which reduce the human error initiation, is sufficient to drive the event frequency well below 1.0×10^{-6} per year without having to use a design alternative to reduce the probability of failure to stop.

Nevertheless, the present analyses investigated other design alternatives that could reduce the probability of failure to stop from the baseline value of 2.58×10^{-3} per demand while holding the initiating event frequency at the baseline value of 0.228 per year.

In the present study, the fault tree model was modified to evaluate the effect of using an electronic system for automatic speed detection and application of emergency brakes. This electronic system reduced the probability of failure to stop to 8.10×10^{-5} per demand and was shown to be dominated by hardware failures.. The application of this design alternative by itself reduces the frequency of runaway to about 1.84×10^{-5} per year, given the initiating frequency remains high at 0.228 per year. This evaluation indicates that it is may not be possible to drive the event frequency to below the 1.0×10^{-6} per year threshold for DBEs by the addition of an automatic emergency brake actuation system by itself (see Table 12).

The present FTAs show that providing a hydraulic braking system as a redundant and diverse backup to the air brake system cannot, by itself, reduce the runaway frequency below the 1.0×10^{-6} per year threshold, because the initiating frequency remains high at 0.228 per year and is dominated by human error. The analyses show, however, that a combination of an automatic emergency brake actuation system and a redundant, diverse brake system reduces the estimated frequency of runaway to 9.59×10^{-8} per year. This frequency is well below the cutoff of 1.0×10^{-6} per year for credible events (see Table 13).

The analyses show that incorporating one or more of the postulated design alternatives will drive the frequency of runaway below the cutoff of 1.0×10^{-6} per year for credible events (see Table 13). The following design alternatives appear to achieve the desired objective:

- Alarm on descent speed, manual emergency brake application (1.18×10^{-7} per year)
- Interlock on dynamic brake, manual emergency brake application (1.95×10^{-9} per year)
- Alarm on descent speed, automatic emergency brake application (3.69×10^{-9} per year)
- Interlock on dynamic brake, automatic emergency brake application (6.13×10^{-11} per year).
- Manual control of descent speed and automatic emergency brake application with redundant air and hydraulic brakes (9.59×10^{-9} per year)

should be 9.59×10^{-8}

The present analysis performed a reliability analysis of a conceptual rail-mounted speed retarder system. Such a system is based on proven technology and appears to be very promising as a diverse means of controlling train speed of descent that is redundant to the on-board dynamic brake and service brake systems.

It is noted that the bases for analysis presented here and based on *Application of Logic Diagrams and Common-Cause Failures to Design Basis Events* (CRWMS M&O 1997b) is very conservative with respect to modeling the large contribution of human error to both initiation and failure to stop a runaway. The present study re-examined the fault trees and incorporated plausible design alternatives that could virtually eliminate the human errors that were assumed in the prior models. It is cautioned that other potential human errors or hardware failures could be revealed when design details are available. Details of the design of the control panels in both the locomotive and control room will be subjected to human-factors evaluation, and continuing reliability evaluations will be performed on the electronic controls and interlocks, brake systems (including dynamic, service, and emergency brake system) to ensure that the frequency of an uncontrolled descent is beyond design basis.

It is concluded that design features that are within the state of the art can be incorporated into the electronic controls and brake mechanical systems for the transporter train and/or rail system to ensure that the runaway event can be regarded as "beyond design basis."

8. INPUTS AND REFERENCES

8.1 DOCUMENT CITED

Air Brake Association 1975. *Engineering Design of Railway Brake Systems.* Chicago, Illinois: Air Brake Association. TIC: 245141.

Air Brake Association 1998. *Management of Train Operation and Train Handling.* Chicago, Illinois: Air Brake Association. TIC: 245636.

Arno, R.G. 1981. *Nonelectronic Parts Reliability Data.* NPRD-2. Pages 24 and 25. Rome, New York: Reliability Analysis Center. TIC: 245435.

Avallone, E.A. and Baumeister, T., III, ed. 1987. *Marks' Standard Handbook for Mechanical Engineers.* 9th Edition. New York, New York: McGraw-Hill. TIC: 206891.

Balco, Inc. 1998. 60 Ton Trolley/Battery Locomotive. Blairsville, Pennsylvania: Balco. TIC: 239719.

Blader, F.B. 1990. *A Review of Literature and Methodologies in the Study of Derailments Caused by Excessive Forces at the Wheel/Rail Interface.* R-717. Chicago, Illinois: Association of American Railroads. TIC: 244198.

CRWMS M&O (Civilian Radioactive Waste Management System Management and Operating Contractor) 1996. *ESF Layout Calculation.* BABEAD000-01717-0200-00003 REV 04. Las Vegas, Nevada: CRWMS M&O. ACC: MOL.19960930.0095.

CRWMS M&O 1997a. *Repository Subsurface Layout Configuration Analysis.* BCA000000-01717-0200-00008 REV 00. Las Vegas, Nevada: CRWMS M&O. ACC: MOL.19971201.0879.

CRWMS M&O 1997b. *Application of Logic Diagrams and Common-Cause Failures to Design Basis Events.* BCA000000-01717-0200-00018 REV 00. Las Vegas, Nevada: CRWMS M&O. ACC: MOL.19980206.0272.

CRWMS M&O 1997c. *DBE/Scenario Analysis for Preclosure Repository Subsurface Facilities.* BCA000000-01717-0200-00017 REV 00. Las Vegas, Nevada: CRWMS M&O. ACC: MOL.19980218.0237.

CRWMS M&O 1998a. *Waste Package Transporter Design.* BCAF00000-01717-0200-00007 REV 00. Las Vegas, Nevada: CRWMS M&O. ACC: MOL.19981222.0039.

CRWMS M&O 1998b. *Mobile Waste Handling Support Equipment.* BCAF00000-01717-0200-00006 REV 00. Las Vegas, Nevada: CRWMS M&O. ACC: MOL.19980819.0397.

CRWMS M&O 1999a. *Classification of the MGR Waste Emplacement System.* ANL-WES-SE-000001 REV 00. Las Vegas, Nevada: CRWMS M&O. ACC: MOL.19990927.0477.

CRWMS M&O 1999b. *Outline Dimensions, Unit Weights and External Features for all WPs to be Emplaced.* Input Transmittal EBS-WP-99370.T. Las Vegas, Nevada: CRWMS M&O. ACC: MOL.19991220.0304.

CRWMS M&O 1999c. *Waste Emplacement and Waste Retrieval - 12012124MA.* Activity Evaluation, September 22, 1999. Las Vegas, Nevada: CRWMS M&O. ACC: MOL.19991020.0135.

CRWMS M&O 2000a. *Subsurface Transporter Safety Systems Analysis.* Development Plan TDP-WER-ME-000001 REV 01. Las Vegas, Nevada: CRWMS M&O. ACC: MOL.20000202.0179.

CRWMS M&O 2000b. *Waste Package Transport and Transfer Alternatives.* ANL-WES-ME-000001 REV 00. Las Vegas, Nevada: CRWMS M&O. ACC: MOL.20000317.0261.

CRWMS M&O 2000c. *Waste Emplacement/Retrieval System Description Document.* SDD-WES-SE-000001 REV 00. Volume I. Las Vegas, Nevada: CRWMS M&O. ACC: MOL.20000214.0302.

CRWMS M&O 2000d. *Site Recommendation Subsurface Layout.* ANL-SFS-MG-000001 REV 00. Las Vegas, Nevada: CRWMS M&O. Submit to RPC URN-0220

CRWMS M&O 2000e. *Subsurface Transporter Safety Systems Analysis.* ANL-WER-ME-000001 REV 00. Las Vegas, Nevada: CRWMS M&O. ACC: MOL.20000225.0052.

DOE (U.S. Department of Energy) 1998. *Preliminary Design Concept for the Repository and Waste Package.* Volume 2 of *Viability Assessment of a Repository at Yucca Mountain.* DOE/RW-0508. Washington, D.C.: U.S. Department of Energy, Office of Civilian Radioactive Waste Management. ACC: MOL.19981007.0029.

DOE (U.S. Department of Energy) 2000. *Quality Assurance Requirements and Description.* DOE/RW-0333P, Rev. 10. Washington, D.C.: U.S. Department of Energy, Office of Civilian Radioactive Waste Management. ACC: MOL.20000427.0422.

DOT (U.S. Department of Transportation) 1998. *Improving Railroad Safety and Rail Passenger Technology through Targeted Research and Demonstrations, 1992-1997.* DOT/FRA/ORD-98. Draft. Washington, D.C.: U.S. Department of Transportation. TIC: 243980.

Dyer, J.R. 1999. "Revised Interim Guidance Pending Issuance of New U.S. Nuclear Regulatory Commission (NRC) Regulations (Revision 01, July 22, 1999), for Yucca Mountain, Nevada." Letter from J.R. Dyer (DOE/YMSCO) to D.R. Wilkins (CRWMS M&O), September 3, 1999, OL&RC:SB-1714, with enclosure, "Interim Guidance Pending Issuance of New NRC Regulations for Yucca Mountain (Revision 01)." ACC: MOL.19990910.0079.

Eide, S.A. and Calley, M.B. 1993. "Generic Component Failure Data Base." *PSA '93, Proceedings of the International Topical Meeting on Probabilistic Safety Assessment, Clearwater Beach, Florida, January 26-29, 1993.* 2, 1175-1182. La Grange Park, Illinois: American Nuclear Society. TIC: 247455.

Goodman Equipment Corporation 1971a. *Goodman Mining Machine Sales Manual - Locomotive General Data Trolley Locomotive Calculations.* Section 4068. Bedford Park, Illinois: Goodman Equipment Corporation. TIC: 237874.

Goodman Equipment Corporation. 1971b. Goodman Mining Machine Sale Manual, Locomotive Standards. Section 4060-B. Bedford Park, Illinois: Goodman Equipment Corporation. TIC: 246930.

Kratville, W.W., ed. 1997. *The Car and Locomotive Cyclopedia of American Practices.* 6th Edition. Omaha, Nebraska: Simmons-Boardman Books. TIC: 237933.

McConnell, J.W.; Ayers, A.L. Jr.; and Tyacke, M.J. 1996. *Classification of Transportation Packaging and Dry Spent Fuel Storage System Components According to Importance to Safety.* NUREG/CR-6407. Washington, D.C.: U.S. Nuclear Regulatory Commission. TIC: 240459.

NTSB (National Transportation Safety Board) 1998. *Railroad Accident Report - Derailment of Union Pacific Railroad Unit Freight Train 6205 West Near Kelso, California January 12, 1997.* NTSB/RAR-98/01. Washington, D.C.: National Transportation Safety Board. TIC: 244169.

Swain, A.D. and Guttmann, H.E. 1983. *Handbook of Human Reliability Analysis with Emphasis on Nuclear Power Plant Applications Final Report.* NUREG/CR-1278. Washington, D.C.: U.S. Nuclear Regulatory Commission. TIC: 246563.

Ultra Dynamics, Inc. 1997. *Freight Car Continuous Speed Control System.* Columbus, Ohio: Ultra Dynamics, Inc. TIC: 245289.

8.2 CODES, STANDARDS, REGULATIONS, AND PROCEDURES

30 CFR 75. 1998. Mineral Resources: Mandatory Safety Standards. Underground Coal Mines. Readily Available

AAR (Association of American Railroads) 1999. *Manual of Standards and Recommended Practices: Section E-Brakes and Brake Equipment.* Washington, D.C.: Association of American Railroads. TIC: 244145.

AP-3.10Q, Rev. 2, ICN 2. *Analyses and Models.* Washington, D.C.: U.S. Department of Energy, Office of Civilian Radioactive Waste Management. ACC: MOL.20000619.0576.

AP-3.15Q, Rev. 1, ICN 2. *Managing Technical Product Inputs.* Washington, D.C.: U.S. Department of Energy, Office of Civilian Radioactive Waste Management. ACC: MOL.20000713.0363.

AP-SI.1Q, Rev. 2, ICN 4. *Software Management.* Washington, D.C.: U.S. Department of Energy, Office of Civilian Radioactive Waste Management. ACC: MOL.20000223.0508.

AP-SV.1Q, Rev. 0, ICN 1. *Control of the Electronic Management of Data.* Washington, D.C.: U.S. Department of Energy, Office of Civilian Radioactive Waste Management. ACC: MOL.20000512.0068.

QAP-2-0, Rev. 5. *Conduct of Activities.* Las Vegas, Nevada: CRWMS M&O. ACC: MOL.19980826.0209.

QAP-2-3, Rev. 10. *Classification of Permanent Items.* Las Vegas, Nevada: CRWMS M&O. ACC: MOL.19990316.0006.

Goodman Ref:
BRIAN WILTSEE

SILVIO MARTINO

9. ATTACHMENTS

Attachment I – Vender Information

Attachment II – Figure Calculation Data

Attachment III – CD-ROM Electronic Media

INTENTIONALLY LEFT BLANK

ATTACHMENT I

VENDER INFORMATION

INTENTIONALLY LEFT BLANK

ULTRA Dynamics

TrackMaster &
HC Retarders.
Marine Jet Drives
Surface Drives.

Ultra Dynamics, Inc. • 1110A Claycraft Road • Columbus, Ohio 43230
Telephone (614) 759-9000 • Fax (614) 759-9046 • E-Mail 70414.1337@compuserve.com

August 17, 1999

Please visit our web site at www.ultradynamics.com

Richard Silva
MORRISON KNUDSEN
1261 Town Center DR
Las Vegas, NE 89144

Fax: 702-295-4435

Dear Richard:

Here is some data to assist your basic calculation.

In addition to the Retarder energy there is always rolling resistance (normally 2lb/ton for a good roller) and curve resistance which can be significant. There are also switch factors.

Sorry for the mixed units.

Projected energy extraction for a 5 mph Ultra TrackMaster Retarder

5mph	1585 Joules
6mph	1670 J
7mph	1740 J
8mph	1820 J
9mph	1900 J

Please call if you have any questions.

Best regards.

Peter Raine

☐ TM Package ☐ TM Video ☐ Other-See GS

Printed by Peter on 17 Aug 99

ULTRA *Dynamics*

Ultra Dynamics, Inc.
1110A Claycraft Road,
Columbus, Ohio 43230
Tel: (614) 759 9000 Fax: (614) 759 9046
E-mail 70414.1337@compuserve.com

Marine Propulsion
Railroad Products

July 15, 1999

Richard Silva

MORRISON KNUDSEN
1261 Town Centre DR
Las Vegas, NE 89144

Dear Richard:

Here is the generic literature you requested for Ultra Rail Mounted Retarders.

I have conducted some provisional calculations and conclude that it should be possible to control the 190 Ton (380,000 lb) car on the 2.25% grade with no brakes on a straight grade.

The number of Ultra Retarders required is approximately 420 per 100 meters which would require tie spacing to be slightly closer than normal.

If the scenario considered has the two 50 ton (100,0000 lb) locomotives attached then appreciably fewer Ultra Retarders are required.

Curves negotiated during descent will also reduce the number of retarders required as there are appreciable losses involved with curve and switch negotiations.

Please contact me if you have any questions.

If required I could send you a video which may clarify the operation of the equipment.

Yours sincerely

Peter Raine

P.S.R.

Printed by Peter on 15 Jul, 99

ATTACHMENT II

FIGURE CALCULATION DATA

INTENTIONALLY LEFT BLANK

Microsoft Excel 97 SR-2 was used to develop seven figures (Figure 11 through Figure 16, and Figure 19). The data used to create these figures are presented in Attachment III as an electronic attachment in the form of Excel spreadsheets. All figures and data are contained within one Excel file and are organized into logical "sheets". Each Excel sheet contains one or more tables and figures, as listed below:

Table II-1. Microsoft Excel Spreadsheet Data

Sheet	Table/Figure	Description
Sheet 1 - Resistance	Table III-1	Initial Conditions for Resistance Data
	Table III-2	Resistance Data for Figure 11
	Figure 11	Rolling Resistance
Sheet 2 - Scenario 1	Table III-3	Velocity Data - Runaway Scenario 1
	Figure 12	Train Velocity - Scenario 1
Sheet 3 - Scenario 2	Table III-4	Velocity Data - Runaway Scenario 2
	Figure 13	Train Velocity - Scenario 2
Sheet 4 - Scenario 3	Table III-5	Velocity Data - Runaway Scenario 3
	Figure 14	Train Velocity - Scenario 3
Sheet 5 - Scenario 4	Table III-6	Velocity Data - Runaway Scenario 4
	Figure 15	Train Velocity - Scenario 4
Sheet 6 - Nadal Criterion	Table III-7	Stopping Distance for Figure 22
	Figure 19	Nadal Criterion
Sheet 7 - Stopping Distance	Table III-8	Initial Conditions for Stopping Distance Calculations
	Table III-9	Stopping Distance for Figure 16
	Figure 16	Stopping Distance

The equations that manipulate the data are presented below in their native Excel format, along with a basic description of the original equation and the expected results.

Table III-3 presents the runaway speed data for Scenario 1, which is used in Figure 12 and Table 5, for various frictional conditions and locations within the North Ramp and North Ramp Extension Curve. Starting from Point A (Station 01+62.500), Table III-3 used initial velocity conditions of 0 m/s and 2.222 m/s. Sheets *Scenario 2* through *Scenario 4* present the runaway speeds used in Figure 13 through Figure 15 and Table 6 through Table 8, respectively. The initial conditions for the rolling resistance calculations are presented in Table III-1. The calculations for Scenario 2 through Scenario 4 utilize the same calculations and procedures as Scenario 1, therefore only explanation of Scenario 1 is required by AP-SI.1Q.

Rolling Resistance Values

Table III-2 presents resistance values used in Figure 11 for a range of velocities based on Equation 17, 18, and 19 as presented in Section 6.3.2.1. The initial conditions for the equations are listed in Table III-1.

Table III-2 contains 5 columns labeled from A through E. Each row utilizes the same equation within each respective column, and therefore, only one arbitrary row will be described (i.e. row 26).

Column A of the data increments the speed by five miles per hour.

=SUM(A25+5)

Columns B through D calculate the resistance using Equations 17 through 19 respectively.

B: =SUM(1.3*Weight+29*N+0.045*Weight*A26+0.0005*Area*A26^2)

$$R = 1.3W + 29n + 0.045Wv + 0.0005Av^2 \qquad \text{(Eq. 17)}$$

This calculation can be hand verified using row 26 (Speed = 50) as:

$$(1.3 \times 441) + (29 \times 10) + (0.045 \times 441 \times 50) + (0.0005 \times 128.5 \times 50^2) = 2016.18 \text{ (0.0\% error)}$$

C: =SUM(1.3*Weight+29*N+0.045*Weight*A26+0.045*A26^2)

$$R = 1.3W + 29n + 0.045Wv + 0.045v^2 \qquad \text{(Eq. 18)}$$

This calculation can be hand verified using row 26 (Speed = 50) as:

$$(1.3 \times 441) + (29 \times 10) + (0.045 \times 441 \times 50) + (0.045 \times 50^2) = 1968.05 \text{ (0.0\% error)}$$

D: =SUM(0.6*Weight+20*N+0.01*Weight*A26+0.07*A26^2)

$$R = 0.6W + 20n + 0.01Wv + 0.07v^2 \qquad \text{(Eq. 19)}$$

This calculation can be hand verified using row 26 (Speed = 50) as:

$$(0.6 \times 441) + (20 \times 10) + (0.01 \times 441 \times 50) + (0.07 \times 50^2) = 860.10 \text{ (0.0\% error)}$$

Column E calculates that resistance based on Goodman's "rule-of-thumb", as discussed in Section 6.3.2.1. However, this information is not presented in Figure 11 as it is found to be much larger in magnitude than the previous methods (Equations 17 through 19).

E: =SUM(20*Weight)

This calculation can be hand verified using row 26 (Speed = 50) as:

$$20 \times 441 = 8820 \text{ (0.0\% error)}$$

Runaway Velocity for Scenario 1

The determination of runaway velocity is primarily a function of slope, distance traveled, and rolling resistance. However, due to aerodynamic drag, the rolling resistance is a function of velocity. Therefore, the determination of velocity is a function of velocity.

From Section 6.3.2.3, Equation 31 and 32 describe the basic velocity equations used to find the runaway speed.

$$F\Delta s = \frac{1}{2} m(v_1^2 - v_2^2) + mgh \qquad \text{(Eq. 31)}$$

$$v_2 = \sqrt{\frac{-2}{m} F\Delta s + 2gh + v_1^2} \qquad \text{(Eq. 32)}$$

Recall that the rolling resistance is a function of velocity, and to correctly calculate the runaway velocity at any point within the North Ramp, a mathematical technique called stepwise integration is used. This is a numerical-methods technique where a small change in one value is used to determine the next value, and so on in a stepwise fashion (Avallone and Baumeister 1987, p. 2-45).

In the determination of runaway velocity, a small, stepwise drop in elevation (h) is used to step through the velocity equation (Eq. 31 and Eq. 32) and solve for the velocity at any location in the ramp. Generally with stepwise integration, smaller steps result in smaller truncation errors. For this calculation of velocity, an elevation (h) step of 0.1 meters is used. Using Equation 32, the velocity (v_2) for each step is determined using resistance force (F) derived from the velocity of the previous step (v_1). This resistance force is determined from the summation of Equation 17 and Equation 25 for rolling and curve resistance respectively.

Table III-3 contains 16 columns labeled from A through P. Each row utilizes the same equation within each respective column, and therefore, only one arbitrary row will be described (i.e. row 67).

The first column (A) is the stepwise change in elevation. This adds the stepwise change in elevation of 0.1 m to the previous elevation.

=SUM(A66+0.1)

This calculation can be hand verified using row 67 ($\Delta h = 3.3$) as:

3.2+0.1=3.3

The second column (B) is the slope that determines the change in position in column C (Δs) based on the slope of the North Ramp (Equation 42) in degrees derived from Equation 41 and the change in elevation (h).

$$\theta = \tan^{-1}\left(\frac{\%Grade}{100}\right) = \tan^{-1}\left(\frac{2.1486}{100}\right) = 1.2309° \quad \text{(Eq. 41)}$$

$$h = \Delta s \times \sin(\theta) \quad \text{(Eq. 42)}$$

=SUM(A68-A67)/(SIN(ATAN(B67/100)))

This calculation can be hand verified using row 67 ($\Delta h = 3.3$) as:

$$\frac{3.3-3.2}{\sin\left(\tan^{-1}\frac{2.1486}{100}\right)} = 4.66 \text{ (0.00\% error)}$$

Column D determines the overall position in the North Ramp starting from Point A (Station 01+62.500) by adding the change in position (Column C) to the previous position (Column D).

=SUM(D66+C67)

This calculation can be hand verified using row 67 ($\Delta h = 3.3$) as:

311.469+4.66=316.129 (0.0016% error)

Column E determines the rolling resistance for the WP Transporter based on Equation 17 using the velocity (Column K) from the previous step. The initial conditions for rolling resistance calculations are shown in Table III-1.

=SUM(1.3*Weight+29*N+0.045*Weight*K66+0.0005*Area*K66^2)

$$R = 1.3W + 29n + 0.045Wv + 0.0005Av^2 \quad \text{(Eq. 17)}$$

This calculation can be hand verified using row 67 ($\Delta h = 3.3$) as:

$$(1.3 \times 441.00) + (29 \times 10) + (0.045 \times 441 \times 17.8437) + (0.0005 \times 128.5 \times 17.8437^2) = 1237.86 \text{ (0.000\% error)}$$

Column F converts the Column E results from pounds force to Newtons where 1 lb_f=4.448222 N.

=SUM(E67*4.448222)

This calculation can be hand verified using row 67 (Δh = 3.3) as:

Should be 5506.32

$$1237.87 \times 4.448222 = 55506.32 \text{ (0.00\% error)}$$

Column G determines the rolling resistance for a Locomotive based on Equation 17 using the velocity (Column K) from the previous step.

=SUM(1.3*Loco_Weight+29*Nl+0.045*Loco_Weight*K66+0.0005*Area*K66^2)

This calculation can be hand verified using row 67 (Δh = 3.3) as:

$$(1.3 \times 50) + (29 \times 4) + (0.045 \times 50 \times 17.8425) + (0.0005 \times 128.5 \times 17.8425^2) = 241.60 \text{ (0.00\% error)}$$

It should be noted that the cross-sectional area of the WP Transporter (128.5 ft from Section 6.3.2.1) is used because this is the maximum frontal area for the entire train subjected to aerodynamic drag.

Column H converts the Column G results from pounds force to Newtons where 1 lb=4.448222 N.

=SUM(G34*4.448222)

This calculation can be hand verified using row 67 (Δh = 3.3) as:

$$241.60 \times 4.448222 = 1074.69 \text{ (0.0\% error)}$$

Column I determines the curve resistance per metric ton (R_c) of the train which consists of two locomotives and the WP transporter. This resistance only applies where curves fall in the repository layout and it is based on 305-m curve radius.

$$R_c/\theta_c = 1\frac{lb_f}{ton} \times \frac{4.448\frac{N}{lb_f}}{0.9071\frac{MT}{ton}} = 4.9033\frac{N}{MT} \quad \text{(Eq. 24)}$$

$$R_c = \theta_c \times R_c/\theta_c = 5.7262° \times 4.9033\frac{N}{MT} = 28.078\frac{N}{MT} \quad \text{(Eq. 25)}$$

=28.0778262295*(Weight+(2*Loco_Weight))*0.9072

This calculation can be hand-verified using row 524 ($\Delta h = 49$)

$$R_C = 28.078 \times (441 \text{ tons} + (2 \times 50 \text{ tons}))\ 0.9072 \text{ MT/ton}$$

$$= 13{,}780.55 \text{ N (0.00\% error)}$$

Column J utilizes Equation 32 to determine the velocity of the WP Transporter and the two locomotives for the frictional case. The weight of the train is converted from tons to kilograms within the equation (1 ton = 907.1847 kg).

$$v_2 = \sqrt{\frac{-2}{m} F\Delta s + 2gh + v_1^2} \qquad \text{(Eq. 32)}$$

=SUM(((-2*(F66+2*H66+I66)*C66/((Weight+2*Loco_Weight)*907.1847)) +
(2*9.80665*(A67-A66)) + J66^2)^0.5)

This calculation can be hand verified using row 67 ($\Delta h = 3.3$) as:

$$\sqrt{\frac{-2\times(5506.30+2\times1074.71)\times4.66}{(441+2\times50)\times907.1847} + 2\times9.80665\times(3.3-3.2) + 7.97686^2}$$

$$= 8.0899 \text{ m/s (0.0006\% error)}$$

Column K converts the Column J results from meters per second (m/s) to miles per hour (mph) where 1 m/s=2.236936 mph.

=SUM(H34*2.236936)

This calculation can be hand verified using row 67 ($\Delta h = 3.3$) as:

$$8.0899 \times 2.236936 = 18.097 \text{ mph (0.0\% error)}$$

Column L derives the total elapsed time by dividing the change in position by the velocity and adding that value to the previous stepwise time.

=SUM((D67-D66)/J67)+L66

This calculation can be hand verified using row 67 ($\Delta h = 3.3$) as:

$$\frac{316.124 - 311.469}{8.0899} + 28.379 = 28.954 \text{ sec. (0.00\% error)}$$

Column M determines the frictionless velocity based on Equation 7 from Section 6.3.1.

$$v^2 = v_0^2 + 2a(x - x_0) \qquad \text{(Eq. 7)}$$

=SUM((2*9.80665*(A67-A66)+M66^2)^0.5)

This calculation can be hand verified using row 67 ($\Delta h = 3.3$) as:

$$\sqrt{2 \times 9.80665 \times (3.3 - 3.2) + 8.22799^2} = 8.34633 \text{ m/s (0.0\% error)}$$

Column N converts the Column M results from meters per second (m/s) to miles per hour (mph) where 1 m/s=2.236936 mph.

=SUM(M34*2.236936)

This calculation can be hand verified using row 34 ($\Delta h = 3.3$) as:

$$8.34633 \times 2.236936 = 18.670 \text{ mph (0.0\% error)}$$

Column O utilizes Equation 26 to determine the velocity of the WP Transporter and the two locomotives for the Goodman resistance case of 20 pounds resistance force for every ton of weight. The 400 MT rail car will produce 8,820 pounds resistance force and the 50-ton locomotives will create 1000 pounds each. Within Equation 32, the resistance forces are converted from pounds force to Newtons (1 lb_f = 4.448222 N) and the weight of the train is converted from tons to kilograms (1 ton = 907.1847 kg).

=SUM(((-2*((8820+2*1000)*4.448222)*C66/((Weight+2*Loco_Weight)*907.1847)) + (2*9.80665*(A67-A66)) + O66^2)^0.5)

does not account for curve resistance

This calculation can be hand verified using row 67 ($\Delta h = 3.3$) as:

$$\sqrt{\frac{-2 \times (8820 + 2 \times 1000) \times 4.44822}{(441 + 2 \times 50) \times 907.1847} \times 4.66 + 2 \times 9.80665 \times (3.3 - 3.2) + 6.2034^2}$$

$$= 6.28725 \text{ m/s (0.00\% error)}$$

Column P converts the Column O results from meters per second (m/s) to miles per hour (mph) where 1 m/s=2.236936 mph.

=SUM(O67*2.236936)

This calculation can be hand verified using row 67 ($\Delta h = 3.3$) as:

$$6.28725 \times 2.236936 = 14.0642 \text{ mph (0.0\% error)}$$

Nadal Criteria

Table III-7 plots the Nadal Criterion equation (Eq. 47) described in Section 6.4.2 for varying flange angles (δ) and coefficients of friction (μ). Table III-7 contains 8 columns labeled from A

through I (Column C is not used). Each row utilizes the same equation within each respective column, and therefore, only one arbitrary row will be described (i.e. row 19).

$$\frac{L}{V}=\frac{R\sin\delta-F\cos\delta}{R\cos\delta+F\sin\delta}=\frac{\sin\delta-\mu\cos\delta}{\cos\delta+\mu\sin\delta} \qquad \text{(Eq. 47)}$$

Column A increments the flange angle by one degree.

=SUM(A10+1)

The Excel software calculates sine and cosine functions in radians. Therefore, the flange angle is converted to radians in Column B

=SUM(A19*3.1416/180)

Columns D though I calculate the Nadal Criteria for varying coefficients of friction ranging from 0.1 to 0.6 respectively.

D: =SUM((SIN(B19)-0.1*COS(B19))/(COS(B19)+0.1*SIN(B19)))

E: =SUM((SIN(B19)-0.2*COS(B19))/(COS(B19)+0.2*SIN(B19)))

F: =SUM((SIN(B19)-0.3*COS(B19))/(COS(B19)+0.3*SIN(B19)))

G: =SUM((SIN(B19)-0.4*COS(B19))/(COS(B19)+0.4*SIN(B19)))

H: =SUM((SIN(B19)-0.5*COS(B19))/(COS(B19)+0.5*SIN(B19)))

I: =SUM((SIN(B19)-0.6*COS(B19))/(COS(B19)+0.6*SIN(B19)))

These calculations can be hand verified using row 19 (Angle = 10) and using column D where μ=0.1:

$$\frac{\sin_{rad}(0.174533)-0.1\times\cos_{rad}(0.174533)}{\cos_{rad}(0.174533)+0.1\times\sin_{rad}(0.174533)}=0.075005 \text{ (0.0\% error)}$$

Stopping Distances

Table III-8 presents the initial data used to find the stopping distance as shown in Figure 16. This set of data determines the stopping distance at velocity increments of one meter/sec using Equation 43.

Table IIi-9 contains 10 columns labeled from A through J. Each row utilizes the same equation within each respective column, and therefore, only one arbitrary row will be described, i.e., row 64 (29 m/s).

Column A of the data increments the speed by one meter per second.

=SUM(A63+1)

Column B converts the Column A results from meters per second (m/s) to miles per hour (mph) where 1 m/s=2.2369 mph.

=SUM(A64*2.2369)

This calculation can be hand verified using row 64 (Speed = 29) as:

$$29 \times 2.2369 = 64.8701 \text{ (0.0\% error)}$$

Column C determines the rolling resistance for the WP Transporter based on Equation 17 using the velocity (Column B).

=SUM(1.3*Weight+29*N+0.045*Weight*B64+0.0005*Area*B64^2)

$$R = 1.3W + 29n + 0.045Wv + 0.0005Av^2 \qquad \text{(Eq. 17)}$$

This calculation can be hand verified using row 64 (Speed = 29) as:

$$((1.3 \times 441) + (29 \times 10) + (0.045 \times 441 \times 64.8701) + (0.0005 \times 128.5 \times 64.8701^2) = 2421.02 \text{ (0.0\% error)}$$

Column D converts the Column C results from pounds force to Newtons where 1 lb_f=4.4482 N.

=SUM(C64*4.4482)

This calculation can be hand verified using row 64 (Speed = 29) as:

$$2421.02 \times 4.4482 = 10{,}769.18 \text{ (0.0\% error)}$$

Column E determines the rolling resistance for the locomotive based on Equation 17 using the velocity (Column B).

=SUM(1.3*Loco_Weight+29*Nl+0.045*Loco_Weight*B64+0.0005*Area*B64^2)

$$R = 1.3W + 29n + 0.045Wv + 0.0005Av^2 \qquad \text{(Eq. 17)}$$

This calculation can be hand verified using row 64 (Speed = 29) as:

$$((1.3 \times 50) + (29 \times 4) + (0.045 \times 50 \times 64.8701) + (0.0005 \times 128.5 \times 64.8701^2) = 597.34 \text{ (0.002\% error)}$$

Column F converts the Column E results from pounds force to Newtons where 1 lb=4.4482 N.

=SUM(E64*4.4482)

This calculation can be hand verified using row 64 (Speed = 29) as:

$$597.34 \times 4.4482 = 2657.09 \text{ (0.002\% error)}$$

Column G calculates the stopping distance using Equation 43 for standard braking (Brake Ratio = 0.13). The initial conditions for the determination of stopping distance are listed in Table III-8 (i.e. Brake Ratio, Coefficient of Friction for the brakes, etc.). The retardation force (ΣF) is found from Equation 36 and 37 for emergency and standard braking respectively for both the Transporter (400 MT) and the two locomotives (50 ton = 45.359 MT).

$$F_{B\max} = \mu R_B W = \mu R_B mg = 0.30 \times 0.60 \times (400\,\text{MT} + 2 \times 45.359\,\text{MT}) \times 9.80665\,\tfrac{\text{m}}{\text{s}^2} \times 1000\,\tfrac{\text{kg}}{\text{MT}}$$
$$= 866{,}214\ \text{N} \qquad \text{(Eq. 36)}$$

$$F_{B\min} = \mu R_B W = \mu R_B mg = 0.30 \times 0.130 \times (400\,\text{MT} + 2 \times 45.359\,\text{MT}) \times 9.80665\,\tfrac{\text{m}}{\text{s}^2} \times 1000\,\tfrac{\text{kg}}{\text{MT}}$$
$$= 187{,}680\ \text{N} \qquad \text{(Eq. 37)}$$

$$\Delta s = \frac{m(v_1^2 - v_2^2)}{2[\sum F - mg\sin(1.2309)]} \qquad \text{(Eq. 43)}$$

=SUM(((Weight+2*Loco_Weight)*907.18*(A64^2-
Final_Velocity^2))/(2*(D64+F64+(Coefficient_Brake_Friction*Brake_Ratio*(Weight+2*Loco_
Weight)*9.8066*907.18)-((Weight+2*Loco_Weight)*907.18*9.8066*0.0214812))))

NOTE:

1 ton = 907.18 kg
g = 9.8066 m/s^2
sin(1.2309) = 0.021481

This calculation can be hand verified using row 64 (Speed = 29) as:

$$\Delta s = \frac{(441 + 2 \times 50) \times 907.18 \times (29^2 - 0^2)}{2[10769.18 + 2567.09 + (0.3 \times .13 \times (441 + 2 \times 50) \times 9.8066 \times 907.18) - ((441 + 2 \times 50) \times 9.8066 \times 907.18 \times 0.0214812)]}$$
$$= 2{,}111.404 \text{ (0.0\% error)}$$

Column H converts the Column G results from meters to feet where 1 m = 3.28084 ft.

=SUM(G64*3.28083989501)

This calculation can be hand verified using row 64 (Speed = 29) as:

$$5111.404 \times 3.28084 = 6927.18 \text{ (0.0\% error)}$$

Column I calculates the stopping distance using Equation 43 for emergency braking (Brake Ratio = 0.60). The initial conditions for the determination of stopping distance are listed in

Table III-8 (i.e. Brake Ratio, Coefficient of Friction for the brakes, etc.). The retardation force (ΣF) is found from Equation 36 and 37 for emergency and standard braking respectively.

=SUM(((Weight+2*Loco_Weight)*907.18*(A64^2-Final_Velocity^2))/(2*(D64+(Coefficient_Brake_Friction*Emergency_Brake_Ratio*(Weight+2*Loco_Weight)*9.8066*907.18)-((Weight+2*Loco_Weight)*907.18*9.8066*0.021481))))

NOTE:

1 ton = 907.18 kg
g = 9.8066 m/s^2
sin(1.2309) = 0.021481

This calculation can be hand verified using row 64 (Speed = 29) as:

$$\Delta s = \frac{(441+2\times 50)\times 907.18\times(29^2-0^2)}{2[10769.18+2657.09+(0.3\times .60\times(441+2\times 50)\times 9.8066\times 907.18)-((441+2\times 50)\times 9.8066\times 907.18\times 0.0214812)]}$$
$$= 265.822 \text{ (0.343\% error)}$$

Column J converts the Column I results from meters to feet where 1 m = 3.28084

=SUM(J64*3.28084)

This calculation can be hand verified using row 64 (Speed = 29) as:

$$265.822 \times 3.28084 = 872.119 \text{ (0.343\% error)}$$